

INFORMATION TO USERS

This manuscript has been reproduced from the microfilm master. UMI films the text directly from the original or copy submitted. Thus, some thesis and dissertation copies are in typewriter face, while others may be from any type of computer printer.

The quality of this reproduction is dependent upon the quality of the copy submitted. Broken or indistinct print, colored or poor quality illustrations and photographs, print bleedthrough, substandard margins, and improper alignment can adversely affect reproduction.

In the unlikely event that the author did not send UMI a complete manuscript and there are missing pages, these will be noted. Also, if unauthorized copyright material had to be removed, a note will indicate the deletion.

Oversize materials (e.g., maps, drawings, charts) are reproduced by sectioning the original, beginning at the upper left-hand corner and continuing from left to right in equal sections with small overlaps. Each original is also photographed in one exposure and is included in reduced form at the back of the book.

Photographs included in the original manuscript have been reproduced xerographically in this copy. Higher quality 6" x 9" black and white photographic prints are available for any photographs or illustrations appearing in this copy for an additional charge. Contact UMI directly to order.

UMI

A Bell & Howell Information Company
300 North Zeeb Road, Ann Arbor MI 48106-1346 USA
313/761-4700 800/521-0600

TWO DIMENSIONAL AGONISTIC CONTROL

by
Daqing Yang

**A Dissertation
Submitted to the Faculty of
New Jersey Institute of Technology
in Partial Fulfillment of the Requirements for the Degree of
Doctor of Philosophy**

Department of Electrical and Computer Engineering

January 1997

UMI Number: 9721276

**Copyright 1997 by
Yang, Daqing**

All rights reserved.

**UMI Microform 9721276
Copyright 1997, by UMI Company. All rights reserved.**

**This microform edition is protected against unauthorized
copying under Title 17, United States Code.**

UMI
300 North Zeeb Road
Ann Arbor, MI 48103

ABSTRACT

TWO DIMENSIONAL AGONISTIC CONTROL

by
Daqing Yang

The conventional method of precise multiple-axis motion control entails use of a multiple axis positioning system with each axis carrying not only the workpiece but also the positioning system of the remaining axes. The resultant structure is heavy, sluggish, and expensive. An alternative positioning technique is being investigated in which the motion of the workpiece is controlled by pulling it with tendons, each of which has its own actuator. Since the actuators can be mounted on the base of the structure instead of being carried by motion system of the other axes, they can be relatively large and powerful without the need for a massive structure such as is found in a conventional motion control system. This method of control is given the appellation *agonistic*, based on the usages of the word suggesting tension or a contest.

Agonistic control system can be used for low cost accurate positioning of workpiece. The control task can be moving the workpiece from one point to another point and kept there or tracking a given trajectory. While the workpiece moves, the tendons should be always kept in tension.

In this thesis, the model of two dimensional agonistic control (in the case of tendons of infinite elastic modulus) is established. It leads to a nonlinear multi-variable control problem. Based on this nonlinear model, a full-state feedback control law is synthesized. It is composed of two parts. The first part is a feedforward control to cancel the nonlinear dynamics. The second part is a PD control term which requires velocity information. In the practice, velocity measurement may be contaminated by noise. In order of only using position measurement in the control law, a nonlinear observer is designed to provide the velocity information.

Numerical simulation is performed to verify the ability of the proposed control law.

In reality, the tendon has some elasticity. This finite elasticity, if not accounted for, can render the closed-loop system unstable. The investigation shows that the effect of elastic tendons can be compensated for by appropriately modifying the control law designed for inelastic tendons. In particular, the control law is synthesized using the singular perturbation method. It consists of a fast control and a slow control. The fast control is used to stabilize the oscillations incurred by the finite elasticity of the tendon. The slow control drives the system to track the desired trajectory. Robustness of the controller is enhanced by using sliding mode control.

In the chapter 4, the design of observer in the elastic case is addressed. Linear uncertain system theory is used. The observer is globally stable.

The use of decentralized control scheme makes very simple the controller design and reduces the computational complexity. It is very useful for real time agonistic control. A design approach is presented for the decentralized control scheme. A simple linear second order model is used instead of complex nonlinear model used in centralized version. In this approach, the tension in each tendon is treated as disturbance, estimated by an observer, to be compensated.

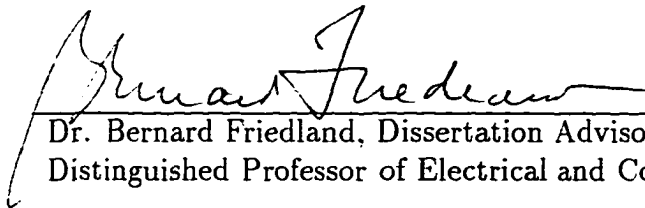
Copyright © 1997 by Daqing Yang

ALL RIGHTS RESERVED

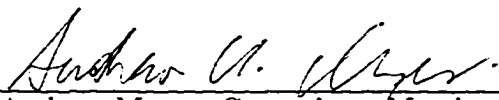
APPROVAL PAGE

Two Dimensional Agonistic Control

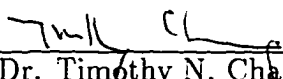
Daqing Yang

 9/26/96


Dr. Bernard Friedland, Dissertation Advisor Date
Distinguished Professor of Electrical and Computer Engineering, NJIT

 9/26/96


Dr. Andrew Meyer, Committee Member Date
Professor of Electrical and Computer Engineering, NJIT

 9/26/96

Dr. Timothy N. Chang, Committee Member Date
Associate Professor of Electrical and Computer Engineering, NJIT

 Sept 26, 1996

Dr. John Tavantzis, Committee Member Date
Professor of Mathematics, NJIT

 9/26/96

Dr. Anthony Tzes, Committee Member Date
Associate Professor of Mechanical, Aerospace and Manufacturing Engineering,
Polytechnic University, New York

BIOGRAPHICAL SKETCH

Author: Daqing Yang

Degree: Doctor of Philosophy

Date: January 1997

Date of Birth: February 21, 1964

Place of Birth: Anhui, P.R.China

Undergraduate and Graduate Education:

- Doctor of Philosophy in Electrical Engineering,
New Jersey Institute of Technology, Newark, NJ, 1997
- Master of Science in Automatic Control,
Beijing University of Aeronautics and Astronautics, Beijing, P.R.China, 1987
- Bachelor of Science in Automatic Control,
Nanjing University of Aeronautics and Astronautics, Nanjing, P.R.China, 1984

Major: Electrical Engineering

Presentations:

Daqing Yang and Bernard Friedland, "Two dimensional agonistic control: stiff case" Proceedings of IEEE Regional Conference on Control Applications, Rutgers University, Piscataway, August 1994

Daqing Yang and Bernard Friedland, "Two dimensional agonistic control: elastic case" Proceedings of Japan-U.S.A. Symposium on Flexible Automation, Boston, July 1996

Daqing Yang and Bernard Friedland, "A decentralized control strategy for agonistic system" submitted to 1997 American Control Conference

This work is dedicated to
my family

ACKNOWLEDGMENT

The author wishes to express his sincere gratitude to his advisor, Dr. Friedland, for his guidance, insight, support and patience.

The author would like to thank Dr. Meyer, Dr. Chang, Dr. Tavantzis and Dr. Tzes for serving the committee members and taking time to review this dissertation.

The author also wish to thank past and current members in the control system lab, Hong Ding and Vincenzo Pappano, for their generous help.

TABLE OF CONTENTS

Chapter	Page
1 INTRODUCTION	1
1.1 Background	1
1.2 Description of an Agonistic System	4
1.3 Control Methodology	7
1.4 Contribution of this Dissertation	10
1.5 Organization of this Dissertation	11
2 DERIVATION OF DYNAMIC MODEL	12
2.1 Stiff Case	13
2.2 Elastic Case	19
2.3 Dynamic Model for Decentralized Control	24
3 CONTROL LAW DESIGN	27
3.1 Centralized Control Strategy	27
3.1.1 Stiff Case	27
3.1.2 Elastic Case	35
3.2 Decentralized Control Strategy	40
3.3 Consideration of DC Motor Characteristics	43
4 OBSERVER DESIGN FOR AGONISTIC CONTROL	46
4.1 Necessity of Observer	46
4.2 Development of the Nonlinear Observer	46
4.3 Observer Design for Agonistic Control: Elastic Case	49
5 PERFORMANCE EVALUATION BY SIMULATION	60
5.1 Centralized Control Strategy	60
5.1.1 Stiff Case	60
5.1.2 Elastic Case	76

Chapter	Page
5.2 Decentralized Control Strategy	86
5.3 Bandwidth of the Agonistic System	99
5.4 Choice of the Control Laws	100
5.5 Comparison with Hummingbird System	101
6 SUMMARY AND CONCLUSIONS	103
REFERENCES	105

LIST OF FIGURES

Figure	Page
1.1 Schematic drawing of XY-table	2
1.2 Model of a single-joint driven by one rotary actuator	3
1.3 Two dimensional agonistic control	5
1.4 Centralized control	9
1.5 Decentralized control	9
3.1 Computed torque control scheme	29
3.2 PD + control scheme	34
3.3 The composite control law is designed to achieve robust tracking	38
3.4 Motor dynamics	44
5.1 Trajectory. computed torque method in the absense of friction	63
5.2 Orbit discrepancy. computed torque method.	63
5.3 Control torques exerted on each motors. They are all positive.	64
5.4 Input voltages	65
5.5 Trajectory. Computed torque method. Friction is present	66
5.6 Control torques exerted on each motors. Friction is present.	67
5.7 Trajectory. computed torque method with observer. friction is added . .	68
5.8 Control torques on each motors	69
5.9 True and estimated velocities	70
5.10 Trajectory. Passivity-based method in the absense of friction	71
5.11 Orbit discrepancy. Passivity-based method.	71
5.12 Trajectory. Passivity-based method. Friction is present	72
5.13 Control torques exerted on each motors. Friction is present.	73
5.14 Trajectory. Passivity-based method with observer. friction is added	74
5.15 Control torques on each motors	75

Figure	Page
5.16 Composite control law performance for the agonistic system with elastic tendons	77
5.17 Orbit discrepancy	77
5.18 Behavior of fast boundary-layer state η	78
5.19 Composite control developed in tracking circular trajectory	79
5.20 Control law maintains positive tensions in the tendons	80
5.21 Fast control	81
5.22 Input voltages are less than allowable level, 24 volts	82
5.23 Composite control law performance	83
5.24 Orbit discrepancy	83
5.25 Control torques are positive, as physically required	84
5.26 True and estimated velocities. The estimated values closely follow the true values	85
5.27 Trajectory, decentralized	87
5.28 Orbit discrepancy. decentralized control strategy. full state feedback . . .	87
5.29 Control torque, decentralized	88
5.30 The base value in each torque	89
5.31 The correction value in each torque	90
5.32 Tensions in each tendon	91
5.33 Input voltages	92
5.34 Angular velocity	93
5.35 Contracted working domain	94
5.36 Unstable system	95
5.37 Tensions become uncontrolled	96
5.38 Trajectory with observer	97
5.39 Angular velocity	98
5.40 The agonistic system has 20 Hz bandwidth	100

CHAPTER 1

INTRODUCTION

1.1 Background

Motion control systems are commercially available that achieve high static accuracy. These machines achieve their accuracy by relying upon a very rigid structure and motion of the object to be controlled is achieved through very precise mechanical drive systems. Not only are such machines very costly, but they are usually very slow, since the motors in the multiple axis positioning system have to move along with the load.

XY-table is an example of conventional positioning system (Jager, 1994). The table consists of three prismatic joints, where two of the joints move parallel to each other and coupled by a spindle with a torsion spring. It has two degrees-of-freedom, moving in the horizontal plane. The target area is a rectangle covered by the end-effector. The x and y coordinates correspond to the position of the "target" point in the horizontal plane. Two current amplifiers feed two permanent magnet DC motors. The transmission consists of cog wheels and timing belts. The two belts that drive the x-slides, and by that the y-slideway, are connected to belt-wheels on the spindle. The spindle is connected to the x-motor by a belt. The belt for the y-slide is connected to a belt-wheel directly mounted on the y-motor, so this motor drives the end-effector without reduction. Pre-tensioned springs connect the belts with the slides. With a flexible spindle, it is not necessary for the y-slideway to be perpendicular to the x-slideway.

Conventional positioning machines are useful for positioning of heavy objects but are inefficient for positioning of light objects such as semiconductor wafers.

There is a need for cheaper and faster means of motion control. A number of techniques have been proposed to address this need. The "Hummingbird" minipositioner was developed at the IBM Thomas J. Watson Research Laboratories (Zai

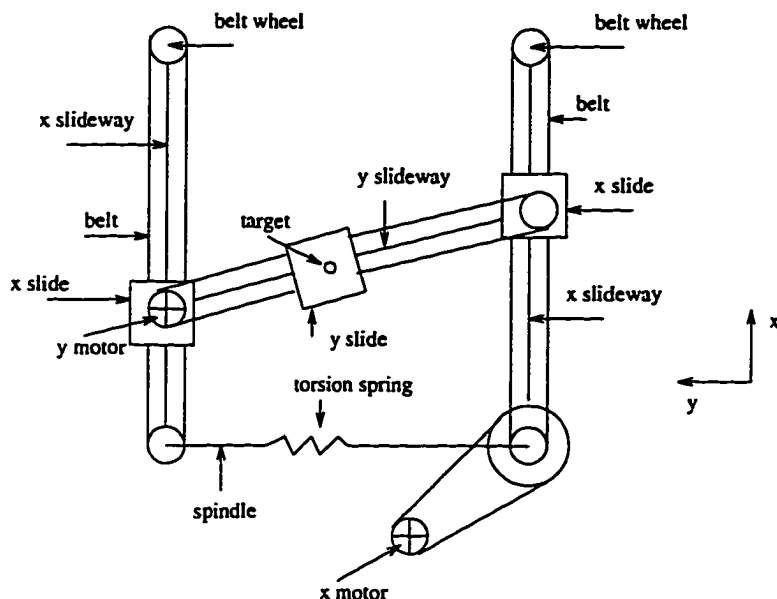


Figure 1.1 Schematic drawing of XY-table

and Durfee et al, 1992). As its name suggests, the Hummingbird system has a small, wing-link actuator structure. It uses more or less conventional mechanical elements, but employs light weight materials, novel configurations, and pays careful attention to details of balance to achieve both precision and high speed operation. A prototype system was demonstrated to have micron precision.

Minipositioner is useful in applications requiring fast incremental motion of very low-mass payloads over a planar workspace. One example of such an application is the electrical probing of high-density electronic components, where the payload is a very small probe and speed is important because of the large number of moves. Other applications are laser beam positioning (Neumann, 1992), semiconductor wafer positioning and disk-drive (L.W. Chang, 1991).

In the mini-positioning system, tendons (cables, ropes and chains) can be used for actuation. The resulting system is so called "tendon-driven" system, Figure 1.2. Teleoperation manipulator is such an example where tendons are used to actuate manipulator remotely (Jacobsen et al, 1989).

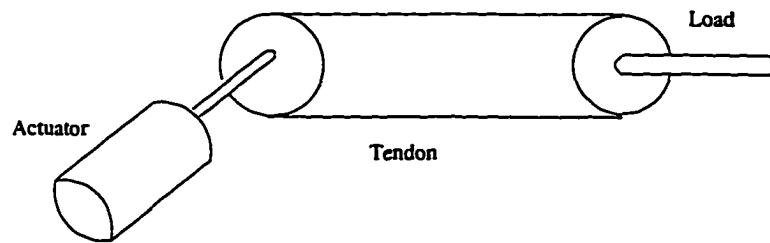


Figure 1.2 Model of a single-joint driven by one rotary actuator

The conventional method of precise multiple-axis motion control entails use of a multiple axis positioning system with each axis carrying not only the workpiece but also the positioning system of the remaining axes. The resultant structure is heavy and sluggish. An alternative positioning technique is being investigated in this dissertation in which the object to be positioned is pulled from remote points on a fixed external framework. The motion of the workpiece is controlled by pulling it with tendons, each of which has its own actuator. Since the actuators can be mounted on the base of the structure instead of being carried by motion system of the other axes, they can be relatively large and powerful without the need for a massive structure such as is found in a conventional motion control system. This method of control is given the appellation *agonistic*, based on the usages of the word suggesting tension or a contest.

The idea of positioning an object by pulling on it is not new, of course, since that is precisely the mechanism used for position control in biological control, since the muscles can effect motion only by pulling their loads. In biology, such control is called “antagonistic.” The latter term, however, suggests a spirit of belligerence, or working at cross purposes, rather than in the highly coordinated manner in which an agonistic control system would have to operate to achieve optimal accuracy.

Agonistic control is very similar to multiple manipulator system where a number of manipulators engage a cooperative task such as carrying a single object.

In the paper (Wendlandt and Sastry, 1994), a special manipulator is considered which is designed for minimally invasive surgery. It is a wrist-like manipulator and

provides the ability to point a tool at a desired location. With this system, surgeons are able to control the pointing direction of the tool by pulling the tendons.

The system developed by S. Kawamura (Kawamura, 1994, 1995) and his students is most similar to the agonistic control system investigated in this thesis. Kawamura called his system as the “radial wire drive system”. It can be used in teleoperation with a master-slave systems. The slave robot performs tasks while human operators use master robot system to control the slave robot. Virtual reality is an example of such application (Ishii and Sato, 1993).

In the radial wire drive systems, the ends of several wires are fixed at the handle and each wire is radially stretched. The other end of each wire is connected to a pulley which is driven by a D.C. servo motor. Since there is no other pulley or outer tube between the handle and the actuator, transmission loss of wire tension is very low.

The use of tendons creates challenges for the controller design. Contrary to the multi-finger system where fingers push an object, tendons can only be pulled in the tendon-driven system. Therefore the common requirement in the controller design of the tendon-driven system is to ensure that the tendons do not go slack.

1.2 Description of an Agonistic System

Agonistic control is a novel method of motion control. It provides X-Y positioning in the horizontal plane. The workpiece (a small object) is pulled by a multiplicity of tendons. Each tendon is controlled by its own actuator. While the workpiece moves, the tendons are required to be kept in tension.

Since the tendons must always be under tension, it is clear that motion in n dimensions requires a minimum of $n + 1$ tendons. But more than the minimum number of tendons can be used. The redundancy can be used to enlarge the size of the region in which the object can move. In particular, if the object is controlled

by tendons passing through a number of fixed passage points, the workpiece can be moved to any point within the convex hull of the set of passage points.

The mechanism of agonistic control is dynamically very similar to manipulators that have been developed in the past. It differs quite significantly and substantially, however, in the details of its dynamically balanced, symmetric actuator/tendon design.

A significant challenge to the control system designer is created by the requirement of careful coordination of the control signals to the actuators that pull the tendons. In particular, our concern is with a two-dimensional positioning system employing four tendons in a symmetric configuration as shown in Figure 1.3. The four actuators are mounted such that the tendons pass through the points A, B, C, and D. Obviously, the domain that the workpiece can reach is limited to the interior of the square ABCD.

Each actuator is a DC motor with an attached pulley, around which the corresponding tendon is wound. The tendons each pass through holes in the supporting structure. The control task is defined either as moving the workpiece from one point to another point and keeping it there (set point problem), or as tracking a prescribed trajectory (tracking problem).

One of the advantages of the agonistic system is high bandwidth. Unlike the conventional multiple axis positioning system (such as X-Y table), the motors in the agonistic system are not needed to move during the movement of the workpiece. So, the system is agile and the workpiece can quickly acquire and track the given trajectory. We know that the system bandwidth is inversely proportional to the response time (Friedland, 1986, page 167). Therefore, the agonistic system is expected to have high bandwidth.

The elastic effect of the tendon tends to reduce the bandwidth of the agonistic system since the elasticity of the tendons may induce oscillations and inhibit the

workpiece from quickly acquiring and following a given trajectory. By suppressing the oscillatory behavior through using composite control law, we expect the bandwidth of the rigid system can be maintained.

Given the development of two dimensional agonistic system, extension to the three dimensional agonistic system is straightforward since the dynamic equations characterizing the system behavior is very similar.

1.3 Control Methodology

The goal of the control system design is the development of a control law that generates the input voltages to the four motors in order to make the workpiece achieve and then follow a specified reference trajectory.

There are two control strategies: centralized vs. decentralized control.

1. Centralized control:

A single controller oversees and controls the operation of each motor in the system. The input torque to each motor is calculated centrally, using a single dynamic model that accounts for all the motor input torques. All the motors in the system are fully coupled and work cooperatively.

2. **Decentralized control:** Based on the desired location of the controlled object, a desired angular motion is calculated for each motor, and each motor is controlled individually so that the actual angular motion equals the desired one. Only the local information (angular position of each motor) is used. This local information is provided by the optical encoder mounted on each motor.

One way of designing the control for each channel is to assume that the tension in the tendon as an unknown constant in each channel. This assumption is of course contrary to fact, because the tension constantly changes with the movement of the workpiece. Moreover, the assumption that the tension in one channel is unrelated to the other is contrary to fact, since the tension in each channel must be coupled

to achieve dynamic balance. Nevertheless, a control law can be designed on the basis of this assumption which can give satisfactory performance. In particular, the assumption that the tension is an unknown constant to be estimated in each of the channels leads to a control law with integral control.

The decentralized control has the advantage of simplicity: if the dynamic interaction between the motors is neglected, for example, that the load torque on each motor is constant, each channel is dynamically independent of the others and hence can be designed as a single axis servo. The simplicity has another advantage, namely, that the controller for each channel can be implemented by one processor in a computer having a parallel-processing architecture, such as a transputer system.

But the decentralized scheme also has disadvantages:

1. The dynamic effect of the interaction of the tendons is not directly accounted for. It is simply viewed as a disturbance.

2. The working domain of the workpiece is smaller than the available area. If the trajectory extends too far from the center, the system may become unstable.

At the expense of much greater control law complexity, a centralized approach avoids these problems. The difficulty of performing the calculation for a centralized control law has its counterpart in implementation.

In the one dimensional (single axis) case, the dynamics of the agonistic system is linear. The centralized control is not very much more complex than the decentralized control. However, in the multi-axis case, the agonistic system is a highly nonlinear, multivariable system. The improved performance that a centralized control law would achieve would come only at the expense of requiring much more analysis at the design level. The control law design appropriate for a multivariable nonlinear system has to be selected from among the various methods currently available. Computed torque control can be used.

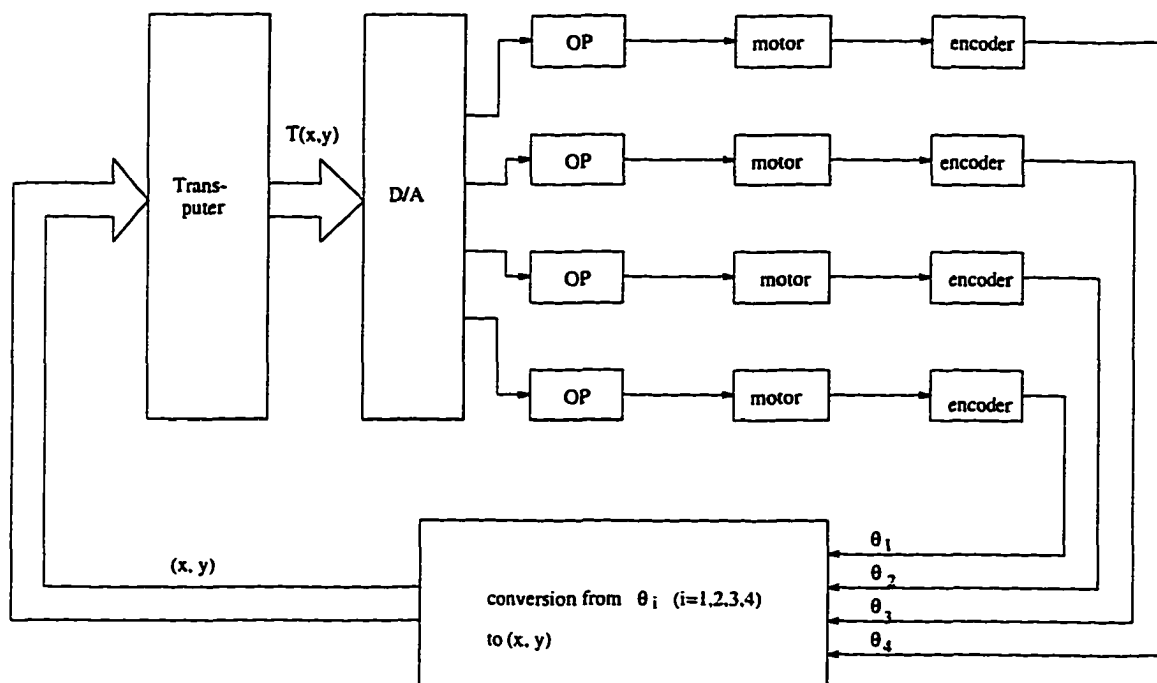


Figure 1.4 Centralized agonistic control. All of the complicated computations are accomplished on one computer

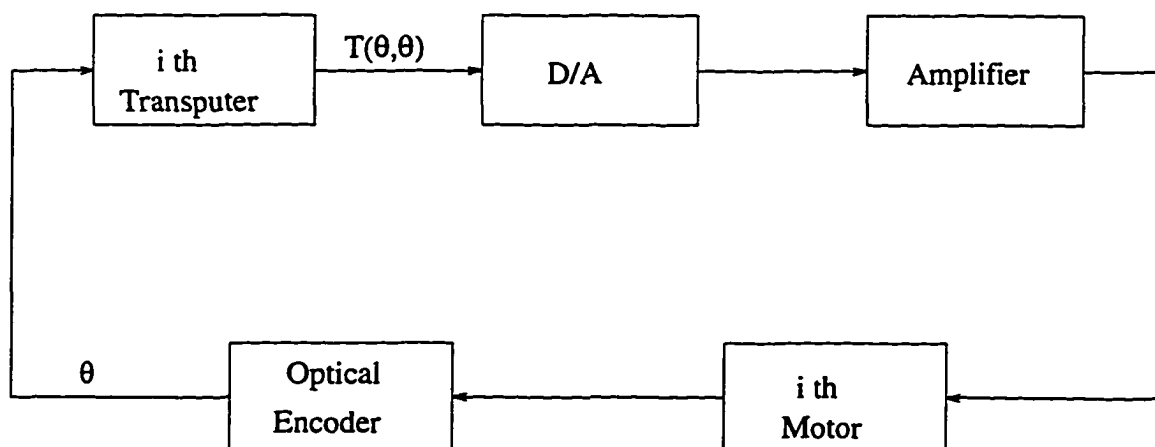


Figure 1.5 Decentralized agonistic control. Four transputers can be used. Each one accomplishes a simple computation. Each subsystem acts as a single axis system

In addition to the basic requirement on the controller to accomplish the control task such as a point-to-point move, or tracking a given trajectory, there are other requirements imposed on the controller:

- The control torques exerted on each motors must be nonnegative. This is required to keep the tendons in tension.
- The input voltage can not exceed its maximum value. In real actuators, there is a physical limitation on the input energy.

Under these requirements, the agonistic control becomes a nonlinear multi-variable control problem with constraints on control input. Let u be the control input, then u must satisfies: $0 \leq u \leq \bar{u}$ where \bar{u} is the maximum allowable value. A lot of work has been done on the energy constraints on the input. However, only a few have dealt with nonnegative control. The general case is not easy.

1.4 Contribution of this Dissertation

The agonistic control was conceived by Dr. Bernard Friedland. Under his supervision, this research has been conducted. The contributions are:

- Establishment of the dynamic model of agonistic system in the stiff case and design of the control law to satisfy the requirement of positive torque. (Technical paper presented in 1994 IEEE Regional Conference on Control Systems, Rutgers University, August 1994)
- Establishment of the dynamic model of agonistic system in the elastic case and using singular perturbation theory to design the control law to suppress the oscillation incurred by finite elasticity. (Technical paper was presented in 1996 Japan-USA Joint Symposium on Flexible Automation, Boston)
- Design of the observer of agonistic system in the elastic case and prove that the observer is linear and globally stable.

- Development of the decentralized control law and propose the “bias torque method” to guarantee the positiveness of the control torque. (Technical paper has been submitted to the 1997 American Control Conference).

1.5 Organization of this Dissertation

The dissertation is organized as follows:

In chapter 1, we give a review on the positioning devices and the description of the agonistic system.

In chapter 2, we present an in-depth investigation of the dynamic modelling of the agonistic system in both ideal and realistic cases. The dynamic equations describing its dynamic motion are established. In addition, the dynamic model for the decentralized control is also developed which is suitable for the decentralized control strategy.

In chapter 3, a control law is synthesized based on the dynamic model established in chapter 2. The controller is designed to address the specific requirements of agonistic control.

In chapter 4, an observer is designed to produce the velocity information which is required for the implementation of the control law.

In chapter 5, results of extensive simulation are reported. Actual scenarios such as friction and parameter variation are incorporated.

Finally, in the chapter 6, we summarize the results and draw some conclusions from above investigation.

CHAPTER 2

DERIVATION OF DYNAMIC MODEL

Notation

l_i :	length of i th tendon ($i=1,2,3,4$)
β_i :	angle between i th tendon and horizontal axis
f_i :	tension of the tendon i
r :	radius of the pulley
J_i :	inertia of the actuator
m :	mass of the workpiece

In the following, we will derive the various dynamic models of the agonistic system under different scenarios. The common ground is Lagrange's equation (Synge and Griffith, 1942):

$$\frac{d}{dt} \left(\frac{\partial L}{\partial \dot{q}} \right) - \frac{\partial L}{\partial q} = \tau \quad (2.1)$$

where q is the coordinate, \dot{q} is the corresponding velocity and τ is either a force or a torque, depending upon whether q is a linear or an angular coordinate.

The Lagrange equation will be utilized throughout this chapter. We will establish different energy functions corresponding to different cases, which leads to the different dynamic equations. Once the dynamic model is obtained, the remaining issue is to design the control law which is the central topic of the next chapter.

In our problem, the generalized coordinates are:

$$q = \left[x \quad y \quad \theta_1 \quad \theta_2 \quad \theta_3 \quad \theta_4 \right]'$$

(x, y) is the positions of the workpiece and θ_i ($i=1,2,3,4$) are the angular positions of the motors.

Each of the four actuators are controlled by individual torque. The vector of generalized force is

$$\tau = \left[0 \quad 0 \quad T_1 \quad T_2 \quad T_3 \quad T_4 \right]'$$

When the workpiece is in the point (x, y) , the length of each tendon is:

$$l_1^2 = (a + x)^2 + y^2 \quad (2.2)$$

$$l_2^2 = (a + y)^2 + x^2 \quad (2.3)$$

$$l_3^2 = (a - x)^2 + y^2 \quad (2.4)$$

$$l_4^2 = (a - y)^2 + x^2 \quad (2.5)$$

2.1 Stiff Case

Under the assumption that the tendons are stiff, the change in the length of the tendons correspond to the movement of the workpiece. So, we have the following holonomic constraints:

$$l_1 - l_1^0 = -r\theta_1$$

$$l_2 - l_2^0 = -r\theta_2$$

$$l_3 - l_3^0 = -r\theta_3$$

$$l_4 - l_4^0 = -r\theta_4$$

Or denoted as

$$\phi(q) = 0. \quad (2.6)$$

where q is the generalized coordinates.

l_i^0 is the initial length of the i th tendon. When the workpiece starts from the origin, $l_i^0 = a$.

The Lagrangian is defined as the difference between the kinetic energy and the potential energy of the system. In the stiff case, the potential energy is zero.

$$L = \frac{1}{2}m(\dot{x}^2 + \dot{y}^2) + \frac{1}{2}J_1\dot{\theta}_1^2 + \frac{1}{2}J_2\dot{\theta}_2^2 + \frac{1}{2}J_3\dot{\theta}_3^2 + \frac{1}{2}J_4\dot{\theta}_4^2$$

Define:

$$\bar{L} = L + \phi'(q)\lambda \quad (2.7)$$

where λ is the Lagrange multiplier.

$$\begin{aligned} \frac{\partial \bar{L}}{\partial q} &= \frac{\partial L}{\partial q} + \left(\frac{\partial \phi}{\partial q}\right)' \lambda, \\ \frac{\partial \bar{L}}{\partial \dot{q}} &= \frac{\partial L}{\partial \dot{q}} \end{aligned}$$

From the Lagrange equation, we obtain:

$$\frac{d}{dt} \left(\frac{\partial L}{\partial \dot{q}} \right) - \frac{\partial L}{\partial q} = \tau - \left(\frac{\partial \phi}{\partial q} \right)' f \quad (2.8)$$

where $f = -\lambda$. f corresponds to the constraint forces in the tendons. Its direction is away from the pulley.

Taking the time derivative on (2.6) results in:

$$\begin{aligned} \frac{\partial \phi}{\partial q} \dot{q} &= 0 \\ \frac{d}{dt} \left(\frac{\partial \phi}{\partial q} \right) \dot{q} + \frac{\partial \phi}{\partial q} \ddot{q} &= 0 \end{aligned} \quad (2.9)$$

let

$$\frac{\partial \phi}{\partial q} = \begin{bmatrix} E_A & E_B \end{bmatrix}, q = \begin{bmatrix} q_A \\ q_B \end{bmatrix}$$

From (2.9) we can obtain

$$\ddot{q}_B = -E_B^{-1} \left[\frac{d}{dt} \left(\frac{\partial \phi}{\partial q} \right) \dot{q} + E_A \ddot{q}_A \right] \quad (2.10)$$

denote

$$\frac{d}{dt}\left(\frac{\partial L}{\partial \dot{q}}\right) - \frac{\partial L}{\partial q} = \begin{bmatrix} D_1 \ddot{q}_A + B_1(q, \dot{q}) \\ D_2 \ddot{q}_B + B_2(q, \dot{q}) \end{bmatrix}$$

Substituting (2.10) into (2.8) gives:

$$\begin{bmatrix} D_1 \\ -D_2 E_B^{-1} E_A \end{bmatrix} \ddot{q}_A + \begin{bmatrix} B_1(q, \dot{q}) \\ B_2(q, \dot{q}) - D_2 E_B^{-1} \frac{d}{dt} \left(\frac{\partial \phi}{\partial \dot{q}} \right) \dot{q} \end{bmatrix} = \tau - \left(\frac{\partial \phi}{\partial q} \right)' f$$

The above equation can be written as

$$\begin{bmatrix} D_1 & \left(\frac{\partial \phi}{\partial q} \right)' \\ -D_2 E_B^{-1} E_A & \end{bmatrix} \begin{bmatrix} \ddot{q}_A \\ f \end{bmatrix} + \begin{bmatrix} B_1(q, \dot{q}) \\ B_2(q, \dot{q}) - D_2 E_B^{-1} \frac{d}{dt} \left(\frac{\partial \phi}{\partial \dot{q}} \right) \dot{q} \end{bmatrix} = \tau \quad (2.11)$$

In our problem,

$$q_A = \begin{bmatrix} x \\ y \end{bmatrix}, q_B = \begin{bmatrix} \theta_1 \\ \theta_2 \\ \theta_3 \\ \theta_4 \end{bmatrix},$$

$$D_1 = mI_2, D_2 = \text{diag}\{J_1, J_2, J_3, J_4\},$$

$$\frac{\partial \phi}{\partial q} = \begin{bmatrix} -\cos \beta_1 & \sin \beta_1 & r & 0 & 0 & 0 \\ -\cos \beta_2 & \sin \beta_2 & 0 & r & 0 & 0 \\ -\cos \beta_3 & \sin \beta_3 & 0 & 0 & r & 0 \\ -\cos \beta_4 & \sin \beta_4 & 0 & 0 & 0 & r \end{bmatrix} \quad B_1 = B_2 = 0$$

We see that

$$E_A = \begin{bmatrix} -\cos \beta_1 & \sin \beta_1 \\ -\cos \beta_2 & \sin \beta_2 \\ -\cos \beta_3 & \sin \beta_3 \\ -\cos \beta_4 & \sin \beta_4 \end{bmatrix}, E_B = rI_4, \quad (2.12)$$

where

$$\begin{aligned} \cos \beta_1 &= -\frac{a+x}{l_1} \\ \sin \beta_1 &= \frac{y}{l_1} \\ \cos \beta_2 &= -\frac{x}{l_2} \end{aligned}$$

$$\begin{aligned}\sin \beta_2 &= \frac{a+y}{l_2} \\ \cos \beta_3 &= \frac{a-x}{l_3} \\ \sin \beta_3 &= \frac{y}{l_3} \\ \cos \beta_4 &= -\frac{x}{l_4} \\ \sin \beta_4 &= -\frac{a-y}{l_4}\end{aligned}$$

Since

$$\begin{aligned}\frac{\partial \beta_i}{\partial x} &= \frac{\sin \beta_i}{l_i}, \\ \frac{\partial \beta_i}{\partial y} &= \frac{\cos \beta_i}{l_i}\end{aligned}$$

and

$$\begin{aligned}\frac{d(-\cos \beta_i)}{dt} &= \frac{\sin \beta_i}{l_i}(\dot{x} \sin \beta_i + \dot{y} \cos \beta_i), \\ \frac{d(\sin \beta_i)}{dt} &= \frac{\cos \beta_i}{l_i}(\dot{x} \sin \beta_i + \dot{y} \cos \beta_i)\end{aligned}$$

We have

$$\frac{d}{dt} \left(\frac{\partial \phi}{\partial \dot{q}} \right) = \begin{bmatrix} \frac{\sin \beta_1}{l_1}(\dot{x} \sin \beta_1 + \dot{y} \cos \beta_1) & \frac{\cos \beta_1}{l_1}(\dot{x} \sin \beta_1 + \dot{y} \cos \beta_1) & 0 & 0 & 0 & 0 \\ \frac{\sin \beta_2}{l_2}(\dot{x} \sin \beta_2 + \dot{y} \cos \beta_2) & \frac{\cos \beta_2}{l_2}(\dot{x} \sin \beta_2 + \dot{y} \cos \beta_2) & 0 & 0 & 0 & 0 \\ \frac{\sin \beta_3}{l_3}(\dot{x} \sin \beta_3 + \dot{y} \cos \beta_3) & \frac{\cos \beta_3}{l_3}(\dot{x} \sin \beta_3 + \dot{y} \cos \beta_3) & 0 & 0 & 0 & 0 \\ \frac{\sin \beta_4}{l_4}(\dot{x} \sin \beta_4 + \dot{y} \cos \beta_4) & \frac{\cos \beta_4}{l_4}(\dot{x} \sin \beta_4 + \dot{y} \cos \beta_4) & 0 & 0 & 0 & 0 \end{bmatrix}$$

Denote:

$$\begin{aligned}\Omega &= \begin{bmatrix} D_1 & & & & & \\ -D_2 E_B^{-1} E_A & \left(\frac{\partial \phi}{\partial \dot{q}} \right)' & & & & \end{bmatrix} \\ &= \begin{bmatrix} mr & 0 & -\cos \beta_1 & -\cos \beta_2 & -\cos \beta_3 & -\cos \beta_4 \\ 0 & mr & \sin \beta_1 & \sin \beta_2 & \sin \beta_3 & \sin \beta_4 \\ J_1 \cos \beta_1 & -J_1 \sin \beta_1 & r & 0 & 0 & 0 \\ J_2 \cos \beta_2 & -J_2 \sin \beta_2 & 0 & r & 0 & 0 \\ J_3 \cos \beta_3 & -J_3 \sin \beta_3 & 0 & 0 & r & 0 \\ J_4 \cos \beta_4 & -J_4 \sin \beta_4 & 0 & 0 & 0 & r \end{bmatrix}\end{aligned}$$

We want to take the inverse of the matrix Ω to decouple the \bar{q}_A and f .

Partitioning the matrix Ω as:

$$\Omega = \begin{bmatrix} \bar{A} & \bar{B} \\ \bar{C} & \bar{D} \end{bmatrix}$$

where

$$\bar{A} = \begin{bmatrix} mr & 0 \\ 0 & mr \end{bmatrix}, \bar{B} = \begin{bmatrix} -\cos \beta_1 & -\cos \beta_2 & -\cos \beta_3 & -\cos \beta_4 \\ \sin \beta_1 & \sin \beta_2 & \sin \beta_3 & \sin \beta_4 \end{bmatrix},$$

$$\bar{C} = \begin{bmatrix} J_1 \cos \beta_1 & -J_1 \sin \beta_1 \\ J_2 \cos \beta_2 & -J_2 \sin \beta_2 \\ J_3 \cos \beta_3 & -J_3 \sin \beta_3 \\ J_4 \cos \beta_4 & -J_4 \sin \beta_4 \end{bmatrix}, \bar{D} = \begin{bmatrix} r & 0 & 0 & 0 \\ 0 & r & 0 & 0 \\ 0 & 0 & r & 0 \\ 0 & 0 & 0 & r \end{bmatrix}$$

Using the matrix identity:

$$\begin{bmatrix} \bar{A} & \bar{B} \\ \bar{C} & \bar{D} \end{bmatrix} = \begin{bmatrix} I & \bar{B} \\ 0 & \bar{D} \end{bmatrix} \begin{bmatrix} \bar{A} - \bar{B}\bar{D}^{-1}\bar{C} & 0 \\ \bar{D}^{-1}\bar{C} & I \end{bmatrix}$$

where I is identity matrix.

We know that

$$\begin{bmatrix} I & \bar{B} \\ 0 & \bar{D} \end{bmatrix}^{-1} = \begin{bmatrix} I & -\bar{B}\bar{D}^{-1} \\ 0 & \bar{D}^{-1} \end{bmatrix}$$

$$\begin{bmatrix} \bar{A} - \bar{B}\bar{D}^{-1}\bar{C} & 0 \\ \bar{D}^{-1}\bar{C} & I \end{bmatrix}^{-1} = \begin{bmatrix} (\bar{A} - \bar{B}\bar{D}^{-1}\bar{C})^{-1} & 0 \\ -\bar{D}^{-1}\bar{C}(\bar{A} - \bar{B}\bar{D}^{-1}\bar{C})^{-1} & I \end{bmatrix}$$

Now,

$$\bar{A} - \bar{B}\bar{D}^{-1}\bar{C} = \frac{1}{r}M$$

where

$$M = \begin{bmatrix} m_{11} & m_{12} \\ m_{21} & m_{22} \end{bmatrix}$$

$$m_{11} = mr^2 + \sum_{i=1}^4 J_i \cos^2 \beta_i$$

$$m_{22} = mr^2 + \sum_{i=1}^4 J_i \sin^2 \beta_i$$

$$m_{12} = -\sum_{i=1}^4 J_i \cos \beta_i \sin \beta_i$$

$$m_{21} = m_{12}$$

We have

$$\Omega^{-1} = \begin{bmatrix} \bar{A} & \bar{B} \\ \bar{C} & \bar{D} \end{bmatrix}^{-1} = \begin{bmatrix} rM^{-1} & 0 \\ -\bar{C}M^{-1} & I \end{bmatrix} \begin{bmatrix} I & -\frac{1}{r}\bar{B} \\ 0 & \frac{1}{r}I \end{bmatrix}$$

Finally, we obtain

$$\Omega^{-1} = \begin{bmatrix} rM^{-1} & -M^{-1}\bar{B} \\ -\bar{C}M^{-1} & \frac{1}{r}(\bar{C}M^{-1}\bar{B} + I) \end{bmatrix}$$

Multiply the (2.11) on both sides by Ω^{-1} , we obtain:

$$\begin{bmatrix} m_{11} & m_{12} \\ m_{21} & m_{22} \end{bmatrix} \begin{bmatrix} \ddot{x} \\ \ddot{y} \end{bmatrix} + \begin{bmatrix} m_{13} \\ m_{23} \end{bmatrix} = \begin{bmatrix} r(\sum_{i=1}^4 T_i \cos \beta_i) \\ -r(\sum_{i=1}^4 T_i \sin \beta_i) \end{bmatrix} \quad (2.13)$$

where

$$m_{13} = -\sum_{i=1}^4 \frac{J_i}{l_i} \cos \beta_i (\dot{x} \sin \beta_i + \dot{y} \cos \beta_i)^2$$

$$m_{23} = -\sum_{i=1}^4 \frac{J_i}{l_i} \sin \beta_i (\dot{x} \sin \beta_i + \dot{y} \cos \beta_i)^2$$

and

$$\begin{bmatrix} f_{1r} \\ f_{2r} \\ f_{3r} \\ f_{4r} \end{bmatrix} = (I - CM^{-1}B(q)) \begin{bmatrix} T_1 + \frac{J_1}{rl_1} (\dot{x} \sin \beta_1 + \dot{y} \cos \beta_1)^2 \\ T_2 + \frac{J_2}{rl_2} (\dot{x} \sin \beta_2 + \dot{y} \cos \beta_2)^2 \\ T_3 + \frac{J_3}{rl_3} (\dot{x} \sin \beta_3 + \dot{y} \cos \beta_3)^2 \\ T_4 + \frac{J_4}{rl_4} (\dot{x} \sin \beta_4 + \dot{y} \cos \beta_4)^2 \end{bmatrix} \quad (2.14)$$

where

$$B(q) = -\bar{B} = \begin{bmatrix} \cos \beta_1 & \cos \beta_2 & \cos \beta_3 & \cos \beta_4 \\ -\sin \beta_1 & -\sin \beta_2 & -\sin \beta_3 & -\sin \beta_4 \end{bmatrix},$$

$$C = \bar{C} = \begin{bmatrix} J_1 \cos \beta_1 & -J_1 \sin \beta_1 \\ J_2 \cos \beta_2 & -J_2 \sin \beta_2 \\ J_3 \cos \beta_3 & -J_3 \sin \beta_3 \\ J_4 \cos \beta_4 & -J_4 \sin \beta_4 \end{bmatrix}$$

Denote $q = \begin{bmatrix} x \\ y \end{bmatrix}$, $\dot{q} = \begin{bmatrix} \dot{x} \\ \dot{y} \end{bmatrix}$, $\begin{bmatrix} m_{13} \\ m_{23} \end{bmatrix}$ can be written as the form $C(q, \dot{q})\dot{q}$:

$$C(q, \dot{q}) = \begin{bmatrix} -\sum_{i=1}^4 \frac{J_i}{l_i} \sin \beta_i \cos \beta_i (\dot{x} \sin \beta_i + \dot{y} \cos \beta_i) & -\sum_{i=1}^4 \frac{J_i}{l_i} \cos^2 \beta_i (\dot{x} \sin \beta_i + \dot{y} \cos \beta_i) \\ \sum_{i=1}^4 \frac{J_i}{l_i} \sin^2 \beta_i (\dot{x} \sin \beta_i + \dot{y} \cos \beta_i) & \sum_{i=1}^4 \frac{J_i}{l_i} \sin \beta_i \cos \beta_i (\dot{x} \sin \beta_i + \dot{y} \cos \beta_i) \end{bmatrix} \quad (2.15)$$

Then, the dynamic equation of the system can be written as

$$M(q)\ddot{q} + C(q, \dot{q})\dot{q} = rB(q)T \quad (2.16)$$

2.2 Elastic Case

In last section, we assume that there is no extension of the tendons. This is an ideal situation. In reality, the tendon will exhibit some elasticity. The requirements of high precision and high speed on the agonistic control calls for the accurate modelling of elastic effect. Based on this modelling in which the elasticity of the tendon is considered, the control law should be designed to compensate the elastic effect.

In the elastic case, due to the elasticity of the tendon, there is no one-to-one correspondence between the position of the workpiece and the angular position of the pulleys.

The extension of each tendon is given by:

$$\Delta l_1 = l_1 - (l_1^0 - r\theta_1)$$

$$\Delta l_2 = l_2 - (l_2^0 - r\theta_2)$$

$$\Delta l_3 = l_3 - (l_3^0 - r\theta_3)$$

$$\Delta l_4 = l_4 - (l_4^0 - r\theta_4)$$

where $l_i^0 (i = 1, 2, 3, 4)$ is the initial length of i th tendon, r_i is the radius of the pulley, θ_i is the angular position of i th pulley.

The Lagrangian for this problem is:

$$\begin{aligned} L = & \frac{1}{2}m(\dot{x}^2 + \dot{y}^2) + \frac{1}{2}J_1\dot{\theta}_1^2 + \frac{1}{2}J_2\dot{\theta}_2^2 + \frac{1}{2}J_3\dot{\theta}_3^2 + \frac{1}{2}J_4\dot{\theta}_4^2 \\ & - \frac{1}{2}k(l_1 - l_1^0 + r\theta_1)^2 - \frac{1}{2}k(l_2 - l_2^0 + r\theta_2)^2 \\ & - \frac{1}{2}k(l_3 - l_3^0 + r\theta_3)^2 - \frac{1}{2}k(l_4 - l_4^0 + r\theta_4)^2 \end{aligned}$$

where k is the elastic modulus of the tendon, m is the mass of the workpiece, J_i is the inertia of the actuator.

From (2.2) to (2.5),

$$\begin{aligned} \dot{l}_i &= \dot{y} \sin \beta_i - \dot{x} \cos \beta_i \\ \ddot{l}_i &= \ddot{y} \sin \beta_i - \ddot{x} \cos \beta_i + \frac{(\dot{x} \sin \beta_i + \dot{y} \cos \beta_i)^2}{l_i} \end{aligned}$$

where β_i is the angle between the i th tendon and horizontal axis.

From Lagrange's equation, we obtain

$$J_1 \ddot{\theta}_1 + kr(l_1 - l_1^0 + r\theta_1) = T_1 \quad (2.17)$$

$$J_2 \ddot{\theta}_2 + kr(l_2 - l_2^0 + r\theta_2) = T_2 \quad (2.18)$$

$$J_3 \ddot{\theta}_3 + kr(l_3 - l_3^0 + r\theta_3) = T_3 \quad (2.19)$$

$$J_4 \ddot{\theta}_4 + kr(l_4 - l_4^0 + r\theta_4) = T_4 \quad (2.20)$$

and

$$\begin{aligned} m\ddot{x} = & (l_1 - l_1^0 + r\theta_1)k \cos \beta_1 + (l_2 - l_2^0 + r\theta_2)k \cos \beta_2 \\ & + (l_3 - l_3^0 + r\theta_3)k \cos \beta_3 + (l_4 - l_4^0 + r\theta_4)k \cos \beta_4 \end{aligned} \quad (2.21)$$

$$\begin{aligned} m\ddot{y} = & -(l_1 - l_1^0 + r\theta_1)k \sin \beta_1 - (l_2 - l_2^0 + r\theta_2)k \sin \beta_2 \\ & - (l_3 - l_3^0 + r\theta_3)k \sin \beta_3 - (l_4 - l_4^0 + r\theta_4)k \sin \beta_4 \end{aligned} \quad (2.22)$$

Define

$$z_1 = (l_1 - l_1^0 + r\theta_1)k \quad (2.23)$$

$$z_2 = (l_2 - l_2^0 + r\theta_2)k \quad (2.24)$$

$$z_3 = (l_3 - l_3^0 + r\theta_3)k \quad (2.25)$$

$$z_4 = (l_4 - l_4^0 + r\theta_4)k \quad (2.26)$$

$$\varepsilon^2 = \frac{1}{k} \quad (2.27)$$

Then, (2.21) and (2.22) become

$$\begin{aligned} m\ddot{x} = & z_1 \cos \beta_1 + z_2 \cos \beta_2 \\ & + z_3 \cos \beta_3 + z_4 \cos \beta_4 \end{aligned} \quad (2.28)$$

$$\begin{aligned} m\ddot{y} = & -(z_1 \sin \beta_1 + z_2 \sin \beta_2 \\ & + z_3 \sin \beta_3 + z_4 \sin \beta_4) \end{aligned} \quad (2.29)$$

From (2.23) and (2.27),

$$\begin{aligned}
 \dot{z}_1 &= (\dot{l}_1 + r\dot{\theta}_1)k \\
 \varepsilon^2 \ddot{z}_1 &= \ddot{l}_1 + r\ddot{\theta}_1 \\
 &= \ddot{y} \sin \beta_1 - \ddot{x} \cos \beta_1 + \frac{(\dot{x} \sin \beta_1 + \dot{y} \cos \beta_1)^2}{l_1} + r\ddot{\theta}_1
 \end{aligned} \tag{2.30}$$

But from (2.17),

$$\ddot{\theta}_1 = \frac{T_1 - kr(l_1 - l_1^0 + r\theta_1)}{J_1} = \frac{T_1 - rz_1}{J_1} \tag{2.31}$$

Substituting (2.31) into (2.30) yields

$$\begin{aligned}
 \varepsilon^2 \ddot{z}_1 &= \ddot{y} \sin \beta_1 - \ddot{x} \cos \beta_1 \\
 &\quad + \frac{(\dot{x} \sin \beta_1 + \dot{y} \cos \beta_1)^2}{l_1} + \frac{r(T_1 - rz_1)}{J_1}
 \end{aligned} \tag{2.32}$$

As $\varepsilon = 0$, the elastic case reduces to the stiff case, and the tension in the tendon becomes the constraint force. In this case

$$\begin{aligned}
 \bar{z}_1 &= \frac{T_1}{r} + \frac{J_1}{r^2}(\ddot{y} \sin \beta_1 - \ddot{x} \cos \beta_1) \\
 &\quad + \frac{J_1}{r^2 l_1}(\dot{x} \sin \beta_1 + \dot{y} \cos \beta_1)^2
 \end{aligned} \tag{2.33}$$

Similarly, for the other tendons, we have:

$$\begin{aligned}
 \varepsilon^2 \ddot{z}_2 &= \ddot{y} \sin \beta_2 - \ddot{x} \cos \beta_2 + \\
 &\quad \frac{(\dot{x} \sin \beta_2 + \dot{y} \cos \beta_2)^2}{l_2} + \frac{r(T_2 - rz_2)}{J_2}
 \end{aligned} \tag{2.34}$$

$$\begin{aligned}
 \varepsilon^2 \ddot{z}_3 &= \ddot{y} \sin \beta_3 - \ddot{x} \cos \beta_3 + \\
 &\quad \frac{(\dot{x} \sin \beta_3 + \dot{y} \cos \beta_3)^2}{l_3} + \frac{r(T_3 - rz_3)}{J_3}
 \end{aligned} \tag{2.35}$$

$$\begin{aligned}
 \varepsilon^2 \ddot{z}_4 &= \ddot{y} \sin \beta_4 - \ddot{x} \cos \beta_4 + \\
 &\quad \frac{(\dot{x} \sin \beta_4 + \dot{y} \cos \beta_4)^2}{l_4} + \frac{r(T_4 - rz_4)}{J_4}
 \end{aligned} \tag{2.36}$$

and

$$\bar{z}_2 = \frac{T_2}{r} + \frac{J_2}{r^2}(\bar{y} \sin \beta_2 - \bar{x} \cos \beta_2) + \frac{J_2}{r^2 l_2}(\dot{x} \sin \beta_2 + \dot{y} \cos \beta_2)^2 \quad (2.37)$$

$$\bar{z}_3 = \frac{T_3}{r} + \frac{J_3}{r^2}(\bar{y} \sin \beta_3 - \bar{x} \cos \beta_3) + \frac{J_3}{r^2 l_3}(\dot{x} \sin \beta_3 + \dot{y} \cos \beta_3)^2 \quad (2.38)$$

$$\bar{z}_4 = \frac{T_4}{r} + \frac{J_4}{r^2}(\bar{y} \sin \beta_4 - \bar{x} \cos \beta_4) + \frac{J_4}{r^2 l_4}(\dot{x} \sin \beta_4 + \dot{y} \cos \beta_4)^2 \quad (2.39)$$

Substituting (2.33) and (2.37)-(2.39) into (2.28)-(2.29) yields

$$\begin{bmatrix} m_{11} & m_{12} \\ m_{21} & m_{22} \end{bmatrix} \begin{bmatrix} \bar{x} \\ \bar{y} \end{bmatrix} + \begin{bmatrix} m_{13} \\ m_{23} \end{bmatrix} = \begin{bmatrix} r(\sum_{i=1}^4 T_i \cos \beta_i) \\ -r(\sum_{i=1}^4 T_i \sin \beta_i) \end{bmatrix} \quad (2.40)$$

where

$$\begin{aligned} m_{11} &= mr^2 + \sum_{i=1}^4 J_i \cos^2 \beta_i \\ m_{22} &= mr^2 + \sum_{i=1}^4 J_i \sin^2 \beta_i \\ m_{12} &= -\sum_{i=1}^4 J_i \sin \beta_i \cos \beta_i \\ m_{21} &= m_{12} \\ m_{13} &= -\sum_{i=1}^4 \frac{J_i}{l_i} \cos \beta_i (\dot{x} \sin \beta_i + \dot{y} \cos \beta_i)^2 \\ m_{23} &= \sum_{i=1}^4 \frac{J_i}{l_i} \sin \beta_i (\dot{x} \sin \beta_i + \dot{y} \cos \beta_i)^2 \end{aligned}$$

These equations are exactly the equations of the stiff case.

Substituting (2.28), (2.29) into (2.32) and (2.34)-(2.36) yields

$$\epsilon^2 \begin{bmatrix} \bar{z}_1 \\ \bar{z}_2 \\ \bar{z}_3 \\ \bar{z}_4 \end{bmatrix} = -\frac{1}{m} \begin{bmatrix} d_1 & c_{12} & c_{13} & c_{14} \\ c_{12} & d_2 & c_{23} & c_{24} \\ c_{13} & c_{23} & d_3 & c_{34} \\ c_{14} & c_{24} & c_{34} & d_4 \end{bmatrix} \begin{bmatrix} z_1 \\ z_2 \\ z_3 \\ z_4 \end{bmatrix}$$

$$+ \begin{bmatrix} \frac{(\dot{x} \sin \beta_1 + \dot{y} \cos \beta_1)^2}{l_1} \\ \frac{(\dot{x} \sin \beta_2 + \dot{y} \cos \beta_2)^2}{l_2} \\ \frac{(\dot{x} \sin \beta_3 + \dot{y} \cos \beta_3)^2}{l_3} \\ \frac{(\dot{x} \sin \beta_4 + \dot{y} \cos \beta_4)^2}{l_4} \end{bmatrix} + \begin{bmatrix} \frac{r}{J_1} T_1 \\ \frac{r}{J_2} T_2 \\ \frac{r}{J_3} T_3 \\ \frac{r}{J_4} T_4 \end{bmatrix} \quad (2.41)$$

where $d_i = 1 + \frac{mr^2}{J_i}$, $c_{ij} = \cos(\beta_i - \beta_j)$.

In compact form, (2.28), (2.29) and (2.41) can be written as:

$$m\ddot{q} = B(q)z \quad (2.42)$$

$$\varepsilon^2 \ddot{z} = -A(q)z + E(q, \dot{q})\dot{q} + Du \quad (2.43)$$

where

$$q = \begin{bmatrix} x \\ y \end{bmatrix}, z = \begin{bmatrix} z_1 \\ z_2 \\ z_3 \\ z_4 \end{bmatrix}, u = \begin{bmatrix} T_1 \\ T_2 \\ T_3 \\ T_4 \end{bmatrix},$$

$$A(q) = \frac{1}{m} \begin{bmatrix} d_1 & c_{12} & c_{13} & c_{14} \\ c_{12} & d_2 & c_{23} & c_{24} \\ c_{13} & c_{23} & d_3 & c_{34} \\ c_{14} & c_{24} & c_{34} & d_4 \end{bmatrix},$$

$$B(q) = \begin{bmatrix} \cos \beta_1 & \cos \beta_2 & \cos \beta_3 & \cos \beta_4 \\ -\sin \beta_1 & -\sin \beta_2 & -\sin \beta_3 & -\sin \beta_4 \end{bmatrix},$$

$$\delta_i = \dot{x} \sin \beta_i + \dot{y} \cos \beta_i$$

$$E(q, \dot{q}) = \begin{bmatrix} \frac{\delta_1}{l_1} \sin \beta_1 & \frac{\delta_1}{l_1} \cos \beta_1 \\ \frac{\delta_2}{l_2} \sin \beta_2 & \frac{\delta_2}{l_2} \cos \beta_2 \\ \frac{\delta_3}{l_3} \sin \beta_3 & \frac{\delta_3}{l_3} \cos \beta_3 \\ \frac{\delta_4}{l_4} \sin \beta_4 & \frac{\delta_4}{l_4} \cos \beta_4 \end{bmatrix},$$

$$D = \text{diag}\left\{\frac{r}{J_1}, \frac{r}{J_2}, \frac{r}{J_3}, \frac{r}{J_4}\right\}$$

These equations are similar to the equations obtained in (Spong, 1987), (Marino and Nicosia, 1985). The system of equations (2.42) and (2.43) is singularly perturbed. The position vector q and its derivatives are slow variables. The tension vector z and its derivatives are fast variables.

2.3 Dynamic Model for Decentralized Control

The centralized control law is based on the workpiece coordinates x and y . Decentralized control law should be based on the individual coordinate of each motor.

In this section, we establish the dynamic model of the whole system using the coordinates $\theta_1 \sim \theta_4$ which describes the true dynamic behavior of the system.

Since in agonistic control, the workpiece is pulled to move by multiple tendons, the basic requirement is that each tendon in the system must always be under tension. This implies the control torque exerted on each motor must be positive all the time.

$$q = \begin{bmatrix} q_A \\ q_B \end{bmatrix}, q_A = \begin{bmatrix} x \\ y \end{bmatrix}, q_B = \begin{bmatrix} \theta_1 \\ \theta_2 \\ \theta_3 \\ \theta_4 \end{bmatrix} \quad (2.44)$$

and l_i^0 is the initial length of the tendon i .

When the workpiece starts from the origin, $l_i^0 = a$.

Now, we derive the actual dynamic model of the system based on the coordinates θ_1 to θ_4 . The dynamic model is obtained with the aid of Lagrange's equations:

$$\frac{d}{dt} \left(\frac{\partial L}{\partial \dot{q}} \right) - \frac{\partial L}{\partial q} = \tau - \left(\frac{\partial \phi}{\partial q} \right)' f \quad (2.45)$$

where f corresponds to the constraint forces in the tendons. Its direction is away from the pulley.

In this application, the Lagrangian is

$$L = \frac{1}{2}m(\dot{x}^2 + \dot{y}^2) + \frac{1}{2}J_1\dot{\theta}_1^2 + \frac{1}{2}J_2\dot{\theta}_2^2 + \frac{1}{2}J_3\dot{\theta}_3^2 + \frac{1}{2}J_4\dot{\theta}_4^2 \quad (2.46)$$

$$\begin{aligned} \tau &= [0 \ 0 \ T_1 \ T_2 \ T_3 \ T_4]', \\ \frac{\partial L}{\partial q} &= 0, \\ \frac{\partial L}{\partial \dot{q}} &= [m\dot{x} \ m\dot{y} \ J_1\dot{\theta}_1 \ J_2\dot{\theta}_2 \ J_3\dot{\theta}_3 \ J_4\dot{\theta}_4]' \end{aligned}$$

From (2.6),

$$\begin{aligned} \frac{\partial \phi}{\partial q} &= \begin{bmatrix} -\cos \beta_1 & \sin \beta_1 & r & 0 & 0 & 0 \\ -\cos \beta_2 & \sin \beta_2 & 0 & r & 0 & 0 \\ -\cos \beta_3 & \sin \beta_3 & 0 & 0 & r & 0 \\ -\cos \beta_4 & \sin \beta_4 & 0 & 0 & 0 & r \end{bmatrix} \\ &= \begin{bmatrix} -B' & rI_4 \end{bmatrix} \end{aligned} \quad (2.47)$$

(2.9) becomes:

$$B' \ddot{q}_A = r \ddot{q}_B + \frac{d}{dt} \left(\frac{\partial \phi}{\partial q} \right) \dot{q} \quad (2.48)$$

Reduction of dimensionality: Under the holonomic constraint (2.6), the dimension of the system is reduced. We can take advantage of this constraint and remove the constraint force from the equation (2.45). The method is based on (Hemami and Weimer, 1981).

Define

$$\begin{aligned} D &= \begin{bmatrix} rc_1 & -rs_1 & 1 & c_{12} & c_{13} & c_{14} \\ rc_2 & -rs_2 & c_{12} & 1 & c_{23} & c_{24} \\ rc_3 & -rs_3 & c_{13} & c_{23} & 1 & c_{34} \\ rc_4 & -rs_4 & c_{14} & c_{24} & c_{34} & 1 \end{bmatrix} \\ &= \begin{bmatrix} D_1 & D_2 \end{bmatrix} \end{aligned}$$

where $c_i = \cos \beta_i$, $s_i = \sin \beta_i$, $c_{ij} = \cos(\beta_i - \beta_j)$, $s_{ij} = \sin(\beta_i - \beta_j)$ and $D_1 = rB'$, $D_2 = B'B$.

The construction of D is intended to satisfy

$$D \left(\frac{\partial \phi}{\partial q} \right)' = 0$$

If the both sides of the the equation (2.45) are premultiplied by the matrix D , the constraint force can be eliminated. We obtain

$$D_1 \begin{bmatrix} m\ddot{x} \\ m\ddot{y} \end{bmatrix} + D_2 \begin{bmatrix} J_1 \ddot{\theta}_1 \\ J_2 \ddot{\theta}_2 \\ J_3 \ddot{\theta}_3 \\ J_4 \ddot{\theta}_4 \end{bmatrix} = D_2 \begin{bmatrix} T_1 \\ T_2 \\ T_3 \\ T_4 \end{bmatrix}$$

i.e.

$$mrB' \ddot{q}_A + B'B J \ddot{q}_B = (B'B)T \quad (2.49)$$

where

$$J = \begin{bmatrix} J_1 & & & \\ & J_2 & & \\ & & J_3 & \\ & & & J_4 \end{bmatrix}, T = \begin{bmatrix} T_1 \\ T_2 \\ T_3 \\ T_4 \end{bmatrix}$$

Substituting (2.48) into (2.49), finally we obtain:

$$[mr^2 I_4 + B'BJ]\ddot{q}_B + mr \frac{d}{dt} \left(\frac{\partial \phi}{\partial \dot{q}} \right) \dot{q} = (B'B)T \quad (2.50)$$

where

$$\frac{d}{dt} \left(\frac{\partial \phi}{\partial \dot{q}} \right) \dot{q} = \begin{bmatrix} \frac{1}{l_1} (\dot{x} \sin \beta_1 + \dot{y} \cos \beta_1)^2 \\ \frac{1}{l_2} (\dot{x} \sin \beta_2 + \dot{y} \cos \beta_2)^2 \\ \frac{1}{l_3} (\dot{x} \sin \beta_3 + \dot{y} \cos \beta_3)^2 \\ \frac{1}{l_4} (\dot{x} \sin \beta_4 + \dot{y} \cos \beta_4)^2 \end{bmatrix}$$

The \dot{x} and \dot{y} in the above expression are related to $\theta_1 \sim \theta_4$ through the following equalities:

$$\begin{aligned} \dot{x} &= \frac{l_1 \dot{l}_1 - l_3 \dot{l}_3}{2a} \\ \dot{y} &= \frac{l_2 \dot{l}_2 - l_4 \dot{l}_4}{2a} \end{aligned}$$

while $\dot{l}_i = -r\dot{\theta}_i$.

(2.50) is the actual dynamic model of the system represented in the coordinates $\theta_1 \dots \theta_4$.

The tensions in each tendon can be computed from (2.14).

CHAPTER 3

CONTROL LAW DESIGN

In this chapter, we will design the control law to accomplish the control task as well as meet other requirements imposed on the control input such as positiveness and actuator saturation. First, we use centralized control strategy. In this scenario, computed-torque method and passivity-based method are investigated.

Based on the investigation of control law design in the stiff case, the control law design in the elastic case will be dealt with. The stiff-based control law will be incorporated into the control law for elastic case.

Finally, we explore the decentralized control strategy and try to use simple linear control law to replace the complicated nonlinear control law.

3.1 Centralized Control Strategy

3.1.1 Stiff Case

The dynamic equation of the system can be written as

$$M(q)\ddot{q} + C(q, \dot{q})\dot{q} = rB(q)T = \tau \quad (3.1)$$

Although the system (3.1) is complex, it has several fundamental properties which can be exploited to facilitate the control law design.

Property 1: The inertia matrix $M(q)$ is symmetric, positive definite.

Property 2: $\frac{1}{2}\dot{M}(q) - C(q, \dot{q})$ is skew-symmetric. It satisfies

$$x^T \left(\frac{1}{2}\dot{M} - C \right) x = 0,$$

$$\dot{m}_{11} = -2 \sum_{i=1}^4 \frac{J_i}{l_i} \sin \beta_i \cos \beta_i (\dot{x} \sin \beta_i + \dot{y} \cos \beta_i),$$

$$\dot{m}_{22} = 2 \sum_{i=1}^4 \frac{J_i}{l_i} \sin \beta_i \cos \beta_i (\dot{x} \sin \beta_i + \dot{y} \cos \beta_i),$$

$$\dot{m}_{12} = \dot{m}_{21} = \sum_{i=1}^4 \frac{J_i}{l_i} (\sin^2 \beta_i - \cos^2 \beta_i) (\dot{x} \sin \beta_i + \dot{y} \cos \beta_i)$$

So,

$$\frac{1}{2} \dot{M} - C = \begin{bmatrix} 0 & \frac{1}{2} \sum_{i=1}^4 \frac{J_i}{l_i} (\dot{x} \sin \beta_i + \dot{y} \cos \beta_i) \\ -\frac{1}{2} \sum_{i=1}^4 \frac{J_i}{l_i} (\dot{x} \sin \beta_i + \dot{y} \cos \beta_i) & 0 \end{bmatrix}$$

Property 3: Linearity in the inertia parameter. Let θ denote the inertia parameters, the equation (2.16) can be written as

$$Y(q, \dot{q}, \ddot{q})\theta = \tau \quad (3.2)$$

This means that the dynamic equation can be linearly parametrized by the inertia parameters. In (3.2), the torque is expressed as a linear regression in terms of the inertia parameters of the system. $Y(q, \dot{q}, \ddot{q})$ is called the regressor. This can be extended to include friction term.

The equations of motion (3.1) may be exactly linearized and decoupled by static nonlinear state feedback (sometimes called inverse dynamics or computed torque in the robotics literature, Spong and Vidyasagar, 1989).

Basically, there are two control methods: computed torque method and passivity-based method

3.1.1.1 Computed Torque Method

$$\tau = M(q)(\ddot{q}_d - k_p e - k_v \dot{e}) + C(q, \dot{q})\dot{q} \quad (3.3)$$

where $e = q - q_d$.

The error dynamics is

$$\ddot{e} + k_v \dot{e} + k_p e = 0 \quad (3.4)$$

The computed torque method is very popular in the control of manipulators. It makes use of the invertibility of the system dynamics to reduce the dynamics to a

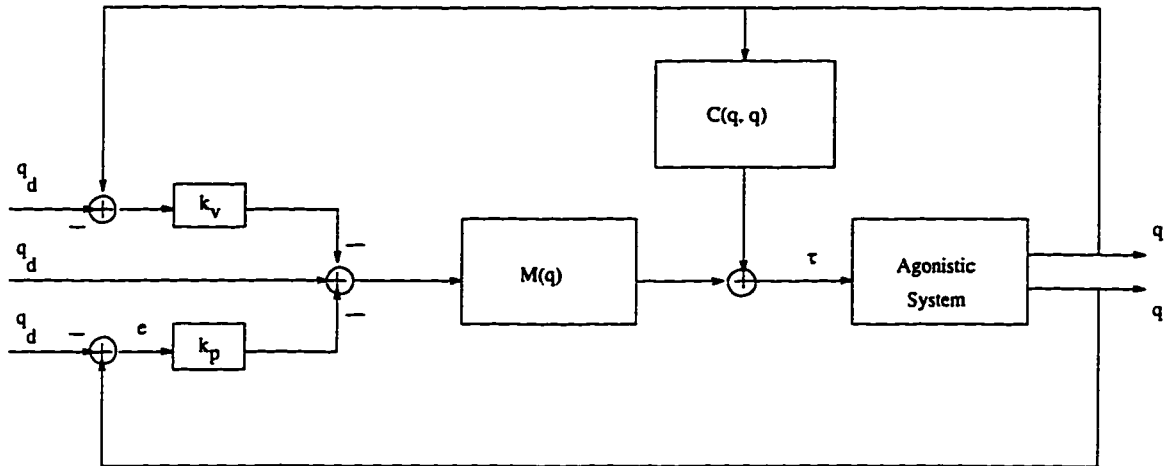


Figure 3.1 Computed torque control scheme

linear second order system with a feedforward control element. Feedback of tracking errors is then employed to position the error poles at desired locations.

Computed torque method is essentially a feedback linearization method which is a general method and does not take into account the specific structure of the agonistic control dynamics. It depends on the exact cancellation of the nonlinear terms and hence may be vulnerable with regard to robustness. Its advantage is that the error dynamics are independent of the configuration of the system and therefore the inertia matrix.

The control torques can be determined from:

$$B(q)T = u \quad (3.5)$$

where

$$u = \frac{1}{r}\tau$$

There are infinitely many solutions for the above equation. Among them, B^+u minimizes the norm of the torque vector T , where B^+ is the pseudo-inverse of B . $B^+ = B^T(BB^T)^{-1}$ ($rank B = 2$). The specific point in the agonistic control is that T must be positive all the time. If B^+u alone is used, T may become negative. In order to meet positivity requirement, a second term is added and results in the following

control law:

$$T = B^+u + (I - B^+B)N \quad (3.6)$$

where N is a constant vector.

The second term in (3.6) is used to guarantee $T_i > 0$. It does not alter the relation (3.5). But N can adjust the nominal magnitude of the torque T . Note that $I - B^+B$ is an idempotent matrix. It is nonnegative since its eigenvalues are 0 and 1 (Ben-Israel and Greville, 1974)

The constraint forces can be calculated from (2.14).

In order to ensure the positiveness of the control torque, there two parameters to tune in the control law: the gain and the constant vector N .

Large value of N helps make the total torque positive, but too large value of N can result in actuator saturation.

Large value of control gain can lead to rapid dynamic response. Too large gain, however, will render the total control torques negative. Therefore, we should make a balance in the choice of the control gain and the value of N to compromise the conflicting requirements.

3.1.1.2 Passivity Based Method In distinction to the computed torque method, passivity-based methodology fully exploits the inherent structure of the agonistic dynamics.

The basic idea is to modify the dynamics of the system (2.16) and reshape the natural energy function of the system and shift the equilibrium point of the system (2.16) from its natural point to the desired point q_d . The passivity-based controller uses feedforward to meet a desired energy function for the closed-loop system, and add damping, via velocity feedback, for asymptotic stabilization purposes. Based on

this idea, Takegaki and Arimoto proposed a beautiful, simple solution to the robot set-point problem. Paden and Panja extend it to the tracking problem.

Definition:

A mapping $x \rightarrow y$ is said to be passive if and only if

$$\langle x, y \rangle = \int_0^T x' y dt \geq -\beta$$

for some $\beta > 0$ and for all T .

The following theorem (LaSalle and Lefschetz, 1961) will be useful in proving asymptotic stability of the closed-loop system.

Theorem 1 (LaSalle) *Consider the autonomous nonlinear system*

$$\dot{x} = f(x)$$

and let the origin be an equilibrium point.

Suppose that the Lyapunov function $V(x)$ satisfies

1. $V(x) > 0$

2. $\dot{V}(x) \leq 0$

3. *the set defined by $\dot{V}(x) = 0$ contains no trajectories other than the trivial trajectory $x = 0$*

Then, the origin is asymptotically stable.

• Set point problem:

Denote $e = q - q_d$, for set-point problem, the desired equilibrium point is $(e, \dot{q}) = (0, 0)$. (Takegaki and Arimoto, 1987)

Consider the function:

$$H(e, \dot{q}) = \frac{1}{2} \dot{q}^T M(q) \dot{q} + \frac{1}{2} e^T k_p e \quad (3.7)$$

Let

$$\tau = -k_p e + u \quad (3.8)$$

Where u is the new input to shape the system energy, then,

$$\frac{dH}{dt} = \langle \dot{q}, u \rangle$$

If the mapping: $u \rightarrow \dot{q}$ is passive, we obtain a marginally stable closed-loop system. In order to yield the passive mapping, we introduce the damping term:

$$u = -k_v \dot{q}$$

We get a simple PD control.

$$\tau = -k_p e - k_v \dot{q} \quad (3.9)$$

Now, we use LaSalle's theorem to prove the asymptotic stability.

When $\frac{dH}{dt} = -\dot{q}' k_v \dot{q} = 0$, $\dot{q} = 0$. Then, $\tau = -k_p e$. But from equation (3.1), $\tau = 0$ (due to $\dot{q} = 0$). Hence, $e = 0$.

(3.9) does not depend on the parameters of the system. So, it has immunity to the variations in the parameters. Indeed, a good control law should use as little information about the system as possible.

- Tracking problem:

Let the desired trajectory be $q_d(t)$. We want $q \rightarrow q_d$.

The desired equilibrium point is $(e, \dot{e}) = (0, 0)$, where $e = q - q_d(t)$.

Let

$$\tau = M(q)\ddot{q}_d + C(q, \dot{q})\dot{q}_d - k_p e + u \quad (3.10)$$

where $M(q)\ddot{q}_d + C(q, \dot{q})\dot{q}_d$ is the feedforward compensation.

$$H(e, \dot{e}) = \frac{1}{2} \dot{e}^T M(q) \dot{e} + \frac{1}{2} e^T k_p e \quad (3.11)$$

$$\frac{dH}{dt} = \langle \dot{e}, u \rangle \quad (3.12)$$

After introducing the damping term:

$$u = -k_v \dot{e} \quad (3.13)$$

We get the passive mapping: $u \rightarrow \dot{e}$ and the passivity of the agonistic system is preserved in the closed loop. The closed system can be stabilized by the control law:

$$\tau = M(q)\ddot{q}_d + C(q, \dot{q})\dot{q}_d - k_p e - k_v \dot{e} \quad (3.14)$$

This control law leads to the following error dynamics:

$$M(q)\ddot{e} + C(q, \dot{q})\dot{e} + k_v \dot{e} + k_p e = 0 \quad (3.15)$$

LaSalle's theorem can be used to prove the asymptotic stability.

When $\frac{dH}{dt} = -\dot{e}'k_v \dot{e} = 0$, $\dot{e} = 0$. From (3.15), we have $e = 0$.

Controller (3.14) is a simple PD controller with dynamic feedforward compensation. So, it is named as "PD+" controller (Paden and Panja, 1988). The feedforward compensation constitutes the inner loop, the outside loop is the PD control. In the implementation, this structure allows the simple PD computation to be updated at higher rate than the feedforward compensation. This helps to increase the system bandwidth since in the digital implementation, the gains in the control law is limited by the computer update rate (Under the given computer update rate, too large a control gain will lead to an unstable system). With the higher computer update rate, we can choose the larger values for the control gains to get rapid response time.

The passivity-based control law results in the complicated error dynamics. It is not easy to analyze the effects of the PD gains to the transient behavior of the error dynamics. Judicious choice of the gains in the PD term is important.

In the paper of (Takegaki and Arimoto, 1987), the gains were chosen empirically. Here we give a systematic way to choose these gains which is applicable to both

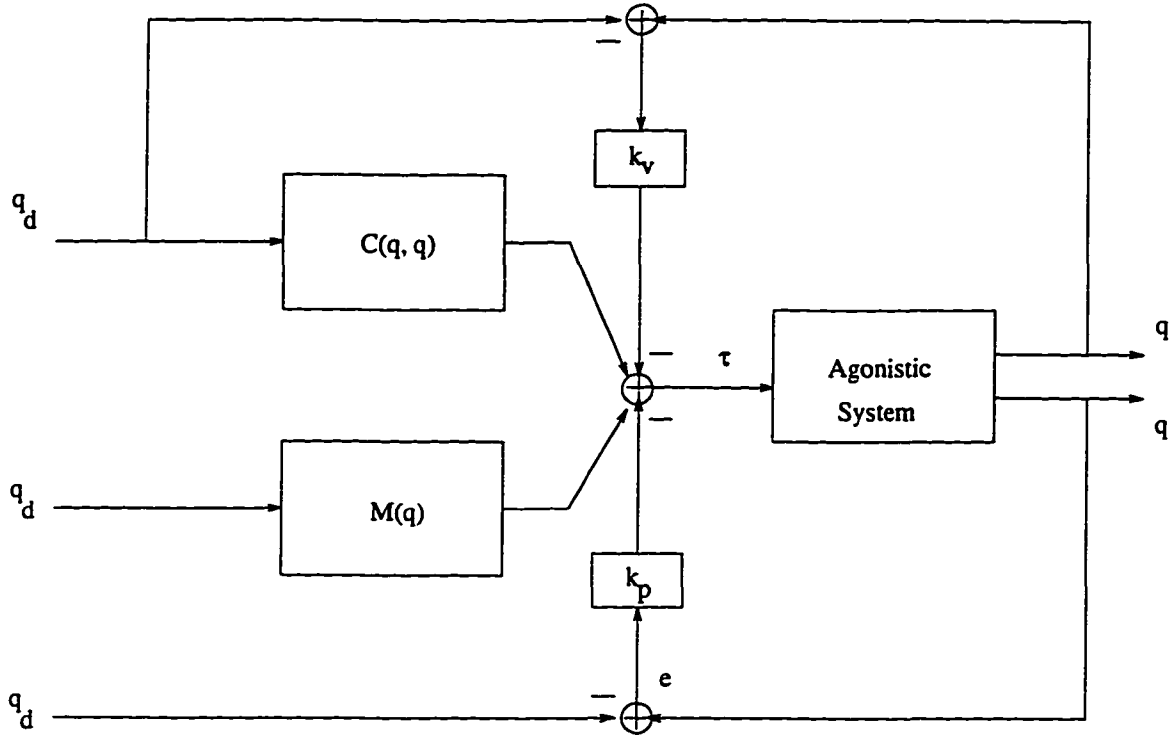


Figure 3.2 PD + control scheme

set-point and tracking problems. In the initial time, the workpiece is in the state $q = q_0, \dot{q} = 0$. $C(q, \dot{q}) = 0$. The error dynamics becomes:

$$M(q_0)\ddot{e} + k_v\dot{e} + k_p e = 0 \quad (3.16)$$

Let

$$k_p = M(q_0)\bar{k}_p, k_v = M(q_0)\bar{k}_v \quad (3.17)$$

We don't need to worry about the effect of the value of the gains on the stability of the error dynamics, since stability is guaranteed by the passivity-based design.

In the simulation, when we choose:

$$\bar{k}_p = \begin{bmatrix} 100 \\ 100 \end{bmatrix}, \bar{k}_v = \begin{bmatrix} 20 \\ 20 \end{bmatrix}$$

We have

$$k_p = \begin{bmatrix} 2.1097 \times 10^{-3} \\ 2.0317 \times 10^{-3} \end{bmatrix}, k_v = \begin{bmatrix} 4.2194 \times 10^{-4} \\ 4.0635 \times 10^{-4} \end{bmatrix}$$

The torque is large at the beginning, if we increase the value of \bar{k}_p and \bar{k}_v to accelerate the convergence rate, the total torque may have negative values at the initial period. In this case, we need to increase the value of N to guarantee the positiveness of the total torque. In the meantime, the magnitude of the constraint forces will be increased since it is determined by N .

The set point problem can be beautifully handled: only position information is needed and the global stability can be guaranteed.

3.1.2 Elastic Case

In the chapter 2 , we considered agonistic control with inelastic tendons in which the elastic modulus of the tendon is assumed to be infinite. (We refer this as the “stiff” case.) In the real world, however, the elastic modulus of the tendon is finite. Using the control law based on the stiff case can lead to oscillatory behavior which can degrade the performance of the system, or even make the system fail. To avoid the problems introduced by finite elasticity, it is necessary to modify the control law. In last chapter, the model in which the finite elasticity is considered was established. It describes the dynamic behavior of agonistic system with elastic tendons. Based on this model, the control law is designed to compensate the elastic effect. It is shown that the finite elasticity can introduce the oscillations. The control problem is quite complex because of resonance phenomena and the nonlinearity itself. Several important control concepts and techniques, such as feedback linearization, singular perturbation, and composite control are useful tools for the investigation of the dynamics and control of agonistic system in the elastic case. In particular, the control law is synthesized using the singular perturbation method. It consists of a fast control and a slow control. The fast control is used to stabilize the oscillations incurred by the finite elasticity of the tendon. The slow control drives the system to track the desired trajectory.

We have established the following model:

$$m\ddot{q} = B(q)z \quad (3.18)$$

$$\varepsilon^2 \ddot{z} = -A(q)z + E(q, \dot{q})\dot{q} + Du \quad (3.19)$$

where

$$q = \begin{bmatrix} x \\ y \end{bmatrix}, z = \begin{bmatrix} z_1 \\ z_2 \\ z_3 \\ z_4 \end{bmatrix}, u = \begin{bmatrix} T_1 \\ T_2 \\ T_3 \\ T_4 \end{bmatrix},$$

$$A(q) = \frac{1}{m} \begin{bmatrix} d_1 & c_{12} & c_{13} & c_{14} \\ c_{12} & d_2 & c_{23} & c_{24} \\ c_{13} & c_{23} & d_3 & c_{34} \\ c_{14} & c_{24} & c_{34} & d_4 \end{bmatrix},$$

$$B(q) = \begin{bmatrix} \cos \beta_1 & \cos \beta_2 & \cos \beta_3 & \cos \beta_4 \\ -\sin \beta_1 & -\sin \beta_2 & -\sin \beta_3 & -\sin \beta_4 \end{bmatrix},$$

$$\delta_i = \dot{x} \sin \beta_i + \dot{y} \cos \beta_i$$

$$E(q, \dot{q}) = \begin{bmatrix} \frac{\delta_1}{l_1} \sin \beta_1 & \frac{\delta_1}{l_1} \cos \beta_1 \\ \frac{\delta_2}{l_2} \sin \beta_2 & \frac{\delta_2}{l_2} \cos \beta_2 \\ \frac{\delta_3}{l_3} \sin \beta_3 & \frac{\delta_3}{l_3} \cos \beta_3 \\ \frac{\delta_4}{l_4} \sin \beta_4 & \frac{\delta_4}{l_4} \cos \beta_4 \end{bmatrix},$$

$$D = \text{diag}\left\{\frac{r}{J_1}, \frac{r}{J_2}, \frac{r}{J_3}, \frac{r}{J_4}\right\}$$

These equations are similar to the equations obtained in (Spong, 1987), (Marino and Nicosia, 1985). The system of equations (3.18) and (3.19) is singularly perturbed. The position vector q and its derivatives are slow variables. The tension vector z and its derivatives are fast variables.

Let

$$z - \bar{z} := \eta(\tau) + O(\varepsilon^2) \quad (3.20)$$

Using the concept of composite control (Chow and Kokotovic, 1978), (Saberi and Khalil, 1985), we choose the control input u of the form

$$u = u_s(q, \dot{q}) + u_f(q, \dot{q}, z, \dot{z})$$

where u_s is the control law for the stiff case. We refer it as “slow” control. \bar{z} is the constraint force in the stiff case. It satisfies

$$A(q)\bar{z} = E(q, \dot{q})\dot{q} + Du_s \quad (3.21)$$

From (3.19) and (3.21), we see that η satisfies the boundary layer equation:

$$\frac{d^2\eta}{d\tau^2} + A(q)\eta = Du_f - \frac{d^2\bar{z}}{d\tau^2} \quad (3.22)$$

where $A(q)$ is positive definite and $\tau = t/\varepsilon$ is the fast time scale. Neglecting $d^2\bar{z}/d\tau^2$ which is very small in the boundary layer, (3.22) becomes

$$\frac{d^2\eta}{d\tau^2} + A(q)\eta = Du_f \quad (3.23)$$

This is a linear system in η parameterized by q . It has the eigenvalues on the $j\omega$ axis. If the control law derived from stiff case is applied to the elastic system (3.18) (3.19), the fast variables will exhibit oscillation. In practice, dissipation will be present to damp these oscillations. But the damping may not be sufficient. The control u_f is used to provide additional damping.

Based on the dynamics given by (3.23), the control law for u_f is:

$$\begin{aligned} u_f &= D^{-1}\left[A(q)\eta + k_1\eta + k_2\frac{d\eta}{d\tau}\right] \\ &= D^{-1}\left[A(q)\eta + k_1\eta + k_2\varepsilon\frac{d(z - \bar{z})}{dt}\right] \end{aligned} \quad (3.24)$$

Since $d\bar{z}/dt$ is not easily obtained and, moreover, it is very small compared to dz/dt in the boundary layer, it is simply neglected. The proposed control law becomes:

$$u_f = D^{-1}\left[A(q)\eta + k_1\eta + k_2\varepsilon\frac{dz}{dt}\right] \quad (3.25)$$

This control law requires the knowledge of η and dz/dt . The measurements of the workpiece position (x, y) and the measurements of the angular positions $\theta_1, \dots, \theta_4$ are necessary to determine η .

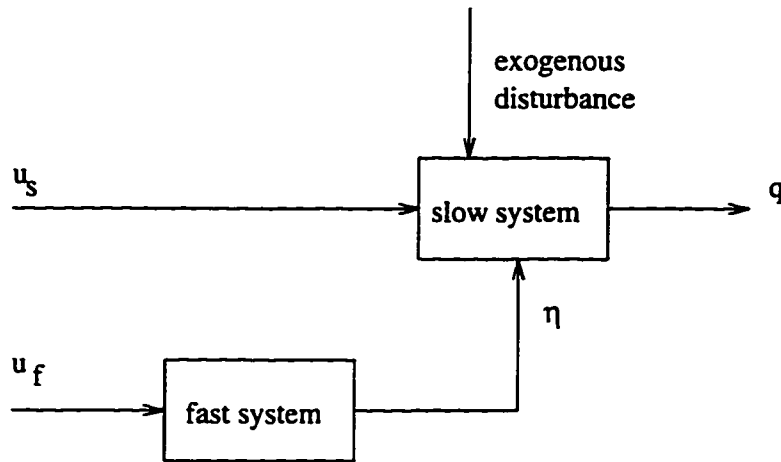


Figure 3.3 The composite control law is designed to achieve robust tracking

When the fast variable η asymptotically goes to zero, from Tikhonov's theorem (Hoppensteadt, 1971) the orbits of the elastic system driven by the composite control will tend to the orbits of the stiff system. Although η can not be damped to exactly zero because the presence of $d\bar{z}/dt$, as long as η decays to a sufficiently small amplitude, it can be viewed as a persistent disturbance to the stiff system. This disturbance prevents the tracking error from going to zero. In addition to this disturbance, there are other things to affect the tracking error such as unmodeled dynamics, parameter variation or lack of knowledge of exact values, and exogenous disturbance. This suggests that the proposed control law must be robust. Based on this consideration, sliding mode control is used.

The sliding mode control law is designed to drive the system to the sliding surface. Once the sliding surface is reached, the system will evolve along the sliding surface and the tracking error will exponentially decay to zero. The sliding surface is independent of the parameters of the system. Therefore the variation in the parameters and disturbance will not affect the performance of the system. The disturbance rejection and robustness to the variation in the parameters is achieved.

Define the sliding surface:

$$e_1(t) = (x(t) - x_d(t)) + \lambda(\dot{x}(t) - \dot{x}_d(t)) \quad (3.26)$$

$$e_2(t) = (y(t) - y_d(t)) + \lambda(\dot{y}(t) - \dot{y}_d(t)) \quad (3.27)$$

$\lambda > 0$ controls the convergence rate of $e(t)$.

The sliding mode control law is designed as (Slotine and Li, 1991):

$$\tilde{u}(t) = -\sigma(e(t)) \quad (3.28)$$

σ should be large enough to overcome the influence of disturbance. When σ is increased, N should be also increased to ensure the positiveness of the control torques. The sliding mode control \tilde{u} is added to the *PD* part in the slow control u_s . The modified slow control is denoted as \tilde{u}_s .

The complete control law is:

$$u = \tilde{u}_s + u_f \quad (3.29)$$

After the sliding mode control law (3.28) is introduced, the right-hand side of the differential equations (3.18) and (3.19) of the dynamical system is discontinuous, chattering phenomenon occurs. In order to reduce the chattering, a saturation function is used to replace the signum function (Slotine and Sastry, 1983). It defines a boundary layer.

$$\tilde{u}(t) = -\sigma \text{sat}(e)$$

$$\text{sat}(e) = \begin{cases} 1 & e \geq \delta \\ \frac{e}{\delta} & -\delta < e < \delta \\ -1 & e \leq -\delta \end{cases}$$

where δ is the thickness of the boundary layer.

There is no abrupt change across the boundary layer. Therefore, the right-hand side of the differential equations of the dynamical system is continuous. Indeed, the chattering is avoided and the smooth tracking is obtained. But there is a penalty to be paid on the tracking error. The tracking error will not asymptotically tend to zero anymore. There is a discrepancy between the desired trajectory and the true trajectory. The difference depends on the thickness δ of the boundary layer which can be adjusted at the designer's will.

3.2 Decentralized Control Strategy

The agonistic control system was proposed and analyzed in previous sections where a centralized control strategy was considered. In centralized version, a thorough analysis must be performed at the design level and the complex dynamics model must be established. The complicated model requires extensive computation and real time control becomes a problem. In this section, we develop a decentralized strategy for agonistic control. Compared with the centralized version, it uses a simplified model and controller complexity is considerably reduced. Under the assumption of the stiff tendons, the desired movement of the workpiece can be transformed to the desired movement of the angular positions of individual motors. In the decentralized scheme, each motor is independently controlled using only local information. The dynamics of each subsystem can be expressed as a independent linear time-invariant second order system with the tension being viewed as a disturbance which is assumed as constant and is estimated by an observer.

The use of decentralized control scheme makes very simple the controller design and reduces the computational complexity. The control tasks can be distributed onto several processors. The i th subsystem is associated with the i th controller which generates the torque T_i to affect only the angle θ_i . The decentralized controller allows the real-time parallel implementation.

Centralized control law is based on the workpiece coordinates x and y . Decentralized control law should based on the individual coordinate of each motor.

The control scheme is based on the following key idea: the total control torque is the superposition of the base value and the correction term, that is:

$$T_i = T_{base}^i + \Delta T_i \quad (3.30)$$

The base value is exerted to keep the tendon from becoming slack. It does not contribute to the motion of the workpiece. Actually, it serves to establish an equilibrium point. The correction term is responsible for the movement of the

workpiece such as tracking and positioning. The correction term actually fluctuates around the base value. Choosing the base value of the torque being sufficient large can guarantee total torque exerted on each motor be positive.

An agonistic system is analogous to cooperative multiple robots (Wendlandt and Sastry, 1994), (Arimoto, Miyazaki and Kawamura, 1987). The base value corresponds to the internal force in the cooperative multiple robots.

The base value can be computed from the so-called “equilibrium condition”. Since the tendons are not allowed to be slack, when the workpiece is in standstill, the torque exerted on each motor should satisfy the following equilibrium condition.

$$BT_{base} = 0 \quad (3.31)$$

There are infinite ways to choose the values of the base torque. Among them, we want a nonnegative value because the purpose of introducing the base torque is to obtain the nonnegative value of the total torque.

The base value of the torque are chosen as

$$T_{base} = (I - B^+B)N$$

where $B^+ = B'(BB')^{-1}$ is the pseudo-inverse of the matrix B and N is a constant vector. It can adjust the nominal magnitude of the base torque.

Note that as long as the base torque satisfies the equilibrium condition, the system dynamic behavior remains unchanged.

Each motor is treated as a subsystem which has a simple second order linear dynamics.

$$J_i\ddot{\theta}_i = T_i - r f_i \quad (3.32)$$

where f_i represents the tension in each tendon.

Just as the torque consists of two components, the tension f_i is decomposed as:

$$f_i = f_{base}^i + \Delta f_i \quad (3.33)$$

where f_{base}^i is the equilibrium force, $f_{base}^i = \frac{1}{r}T_{base}^i$. Δf_i corresponds to the movement of the workpiece. Δf_i represents the variation away from the equilibrium value. For simplicity, Δf_i is treated as a constant disturbance and is estimated from an observer.

The dynamics of each motor then becomes

$$J_i \ddot{\theta}_i = T_i - \Delta f_i r - r f_{base}^i \quad (3.34)$$

In state space form,

$$\frac{d}{dt} \begin{bmatrix} \theta_i \\ \dot{\theta}_i \\ \Delta f_i \end{bmatrix} = \begin{bmatrix} 0 & 1 & 0 \\ 0 & 0 & -\frac{r}{J_i} \\ 0 & 0 & 0 \end{bmatrix} \begin{bmatrix} \theta_i \\ \dot{\theta}_i \\ \Delta f_i \end{bmatrix} + \begin{bmatrix} 0 \\ \frac{1}{J_i} T_i - \frac{r}{J_i} f_{base}^i \\ 0 \end{bmatrix} \quad (3.35)$$

The correction term is designed based on the each independent simple subsystem according to the simple PD control law:

$$\Delta T_i = J_i [\ddot{\theta}_i^d + k_p(\theta_i - \theta_i^d) + k_v(\dot{\theta}_i - \dot{\theta}_i^d)] + \Delta f_i r \quad (3.36)$$

where θ_d is the desired position of the workpiece.

The actual tensions in each tendon can be calculated from (2.14). The following observer is used to construct the estimates of θ_i , $\dot{\theta}_i$ and f_i .

$$\dot{z}_1 = z_2 + k_1(\theta_i - z_1) \quad (3.37)$$

$$\dot{z}_2 = -\frac{r}{J_i} z_3 - \frac{r}{J_i} f_{base}^i + \frac{1}{J_i} T_i + k_2(\theta_i - z_1) \quad (3.38)$$

$$\dot{z}_3 = k_3(\theta_i - z_1) \quad (3.39)$$

where

$$[z_1, z_2, z_3] = [\hat{\theta}_i, \hat{\dot{\theta}}_i, \hat{\Delta f}_i]$$

Choice of the gains in the observer:

When we select large gains in the control law to obtain quick response, the gains in the observer should also be chosen large values so that the state variables of the observer can acquire and track the state variables of the true system.

Under the physical values we use for r and J ($r = 0.01m, J = 10^{-6}kg - m^2$), the characteristic equation of the observer is:

$$s^3 + k_1s^2 + k_2s - 10000k_3 = 0$$

The set of values $k_1 = 100, k_2 = 3100, k_3 = -3$ corresponds to the eigenvalues: -20, -30 and -50 which were used in the simulation studies reported in the next chapter.

The observer-based PD control law is:

$$\Delta T_i = J_i[\ddot{\theta}_i^d + k_p(\hat{\theta}_i - \theta_i^d) + k_v(\dot{\hat{\theta}}_i - \dot{\theta}_i^d)] + \Delta \hat{f}_i r \quad (3.40)$$

Each controller uses only its own local information, the angular position information, provided by the shaft encoder attached to the motor.

In simulation, the control torques T_i are exerted to the actual system model (2.50).

3.3 Consideration of DC Motor Characteristics

Now, we have established the dynamic equations of the agonistic system and designed the control law where we assume that the inputs are torques acting on the motors. However these torques are supplied by actuators. In agonistic control, the electric direct current (DC) motors are used, with voltage as inputs. Therefore, after obtaining the required torque for agonistic control, correct input voltage values are needed to generate the desired torque. Also, the input voltage has a maximum value which can not be exceeded. Consequently, we have to take this factor into account in the controller development.

The motor dynamics is derived in (Friedland, 1986). The torque developed at the shaft of a motor is proportional to the input current to the motor. $\tau = k_1 i$, where k_1 is the torque constant. The induced emf ("back emf") E is proportional to the angular speed ω of the motor. $E = k_2 \omega$, where k_2 is the back emf constant, $\omega = \frac{d\theta}{dt}$, θ is the angular position of the motor.

Let u be the input voltage to the motor, from Ohm's law, we have the following relation:

$$u = E + Ri$$

where R is the resistance of the motor armature.

We obtain

$$\frac{R}{k_1} \tau + k_2 \frac{d\theta}{dt} = u \quad (3.41)$$

From above relation, given the desired torque τ , we can easily calculate the input voltage u .

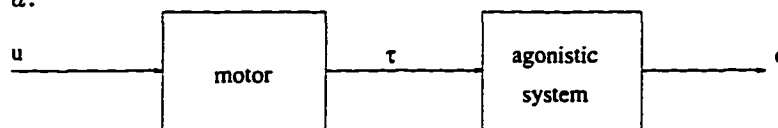


Figure 3.4 Combining motor dynamics with agonistic system. voltage as the input and the position of the workpiece as the output

The electric motor is an electro-mechanical energy transducer. When the energy conversion is 100 percent efficient, the electrical input power $P_e = Ei = \frac{k_2}{k_1} \omega \tau$ should be equal to the mechanical output power $P_m = \omega \tau$, thus $k_1 = k_2$.

Note (3.41) is derived under the assumption that the inductance of the motor armature is negligible. If the inductance is not negligible, combining the motor dynamics with the motion equation of the agonistic system will lead to a third order nonlinear system (Tarn, 1991). In that case, it is very difficult to design the control law for the input voltage. In addition, control problem is further complicated

in agonistic control by the requirement that the torque should be kept positive all the time.

Determination of $\frac{d\theta}{dt}$:

In the calculation of the input voltage u , the value $\frac{d\theta}{dt}$ is needed.

In the stiff case, due to the holonomic constraints: $l_i - l_i^0 = -r\theta_i$, θ_i is related to the velocity of the tendon by $\dot{l}_i = -r\dot{\theta}_i$. While $\dot{l}_i = \dot{y}\sin\beta_i - \dot{x}\cos\beta_i$. Therefore,

$$\dot{\theta}_i = -\frac{1}{r}(\dot{y}\sin\beta_i - \dot{x}\cos\beta_i)$$

In the elastic case, from the relation $z_i = (l_i - l_i^0 + r\theta_i)k$, we can obtain:

$$\dot{\theta}_i = \frac{1}{r}\left(\frac{1}{k}\dot{z}_i - \dot{l}_i\right)$$

where $\dot{l}_i = \dot{y}\sin\beta_i - \dot{x}\cos\beta_i$ and $\dot{z}_i, \dot{x}, \dot{y}$ can be constructed from observer.

In the decentralized case, θ_i itself is the state variable. It is easy to obtain the value of $\dot{\theta}_i$ from the observer.

Choice of the gains in the PD controller:

In the PD (proportional plus derivative) control law, velocity and position gains should be chosen carefully. Too small gains will lead to slow response time and too large gains will result in actuator saturation. In agonistic control, with the increase of the gains, the value of N should be increased accordingly in order to ensure the positiveness of the torques.

PD gains are usually selected for critical damping. $k_v = \omega_n^2, k_p = 2\omega_n$.

In the simulation of agonistic system, parameters of Clifton Precision DC motors were used (model number: JDTH-2250-FN-1C). The relevant data are the following (Catalog, Servo Systems Co.):

$$k_1 = 8 \text{ oz-in/Amp} = 5.76 \times 10^{-3} \text{ kg-m/Amp,}$$

$$\text{resistance } R = 1.2 \text{ ohm}$$

The maximum input voltage is 24 v and the no-load current is 560 mA. Therefore the maximum power is 13.5 watts.

CHAPTER 4

OBSERVER DESIGN FOR AGONISTIC CONTROL

4.1 Necessity of Observer

The control law used in agonistic control is basically PD type. It always requires the velocity information. In the agonistic system with elastic tendons, \dot{q} is used in the slow control law and \dot{z} is used in the fast control law to stabilize the fast system.

Usually, only the position variables q and z are available. We need to construct the velocity variables based on these available quantities. In the elastic case, due to the elasticity of the tendon, there is no one-to-one correspondence between the position of the workpiece and the angular position of the motors. Both these position measurements are needed.

The problem of designing observers for agonistic system is very complex, due to the nonlinear and coupled structure of the related dynamic models. In this chapter, we exploit the structural properties of the agonistic system with elastic tendons and develop a method to reconstruct the velocities of the workpiece. Linear uncertain system theory is used. The observer is shown to be globally stable.

4.2 Development of the Nonlinear Observer

In the PD control law (3.3),(3.4), the position and velocity information of the workpiece is required. The position of the workpiece can be determined from the following relationships:

$$x = \frac{l_1^2 - l_3^2}{4a} \quad (4.1)$$

$$y = \frac{l_2^2 - l_4^2}{4a} \quad (4.2)$$

while $l_i = l_i^0 - r\theta_i$ ($i = 1, 2, 3, 4$). θ_i are provided by the shaft encoders mounted on the motors.

Although the position sensor can give us accurate position measurement of the workpiece, the velocity measurement is not always possible. Even the velocity information is available, it may contaminate with noise. This will deteriorate the controller performance. So, in order that the PD control law is feasible, we need to estimate the velocity of the workpiece using the position measurements via nonlinear observer.

$$\text{let } [z_1, z_2, z_3, z_4] = [\hat{x}, \dot{\hat{x}}, \hat{y}, \dot{\hat{y}}]$$

observer:

$$\dot{z}_1 = z_2 + k_5(x - z_1) \quad (4.3)$$

$$\dot{z}_2 = -q_1 + v_1 + k_6(x - z_1) \quad (4.4)$$

$$\dot{z}_3 = z_4 + k_5(y - z_3) \quad (4.5)$$

$$\dot{z}_4 = -q_2 + v_2 + k_6(y - z_3) \quad (4.6)$$

Observer-based control law:

$$v_1 = k_1(x - x_d) + k_2(z_2 - \dot{x}_d) + \ddot{x}_d + \hat{q}_1 \quad (4.7)$$

$$v_2 = k_3(y - y_d) + k_4(z_4 - \dot{y}_d) + \ddot{y}_d + \hat{q}_2 \quad (4.8)$$

For passivity-based set-point control, by using only the position measurements, velocity information can be obtained via filtering.

Kelly (Kelly, 1993) used a high pass filter of the form $\frac{bs}{s+a}$ (s is the differential operator) to filter the position measurements and extract the velocity information. Similar idea also appeared in (Middleton and Goodwin, 1988) where the operator $\frac{a}{s+a}$ was used to avoid the measurement of acceleration.

Let q_i represent the position state. Define:

$$\theta_i = \frac{b_i s}{s + a_i} q_i \quad (4.9)$$

then θ_i can be viewed as velocity approximation and be used to replace the true velocity \dot{q}_i in the implementation of the set point control law.

$$\begin{bmatrix} \theta_1 \\ \theta_2 \end{bmatrix} = \begin{bmatrix} \frac{b_1 s}{s+a_1} & 0 \\ 0 & \frac{b_2 s}{s+a_2} \end{bmatrix} \begin{bmatrix} q_1 \\ q_2 \end{bmatrix} \quad (4.10)$$

Define

$$A = \text{diag}\{a_i\}, B = \text{diag}\{b_i\} \quad (4.11)$$

we have

$$\dot{x} = -Ax - ABq \quad (4.12)$$

and

$$\theta = x + Bq \quad (4.13)$$

By substituting the velocity approximation θ instead the true velocity \dot{q} into the control law (3.9), we have the following proposed control law:

$$\tau = -k_p(q - q_d) - k_v\theta = k_p\tilde{q} - k_v\theta \quad (4.14)$$

where $\tilde{q} = q_d - q$.

Then, the overall closed loop system is:

$$\frac{d}{dt} \begin{bmatrix} \tilde{q} \\ x \\ \dot{q} \end{bmatrix} = \begin{bmatrix} -\dot{q} \\ -Ax - ABq \\ M^{-1}(q)[k_p\tilde{q} - k_v(x + Bq)] - C(q, \dot{q})\dot{q} \end{bmatrix} \quad (4.15)$$

This is an autonomous system with an unique equilibrium point at $(\tilde{q}, x, \dot{q}) = (0, -Bq_d, 0)$. In order to shift the equilibrium to the origin, introduce the variable $\xi = x + Bq_d$, the new closed system becomes:

$$\frac{d}{dt} \begin{bmatrix} \tilde{q} \\ \xi \\ \dot{q} \end{bmatrix} = \begin{bmatrix} -\dot{q} \\ -A\xi + AB\tilde{q} \\ M^{-1}(q)[(k_p + k_v B)\tilde{q} - k_v\xi] - C(q, \dot{q})\dot{q} \end{bmatrix} \quad (4.16)$$

It has an unique equilibrium point at origin.

Define the Lyapunov function candidate:

$$V = \frac{1}{2}\dot{q}^T M(q)\dot{q} + \frac{1}{2}\tilde{q}^T k_p \tilde{q} + \frac{1}{2}(\xi - B\tilde{q})^T k_v B^{-1}(\xi - B\tilde{q}) \quad (4.17)$$

which is positive definite since $M(q)$, k_p and $k_v B^{-1}$ are all positive definite.

$$\dot{V} = -(\xi - B\tilde{q})^T k_v B^{-1} A(\xi - B\tilde{q}) \quad (4.18)$$

Since $k_v B^{-1} A$ is positive definite, \dot{V} is a negative semi-definite function. Hence, the origin is a stable equilibrium.

Now, we use LaSalle's theorem to prove the asymptotically stability. When $\dot{V} = 0$, $\xi - B\tilde{q} = 0$. We have $\theta = x + Bq = 0$ and $\dot{x} = 0$. From (4.13), $\dot{q} = 0$. Hence $\tau = 0$ (from (3.1)). Finally, we have $\tilde{q} = 0$ from (4.14).

We conclude that the origin is the global asymptotically stable. Hence

$$\lim_{t \rightarrow \infty} \tilde{q}(t) = 0$$

4.3 Observer Design for Agonistic Control: Elastic Case

In (Yang and Friedland, 1996), we established the dynamic model of agonistic control in the elastic case.

$$m\ddot{q} = B(q)z \quad (4.19)$$

$$\epsilon^2 \ddot{z} = -A(q)z + E(q, \dot{q})\dot{q} + Du \quad (4.20)$$

Although the dynamic equations in the elastic case seem more complicated than those in the stiff case, there is inherent structure (Property 1 through Property 3, in section 3.1.1 of chapter 3). By taking advantage of this inherent structure property, the observer design for the elastic case can be made easier than the observer design in the stiff case.

We note

$$E(q, \dot{q}) = -\dot{B}^T(q) \quad (4.21)$$

Then, (4.20) can be written as

$$\epsilon^2 \ddot{z} = -A(q)z - \dot{B}^T(q)\dot{q} + Du \quad (4.22)$$

Theorem 2 *The system defined by (4.19) and (4.22) is equivalent to the following system:*

$$m\ddot{q} = B(q)z \quad (4.23)$$

$$\dot{v} = -rDz + Du \quad (4.24)$$

$$\epsilon^2 \dot{z} = v - B^T(q)\dot{q} \quad (4.25)$$

Proof: Differentiating (4.25), we have

$$\begin{aligned} \epsilon^2 \ddot{z} &= \dot{v} - \frac{d(B^T(q)\dot{q})}{dt} \\ &= D(u - rz) - \dot{B}^T(q)\dot{q} - B^T(q)\ddot{q} \end{aligned}$$

From (4.19), $\ddot{q} = \frac{1}{m}B(q)z$, we obtain:

$$\epsilon^2 \ddot{z} = D(u - rz) - \dot{B}^T(q)\dot{q} - \frac{1}{m}B^T(q)B(q)z \quad (4.26)$$

But

$$\frac{1}{m}B^T(q)B(q) = A(q) - rD \quad (4.27)$$

we have

$$\epsilon^2 \ddot{z} = -A(q)z - \dot{B}^T(q)\dot{q} + Du \quad (4.28)$$

This is exactly the equation (4.22). $\square\square$

Define $q_1 = q, q_2 = \dot{q}, x = \begin{bmatrix} q_1 \\ q_2 \\ v \\ z \end{bmatrix}$, (4.23) to (4.25) can be written as:

$$\begin{bmatrix} \dot{q}_1 \\ \dot{q}_2 \\ \dot{v} \\ \varepsilon^2 \dot{z} \end{bmatrix} = \begin{bmatrix} 0 & I_2 & 0 & 0 \\ 0 & 0 & 0 & \frac{1}{m}B(q) \\ 0 & 0 & 0 & -rD \\ 0 & -B^T(q) & I_4 & 0 \end{bmatrix} \begin{bmatrix} q_1 \\ q_2 \\ v \\ z \end{bmatrix} + \begin{bmatrix} 0 \\ 0 \\ D \\ 0 \end{bmatrix} u \quad (4.29)$$

where I_l is $l \times l$ identity matrix.

(4.29) can be rewritten as:

$$\dot{x} = F(q)x + Gu \quad (4.30)$$

This is a linear singularly perturbed, parameter-dependent system. q enters the matrix $F(q)$ nonlinearly. When the workpiece moves, q varies accordingly. But its value is known in real time through measurement.

Remark 1: (4.29) is parametrized by a time varying parameter q . Although it is a linear time varying system, the variable t does not explicitly appear in the equation. It is more appropriate to call (4.29) a linear parameter-varying (LPV) system. Its observer design problem is quite different from those for linear time varying systems. It is closely related to the linear uncertain system theory (Barmish, 1985), (Petersen and Hollot, 1986), (Petersen, 1987), (Zhou and Khargonekar, 1988).

Remark 2: We see that by exploiting the inherent structure of the system, some nonlinear system can be converted to linear parameter-varying system.

Remark 3: (4.29) is a linear singularly perturbed system. But it differs with the standard linear singularly perturbed system (Kokotovic, Khalil and O'Reilly, 1986). The standard linear singularly perturbed system has the form:

$$\dot{x} = A_{11}x + A_{12}z$$

$$\varepsilon \dot{z} = A_{21}x + A_{22}z$$

where A_{22} is always assumed to be nonsingular. In (4.29), A_{22} does not exist, much less to say it is nonsingular. Indeed, (4.29) is not directly derived from a physical

system. Rather, it is obtained by artificial manipulation. Therefore, the standard method of the observer design for singularly perturbed systems can not be used.

Assume that the workpiece positions (x, y) and the angular positions of the motor $\theta_i, (i = 1, 2, 3, 4)$ are measurements and the elastic modulus of the tendon is known.

Define q and z as output variables:

$$y = \begin{bmatrix} q \\ z \end{bmatrix} = \begin{bmatrix} I_2 & 0 & 0 & 0 \\ 0 & 0 & 0 & I_4 \end{bmatrix} \begin{bmatrix} q_1 \\ q_2 \\ v \\ z \end{bmatrix} = Hx \quad (4.31)$$

where $H = \begin{bmatrix} I_2 & 0 & 0 & 0 \\ 0 & 0 & 0 & I_4 \end{bmatrix}$.

(4.30) and (4.31) are observable regardless of the values of q . The observability matrix is:

$$\mathcal{O} = \begin{bmatrix} H \\ HF \\ HF^2 \\ \vdots \end{bmatrix} = \begin{bmatrix} I_2 & 0 & 0 & 0 \\ 0 & 0 & 0 & I_4 \\ 0 & I_2 & 0 & 0 \\ 0 & -\frac{1}{\epsilon^2}B^T(q) & \frac{1}{\epsilon^2}I_4 & 0 \\ \vdots & \vdots & \vdots & \vdots \end{bmatrix}$$

The matrix \mathcal{O} has full rank.

Observer Design:

$$\dot{\hat{x}} = F(q)\hat{x} - K^T(q)(y - H\hat{x}) + Gu \quad (4.32)$$

From (4.32), we can reconstruct the state variable (q, \dot{q}, v, z) . As for \dot{z} , it can be calculated from (4.25) after we know v and \dot{q} .

Define the error $e = x - \hat{x}$, then

$$\dot{e} = [F(q) + K^T(q)H]e \quad (4.33)$$

The objective is to choose the gain matrix $K(q)$ to stabilize the system (4.33) for all the possible values of q .

This is a robust stabilization problem. It is not a new problem. It has been haunting in the control community for many years, see (Vinkler and Wood, 1978), (Chang and Peng, 1972).

• **Robust Stabilization**

Robust stabilization theory (Petersen and Hollot, 1986), (Petersen, 1987) involves solving an algebraic Riccati equation (ARE). The solution to this Riccati equation defines a quadratic Lyapunov function which is used to establish the stability of the closed loop system. This leads to the notion of “quadratic stabilizability”.

Consider the linear uncertain system:

$$\dot{x} = (A_0 + \Delta A(q))x + B_0 u \quad (4.34)$$

where x is the state, u is the control input and $q(t)$ is a vector of uncertain parameters which is restricted to a prescribed bounding set.

Definition (quadratic stabilization): (4.34) is said to be quadratic stabilizable via a linear constant control if there exists a linear constant gain feedback law $u = Kx$, a positive definite symmetric matrix P and a constant $\alpha > 0$ such that for any admissible uncertainty $q(t)$, the Lyapunov function $V(x) = x^T P x$ satisfies

$$\dot{V} = x^T [P(A_0 + \Delta A(q) + B_0 K) + (A_0 + \Delta A(q) + B_0 K)^T P] x \leq -\alpha \|x\|^2$$

When the system (4.34) is quadratically stabilizable, The corresponding closed loop system can be shown to be uniformly and asymptotically stable.

There are several ways to represent the uncertainty matrix $\Delta A(q)$.

Decomposition 1:

$$\Delta A(q) = \sum_{j=1}^k A_j \delta_j(q) \quad (4.35)$$

where A_j is a known constant matrix and $\delta_j(q)$ is a scalar which contains the uncertainty. Assume $\delta_j(q) < \bar{r}$ for all j (\bar{r} is a constant).

Decomposition 2: (norm bounded uncertainty)

$$\Delta A(q) = DF(q)E \quad (4.36)$$

Where D and E are known constant matrices. Assume $\|F\| \leq 1$. Here, $\|\cdot\|$ denotes the Euclidean norm.

Decomposition 3: (block-structured norm-bounded uncertainty)

$$\Delta A(q) = \sum_{i=1}^k D_i F_i(q) E_i \quad (4.37)$$

Sometimes, it is more appropriate to represent $\Delta A(q)$ by (4.37) which can be converted to (4.36) since

$$\sum_{i=1}^k D_i F_i(q) E_i = [D_1, \dots, D_k] \begin{bmatrix} F_1(q) & & \\ & \ddots & \\ & & F_k(q) \end{bmatrix} \begin{bmatrix} E_1 \\ \vdots \\ E_k(q) \end{bmatrix}$$

Equation (4.35) represent a larger class of uncertainties in the sense that some uncertainties can not be represented as the form (4.36). Furthermore, (4.35) can be more easily obtained than (4.36). But with the decomposition 2, we can obtain stronger results. More specifically, for decomposition 2, the existence of the positive definite solution of the ARE is sufficient and necessary condition for the quadratic stabilizability of (4.34) (Petersen, 1987). But for decomposition 1, we can only say that the existence of the positive definite solution of the ARE is a sufficient condition. These are given by the following theorems.

Theorem 3 (Petersen and Hollot, 1986) *Consider the system (4.34) with the decomposition 1.*

Suppose A_j be decomposed as the following form:

$$A_j = d_j e_j^T \quad (4.38)$$

where d_j and e_j are "rank 1" vectors.

Let

$$D_1 = \bar{r} \sum_{j=1}^k d_j d_j^T$$

$$E_1 = \bar{r} \sum_{j=1}^k e_j e_j^T$$

Given the positive definite matrices R and Q , if for some positive scalar γ , there is a positive definite solution P for the following algebraic Riccati equation:

$$PA_0 + A_0^T P - P\left(\frac{2}{\gamma} B_0 R^{-1} B_0^T - D_1\right)P + E_1 + \gamma Q = 0 \quad (4.39)$$

Then, the control law

$$u = -\frac{1}{\gamma} R^{-1} B_0^T P x \quad (4.40)$$

stabilizes the system (4.34) for all the possible values of q .

Proof: Under the control law (4.40), the closed loop system becomes

$$\dot{x} = \left(A_0 + \Delta A(q) - \frac{1}{\gamma} B_0 R^{-1} B_0^T P\right)x$$

Constructing the Lyapunov candidate

$$V(x) = x^T P x$$

(4.39) and (4.40) can also be written as

$$PA_0 + A_0^T P - P(2B_0 R^{-1} B_0^T - \gamma D_1)P + \frac{1}{\gamma} E_1 + Q = 0 \quad (4.41)$$

and

$$u = -R^{-1} B_0^T P x \quad (4.42)$$

Theorem 4 (Petersen, 1987) Consider the (4.34) with the decomposition 2

Let Q, R be given positive definite symmetric weighting matrices. (4.34) is quadratic stabilizable if and only if there exists a constant $\gamma > 0$ such that the Riccati equation

$$A_0^T P + PA_0 - P(B_0 R^{-1} B_0^T - \gamma D D^T)P + \frac{1}{\gamma} E^T E + Q = 0 \quad (4.43)$$

The stabilizing control law is given by $u = -R^{-1} B_0^T P x$.

With the above theorems, the quadratic stabilization problem is reduced to the existence of the positive definite solution of an algebraic Riccati equation (ARE).

Remark 1 (Petersen, 1987): The existence of the positive definite solution of (4.43) is independent of the choice of the weighting matrices Q and R .

Remark 2: In either decomposition 1 or decomposition 2, the choices of d_j, e_j and D, E are not unique.

(4.43) plays an important role in the quadratic stabilization. Let's look at this ARE.

$$PA + A^T P - P\tilde{R}P + \tilde{Q} = 0 \quad (4.44)$$

Here, we assume (A, B) is controllable and \tilde{R}, \tilde{Q} are symmetric.

(4.44) is associated with a Hamiltonian matrix \tilde{H} defined as:

$$\tilde{H} = \begin{bmatrix} A & -\tilde{R} \\ -\tilde{Q} & -A^T \end{bmatrix} \quad (4.45)$$

\tilde{H} has some properties.

Property 1: If $\lambda \in \text{eig}(\tilde{H})$, then $-\lambda \in \text{eig}(\tilde{H})$.

Property 2: If \tilde{H} has no eigenvalues on $j\omega$ -axis, then (4.44) has a positive definite solution.

It seems that whether \tilde{H} has eigenvalues on $j\omega$ -axis or not is closely related to the matrix \tilde{R} . When \tilde{R} is not sign definite, \tilde{H} generally has eigenvalues on $j\omega$ -axis. In the algorithm of quadratic stabilization, $\tilde{R} = B R^{-1} B^T - \gamma D D^T$, decreasing γ has two meanings. The first one is reducing the effect of the uncertainty. The second one is rendering \tilde{H} be sign definite (here nonnegative definite).

Back to our problem. Let's consider the dual system of (4.33).

$$\dot{\xi} = (A_0 + \Delta A(q) + B_0 K)\xi \quad (4.46)$$

where $A_0 + \Delta A(q) = F^T(q)$, $B_0 = H^T$.

We have

$$A_0 = \begin{bmatrix} 0 & 0 & 0 & 0 \\ I_2 & 0 & 0 & 0 \\ 0 & 0 & 0 & \frac{1}{\varepsilon^2} I_4 \\ 0 & 0 & -rD & 0 \end{bmatrix}, \Delta A(q) = \begin{bmatrix} 0 & 0 & 0 & 0 \\ 0 & 0 & 0 & -\frac{1}{\varepsilon^2} B(q) \\ 0 & 0 & 0 & 0 \\ 0 & \frac{1}{m} B^T(q) & 0 & 0 \end{bmatrix}, B_0 = \begin{bmatrix} I_2 & 0 \\ 0 & 0 \\ 0 & 0 \\ 0 & I_4 \end{bmatrix}$$

In our problem, q is known in real time, we can capitalize on this and use a feedback control to cancel the term $\frac{1}{m} B^T(q)$ (however we can not cancel all the uncertainties due to the constraint of the matrix B).

$$u = K_1 x \quad (4.47)$$

where $K_1 \in R^{6 \times 12}$.

$$K_1 = \begin{bmatrix} 0 & 0 & 0 & 0 \\ 0 & -\frac{1}{m} B^T(q) & 0 & 0 \end{bmatrix}$$

After cancelling the term $\frac{1}{m} B^T(q)$, $\Delta A(q)$ becomes

$$\Delta A(q) = \begin{bmatrix} 0 & 0 & 0 & 0 \\ 0 & 0 & 0 & -\frac{1}{\varepsilon^2} B(q) \\ 0 & 0 & 0 & 0 \\ 0 & 0 & 0 & 0 \end{bmatrix}$$

It can be decomposed as

$$\Delta A(q) = DF(q)E \quad (4.48)$$

where

$$F(q) = \text{diag}\{\cos \beta_1, \sin \beta_1, \cos \beta_2, \sin \beta_2, \cos \beta_3, \sin \beta_3, \cos \beta_4, \sin \beta_4\}, \quad (4.49)$$

$$D = \begin{bmatrix} 0 & 0 & 0 & 0 & 0 & 0 & 0 & 0 \\ 0 & 0 & 0 & 0 & 0 & 0 & 0 & 0 \\ 0 & 0 & 0 & 0 & 0 & 0 & 0 & 0 \\ 0 & 0 & 0 & 0 & 0 & 0 & 0 & 0 \\ 0 & 0 & 0 & 0 & 0 & 0 & 0 & 0 \\ 0 & 0 & 0 & 0 & 0 & 0 & 0 & 0 \\ 0 & 0 & 0 & 0 & 0 & 0 & 0 & 0 \\ 0 & 0 & 0 & 0 & 0 & 0 & 0 & 0 \\ \frac{1}{\varepsilon^2} & \frac{1}{\varepsilon^2} & 0 & 0 & 0 & 0 & 0 & 0 \\ 0 & 0 & \frac{1}{\varepsilon^2} & \frac{1}{\varepsilon^2} & 0 & 0 & 0 & 0 \\ 0 & 0 & 0 & 0 & \frac{1}{\varepsilon^2} & \frac{1}{\varepsilon^2} & 0 & 0 \\ 0 & 0 & 0 & 0 & 0 & 0 & \frac{1}{\varepsilon^2} & \frac{1}{\varepsilon^2} \end{bmatrix}, \quad (4.50)$$

$$E = \begin{bmatrix} 0 & 0 & -1 & 0 & 0 & 0 & 0 & 0 & 0 & 0 & 0 & 0 \\ 0 & 0 & 0 & 1 & 0 & 0 & 0 & 0 & 0 & 0 & 0 & 0 \\ 0 & 0 & -1 & 0 & 0 & 0 & 0 & 0 & 0 & 0 & 0 & 0 \\ 0 & 0 & 0 & 1 & 0 & 0 & 0 & 0 & 0 & 0 & 0 & 0 \\ 0 & 0 & -1 & 0 & 0 & 0 & 0 & 0 & 0 & 0 & 0 & 0 \\ 0 & 0 & 0 & 1 & 0 & 0 & 0 & 0 & 0 & 0 & 0 & 0 \\ 0 & 0 & -1 & 0 & 0 & 0 & 0 & 0 & 0 & 0 & 0 & 0 \\ 0 & 0 & 0 & 1 & 0 & 0 & 0 & 0 & 0 & 0 & 0 & 0 \end{bmatrix} \quad (4.51)$$

With decomposition 1, we have

$$D_1 = \text{diag}\left\{0, 0, \frac{4}{m^2}, \frac{4}{m^2}, 0, 0, 0, 0, \frac{2}{\varepsilon^4}, \frac{2}{\varepsilon^4}, \frac{2}{\varepsilon^4}, \frac{2}{\varepsilon^4}\right\},$$

$$E_1 = \text{diag}\{0, 0, 4, 4, 0, 0, 0, 0, 2, 2, 2, 2\}$$

We can't render \tilde{R} be sign definite. If we cancel the term $\frac{1}{m}B^T(q)$ by feedback, then we obtain the new decomposition matrices:

$$D_1 = \text{diag}\left\{0, 0, 0, 0, 0, 0, 0, 0, \frac{2}{m^2}, \frac{2}{m^2}, \frac{2}{m^2}, \frac{2}{m^2}\right\},$$

$$E_1 = \text{diag}\{0, 0, 4, 4, 0, 0, 0, 0, 0, 0, 0, 0\}$$

The original uncertainty matrix $\Delta A(q)$ does not satisfy the matching condition $\Delta A(q) = B\Delta N(q)$. The matching condition is not a demanding condition imposed by the researcher to make the research easier. It basically means that the uncertainties in the system are not allowed everywhere. If the system does not satisfy the matching condition, it may still be stabilizable, but its stabilizability may not be established via quadratic stabilization method. Therefore the matching condition reveals the inherent mechanism for the success of the quadratic stabilization method. Specifically, when the system does not satisfy the matching condition, it may not be possible to render the matrix \tilde{R} in (4.44) be sign definite, and the ARE may not have the positive definite symmetric solution.

• **Control law design based on the LQG method:**

As a simple and straightforward way, we can design the control law based on the nominal system with $q = 0$. We can use pole placement or LQG method to obtain the gain matrix (Friedland, 1986).

We get the gain matrix K as:

$$K = [K1 \quad K2]$$

where

$$K1 = \begin{bmatrix} 3.7775 & 0 & 2.1348 & 0 & -2.1347 & 0 \\ 0 & 3.7775 & 0 & 2.1348 & 0 & -2.1347 \\ 0.0059 & 0 & 0.0136 & 0 & 0.2661 & 0 \\ 0 & 0.0059 & 0 & 0.0136 & 0 & 0.2661 \\ -0.0059 & 0 & -0.0136 & 0 & 0.2219 & 0 \\ 0 & -0.0059 & 0 & -0.0136 & 0 & 0.2219 \end{bmatrix}$$

$$K2 = \begin{bmatrix} 2.1347 & 0 & 0.0059 & 0 & -0.0059 & 0 \\ 0 & 2.1347 & 0 & 0.0059 & 0 & -0.0059 \\ 0.2219 & 0 & 21.883 & 0 & 9.5204 & 0 \\ 0 & 0.2219 & 0 & 21.883 & 0 & 9.5204 \\ 0.2661 & 0 & 9.5204 & 0 & 21.883 & 0 \\ 0 & 0.2661 & 0 & 9.5204 & 0 & 21.883 \end{bmatrix}$$

The simulation results are shown in chapter 5.

CHAPTER 5

PERFORMANCE EVALUATION BY SIMULATION

5.1 Centralized Control Strategy

5.1.1 Stiff Case

To evaluate the effectiveness of the control law proposed in the chapter 3, a number of simulations have been carried out using ALSIM (ALSIM is a software package for the simulation of control systems described by linear or nonlinear differential equations. Inside ALSIM, variable stepsize fourth order Runge-Kutta integration algorithm is used. The matrix operations are made easy by the library functions. User-friendly interface and the graphical display of the simulation results make ALSIM very easy to use.)

In simulation, parameter values corresponding to an experimental apparatus under construction were used:

$$a = 8\text{cm}, \quad m = 10\text{g}, \quad r = 1\text{cm}, \quad J = 10\text{g} - \text{cm}^2$$

We choose the natural frequency $\omega_n = 125.6$ rad/sec (20 Hz) and the damping factor $\zeta = 0.707$. Then, the gains in the computed torque controller are:

$$k_v = 2\zeta\omega_n = 177.6$$

$$k_p = \omega_n^2 = 15775.36$$

The bias level was set at

$$N = 0.055$$

A circular trajectory was chosen. Typical performance is exemplified by the ability of the system to acquire and track a circular trajectory 8cm in diameter. The reference trajectory is defined by

$$x_d = 0.04 \cos(5t), \quad y_d = 0.04 \sin(5t)$$

The results are shown in Figure 5.1 through Figure 5.4. Figure 5.1 shows how the control system acquires and follows the reference trajectory. It justifies the effectiveness and accuracy of the control algorithms. Figure 5.3 shows the control torques. Note that they are all positive, as required. After the system acquires the circular trajectory, the control torques fluctuate periodically, as expected. Figure 5.4 shows the input voltages. The input voltages are all less than their maximum value 24 volts.

In order to investigate the effect of friction, we add the friction force acting on the pulley. Consider the Coulomb friction: $\alpha_i \text{sgn}(\dot{l}_i)r$, where α_i is the magnitude, \dot{l}_i is the velocity of the tendon.

$$\dot{l}_i = \dot{y} \sin \beta_i - \dot{x} \cos \beta_i \quad (5.1)$$

The input torque becomes:

$$T_i - \alpha_i(\dot{l}_i)r \quad (5.2)$$

where $\alpha_i \text{sgn}(\dot{l}_i)r$ is the resistance torque induced by the friction.

The system dynamics becomes

$$M(q)\ddot{q} + C(q, \dot{q})\dot{q} = rB(T - T_{fric}) \quad (5.3)$$

where T_{fric} is the friction torque.

$$T_{fric} = \begin{bmatrix} \alpha_1(\dot{l}_1)r \\ \alpha_2(\dot{l}_2)r \\ \alpha_3(\dot{l}_3)r \\ \alpha_4(\dot{l}_4)r \end{bmatrix}$$

Take the value $\alpha = 0.2$. Then the friction torque is $\alpha \times r = 2 \times 10^{-3}$. It is about 10% of the average value of the motor torque.

High gain is helpful for overcoming the effect of friction. In simulation, we choose the gains as: $k_v = 222, k_p = 24649$. The value of N is set at $N = 0.05$.

Of course, the gains can not be chosen arbitrarily large. Otherwise, the motor will saturate.

Simulation results are shown in Figure 5.5, Figure 5.6 and Figure 5.7 through Figure 5.9. When α_i is small enough, the effect of the friction is almost negligible. But as α_i increases, the friction force may seriously degrade performance.

Generally, there are two effects due to the friction:

- The orbit discrepancy is increased. (The orbit discrepancy is defined as the difference between the actual radius and the desired radius of the circle).
- The slip-stick phenomenon is observed.

Using an observer makes matters worse. From Figure 5.7, we see that the trajectory is not smooth. The reason is the dynamics of the observer does not incorporate the friction term. This makes the estimates of the velocity \hat{x}, \hat{y} deviate the true values of \dot{x}, \dot{y} . This is evident in Figure 5.9

Combining observer and friction force will leads to serious results: High frequency slip-stick is present and the tracking performance becomes poor.

The simulation results using passivity-based method are shown in Figure 5.10 through Figure 5.11 (Same parameter and gain values used in the computed-torque method are used). Control law performance in the presence of friction are shown in Figure 5.12, Figure 5.13 for full state feedback control and in Figure 5.14, Figure 5.15 for observer-based feedback control law.

Basically, there is no big difference between these two methods except in the passivity-based method with observer in the presence of friction, the control torques are smoother than the control torques in the same case when computed-torque method is used.

To test the robustness of the proposed control law, we changed some parameters in the simulation and observed that practically no change in tracking accuracy has

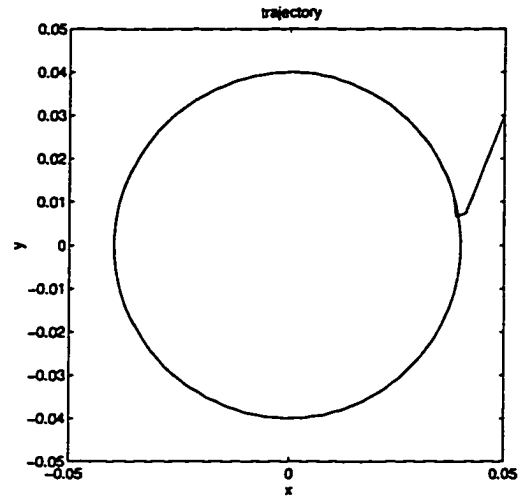


Figure 5.1 Trajectory of the workpiece tracking a circle with radius 4 cm. Computed torque method in the absence of friction.

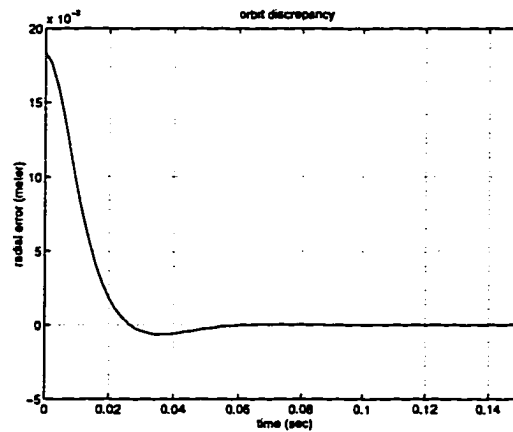


Figure 5.2 Orbit discrepancy. The radial error converges to zero in 60 ms. Computed torque method.

occurred. For example, when we change the mass of the workpiece by 10%, the radius of the true trajectory is still 3.99 cm.

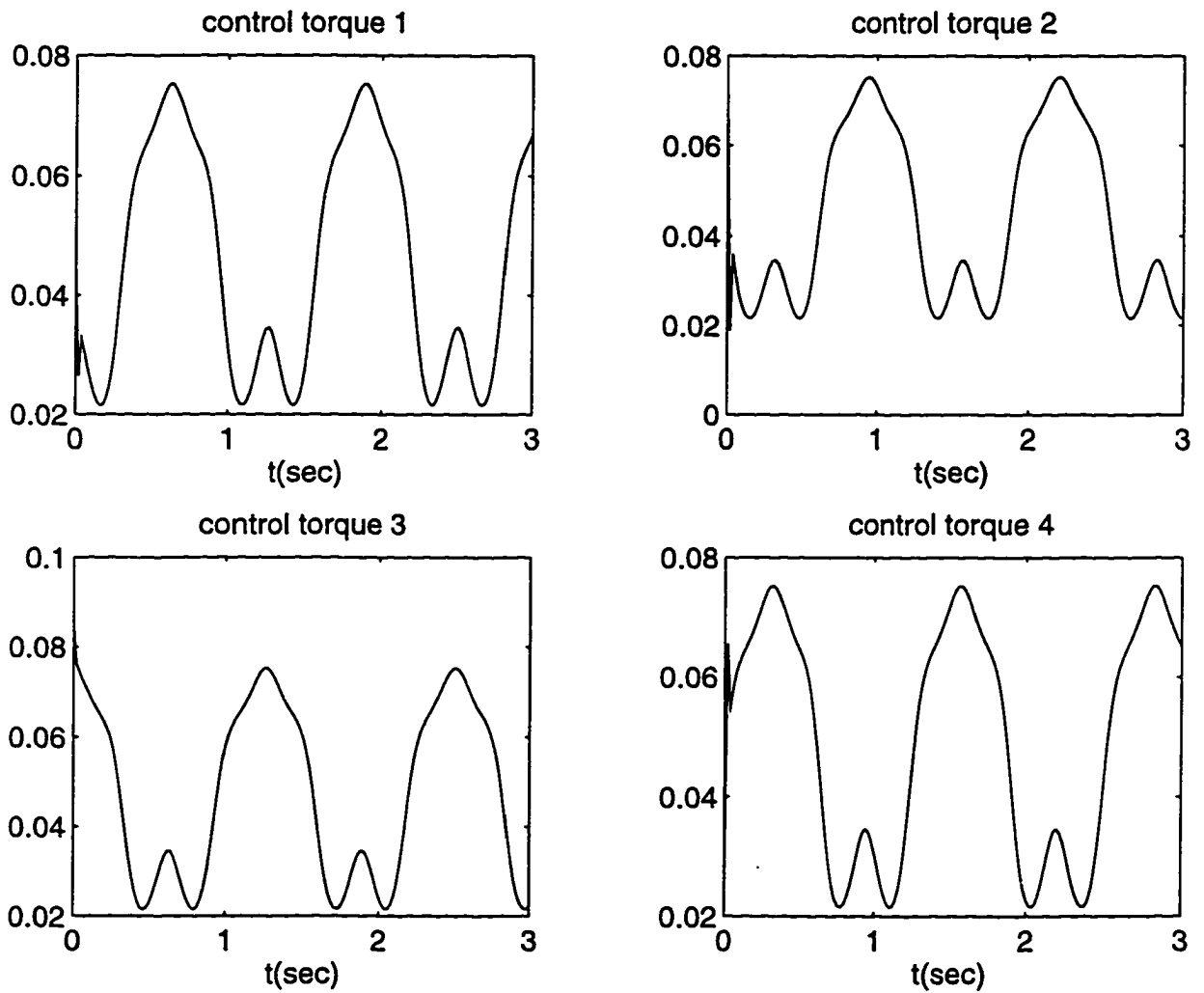


Figure 5.3 Control torques exerted on each motors. They are all positive.

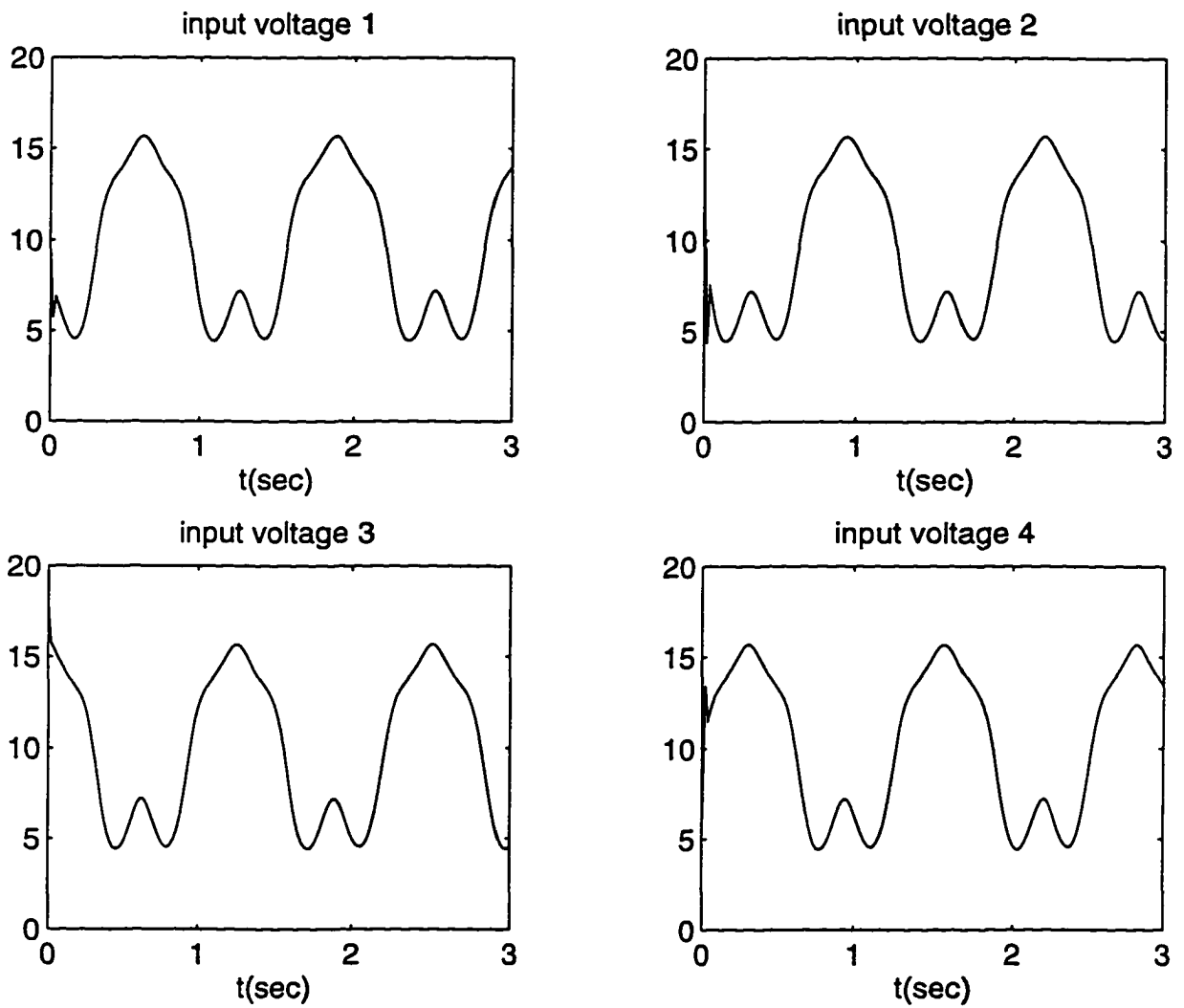


Figure 5.4 Input voltages are less than the allowable level, 24 volts

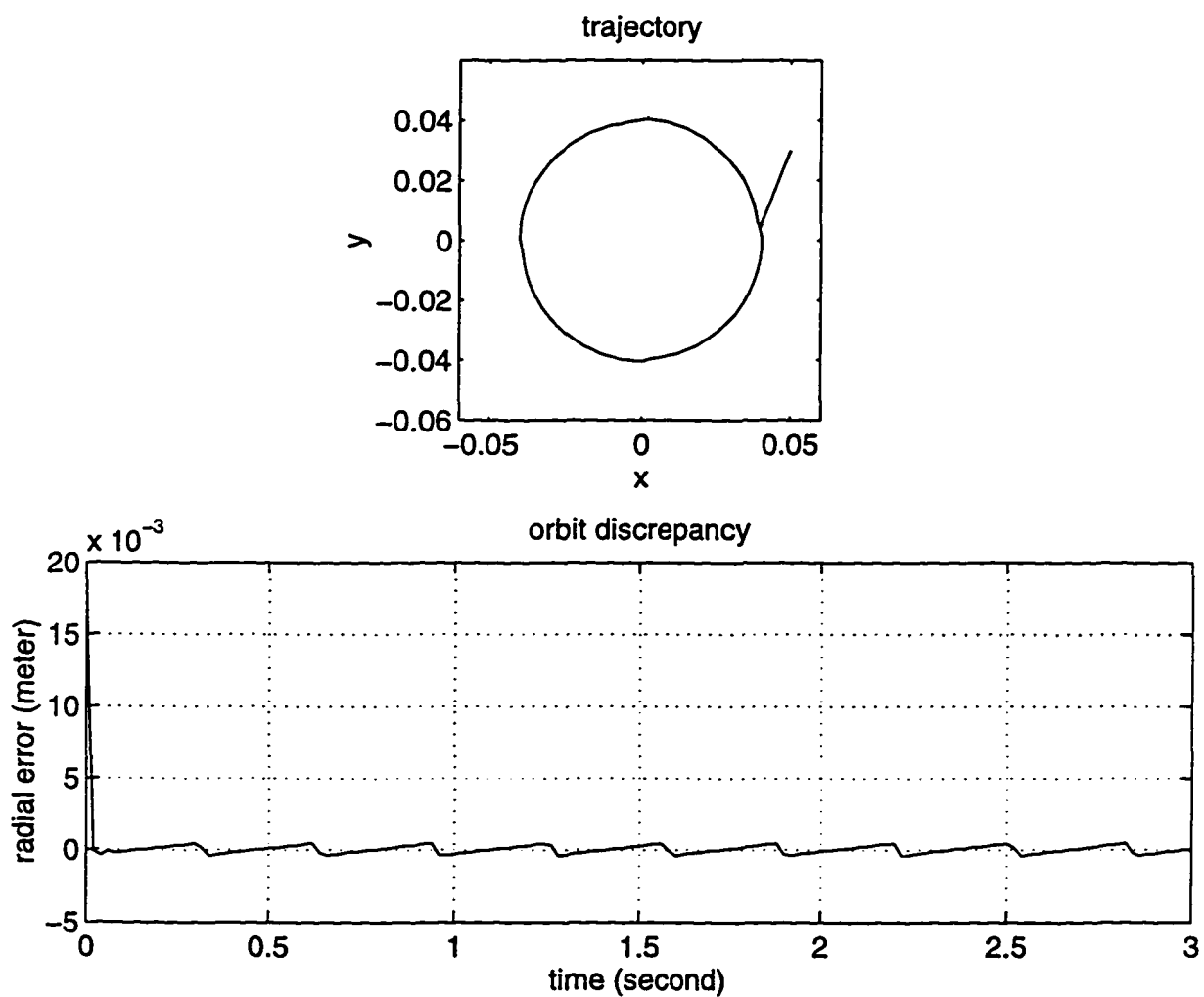


Figure 5.5 Trajectory of the workpiece in the presence of friction. Computed torque method with full state feedback.

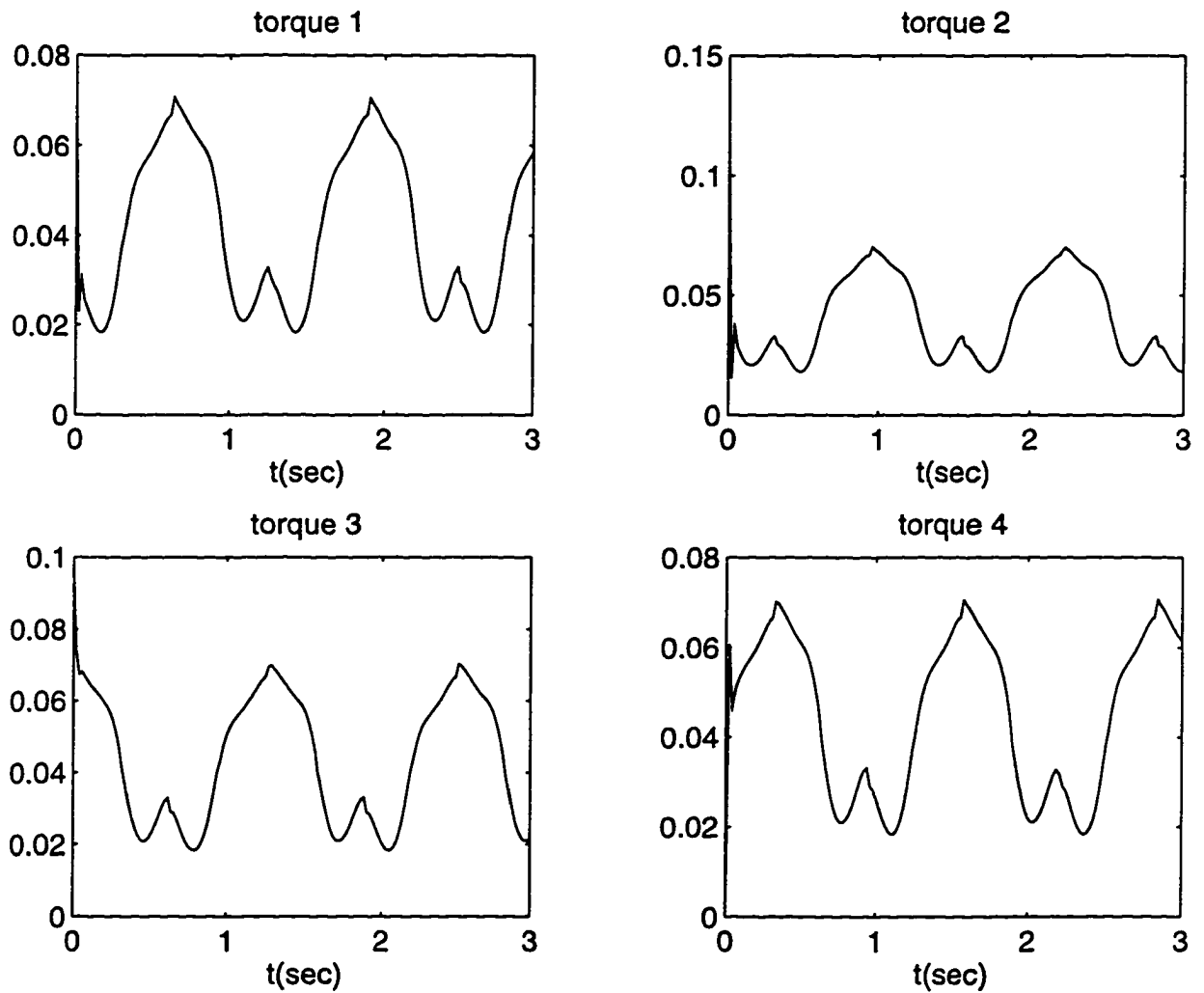


Figure 5.6 Control torques exerted on each motors. Friction is present.

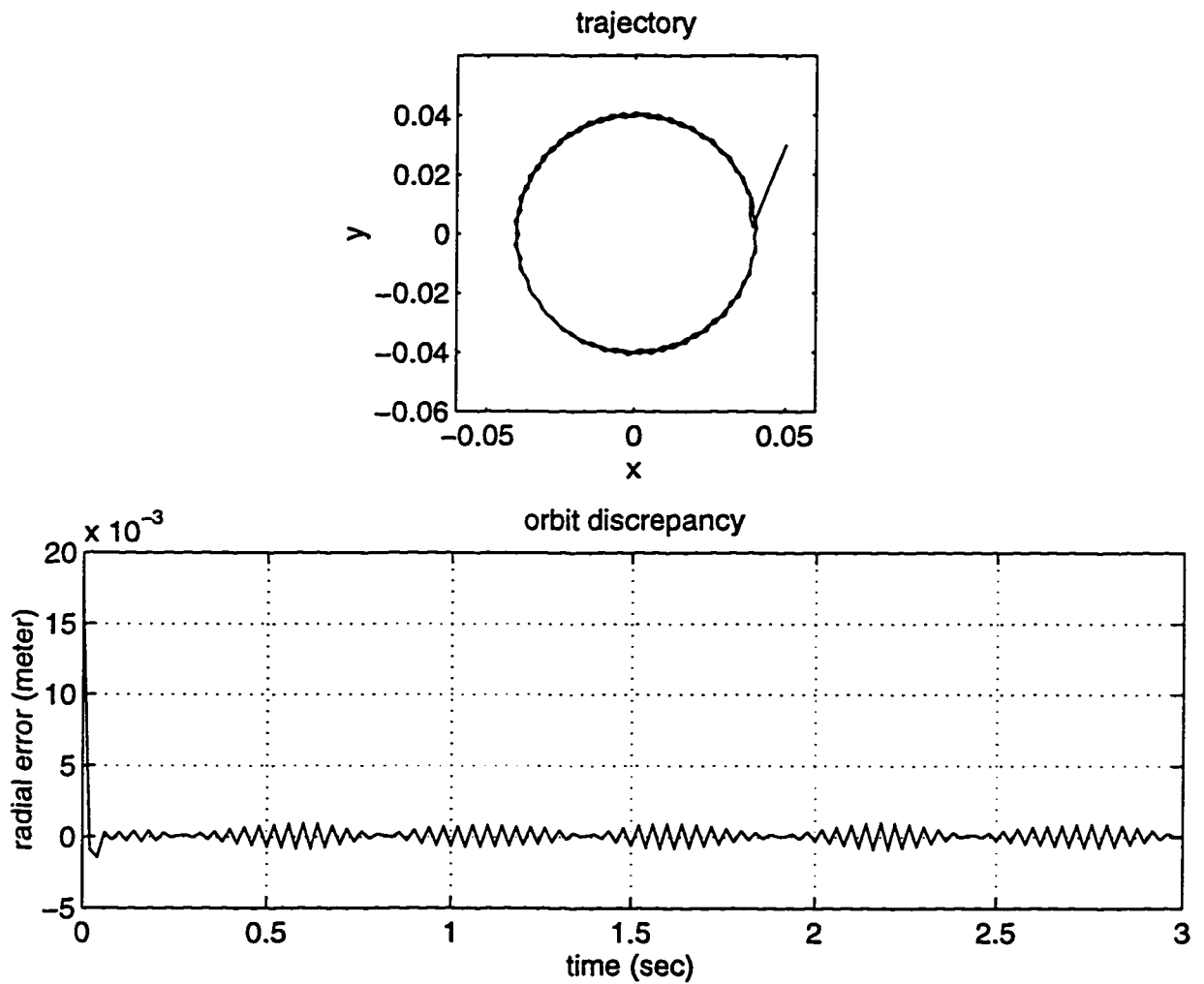


Figure 5.7 Trajectories of the workpiece in the presence of friction. Computed torque method with observer. High frequency slip-stick phenomenon is observed.

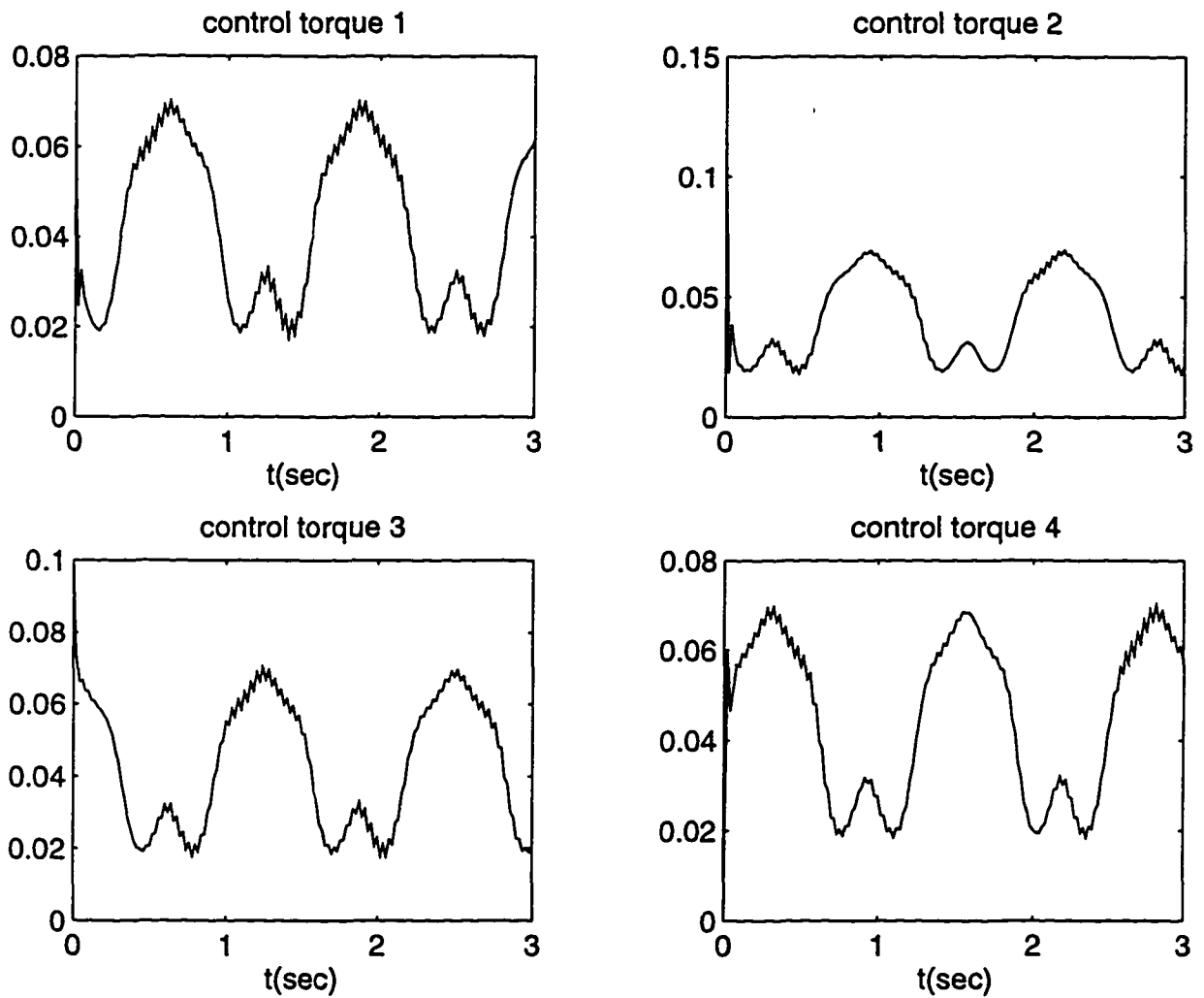


Figure 5.8 Control torques exerted on each motors are not smooth. Friction is present. Observer is used

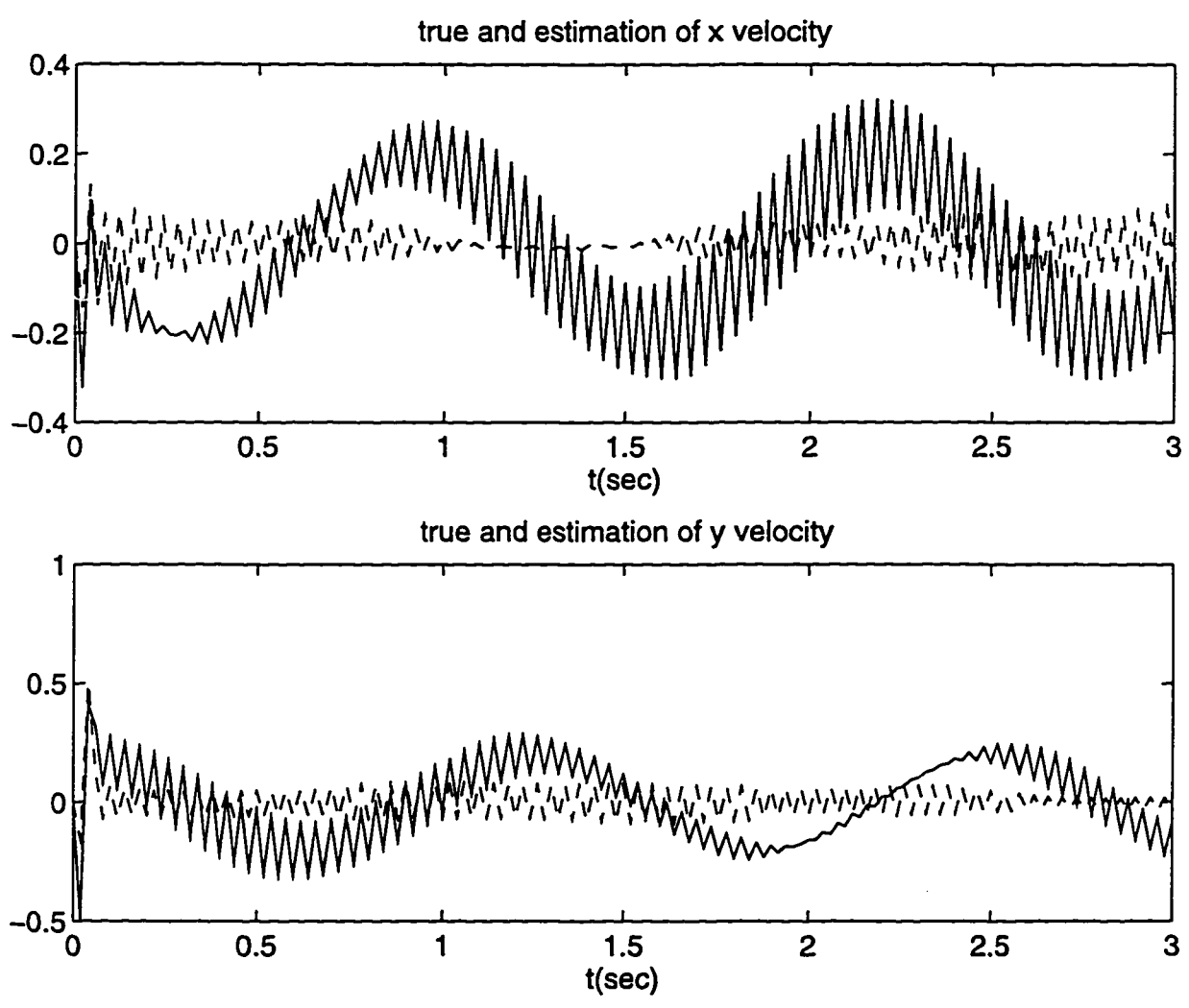


Figure 5.9 True(solid line) and estimated (dashed line) velocities. The poor performance is the result of the unmodeled friction term in the construction of observer

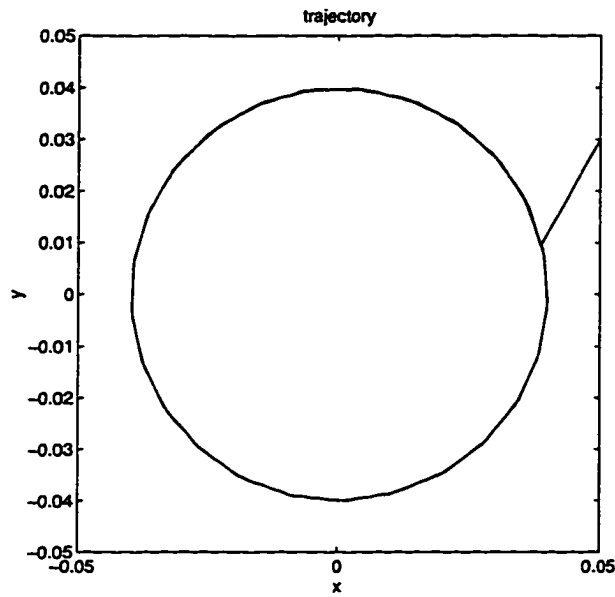


Figure 5.10 Trajectory of the workpiece tracking a circle with radius 4 cm. Passivity-based method in the absence of friction.

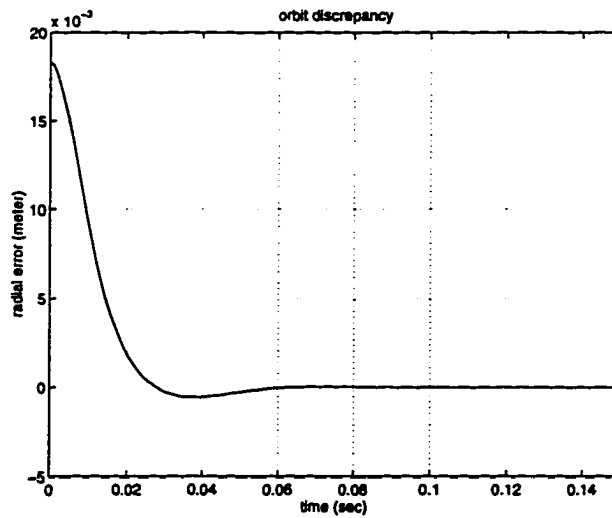


Figure 5.11 Orbit discrepancy. The radial error converges to zero in 60 ms. Passivity-based method.

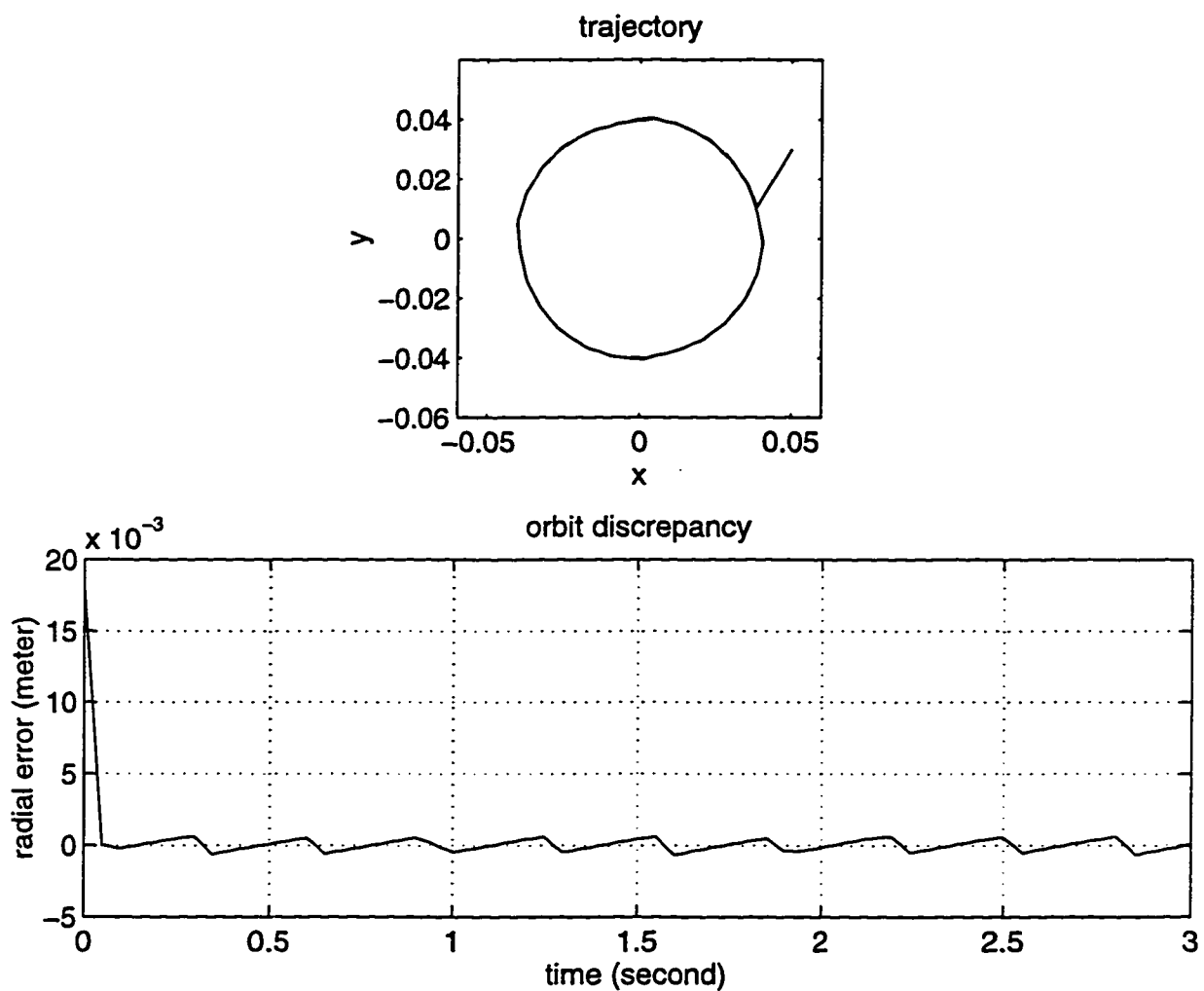


Figure 5.12 Trajectory of the workpiece in the presence of friction. Passivity-based method with full state feedback.

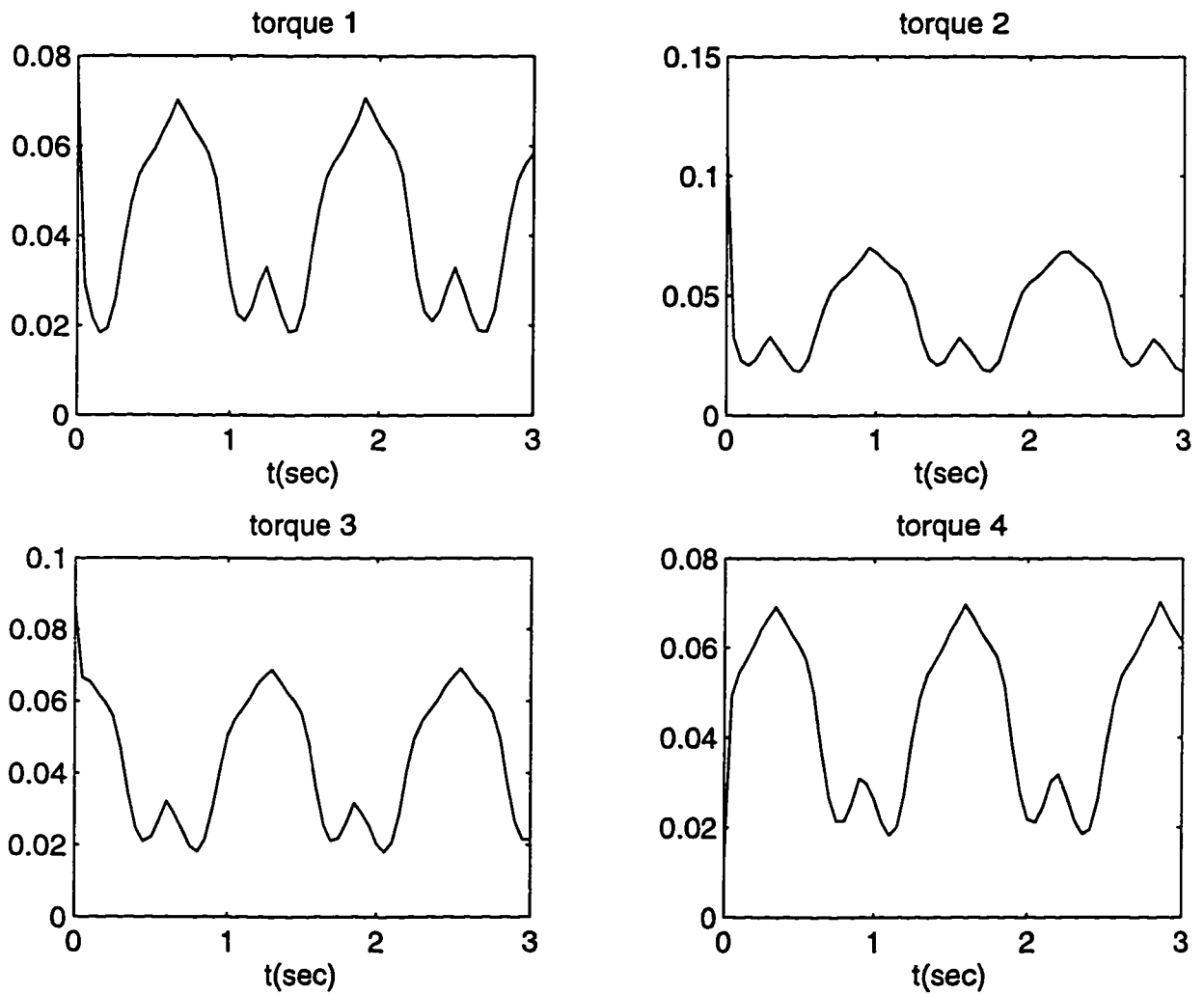


Figure 5.13 Control torques exerted on each motors. Friction is present.

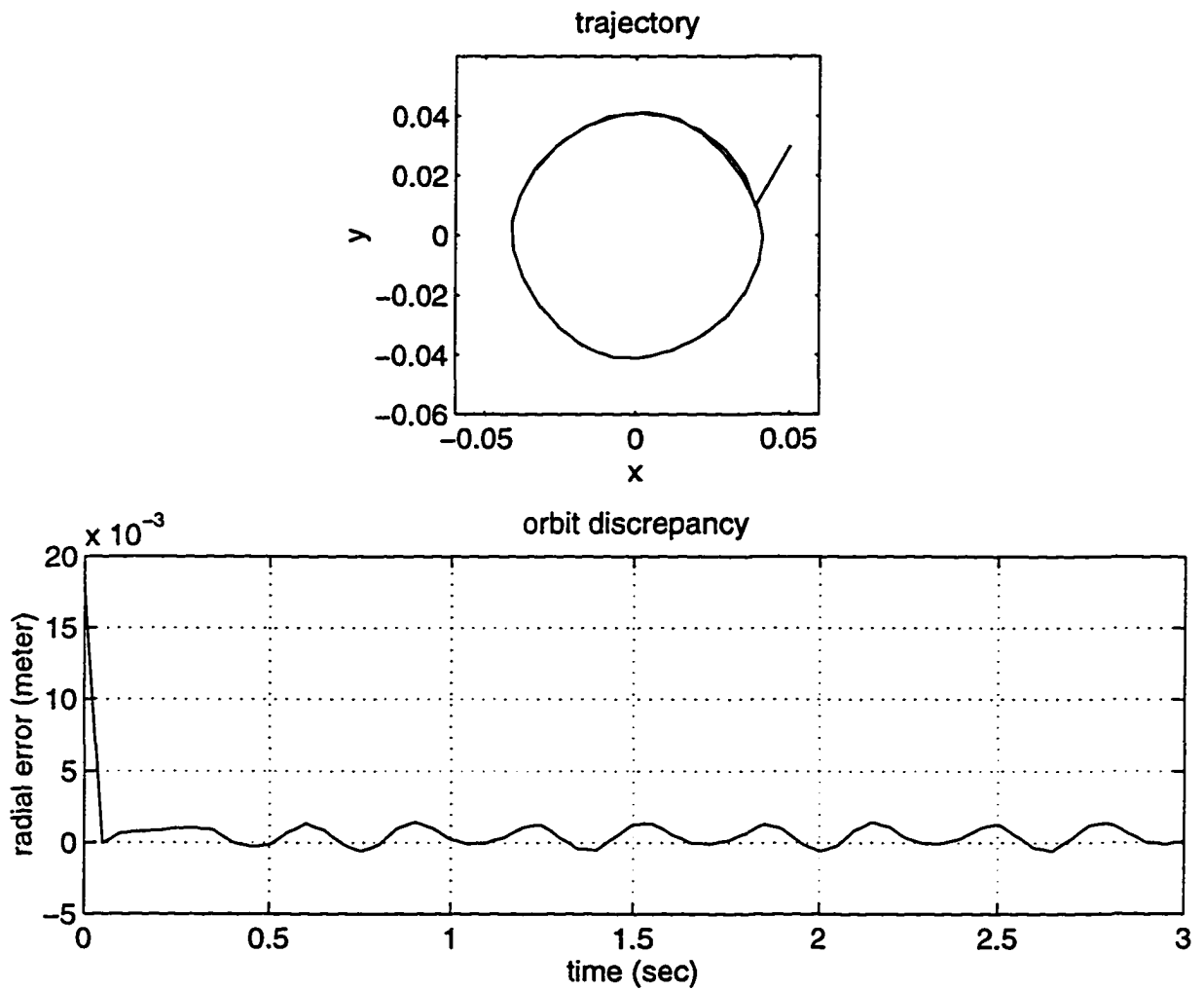


Figure 5.14 Trajectories of the workpiece in the presence of friction. Passivity-based method with observer.

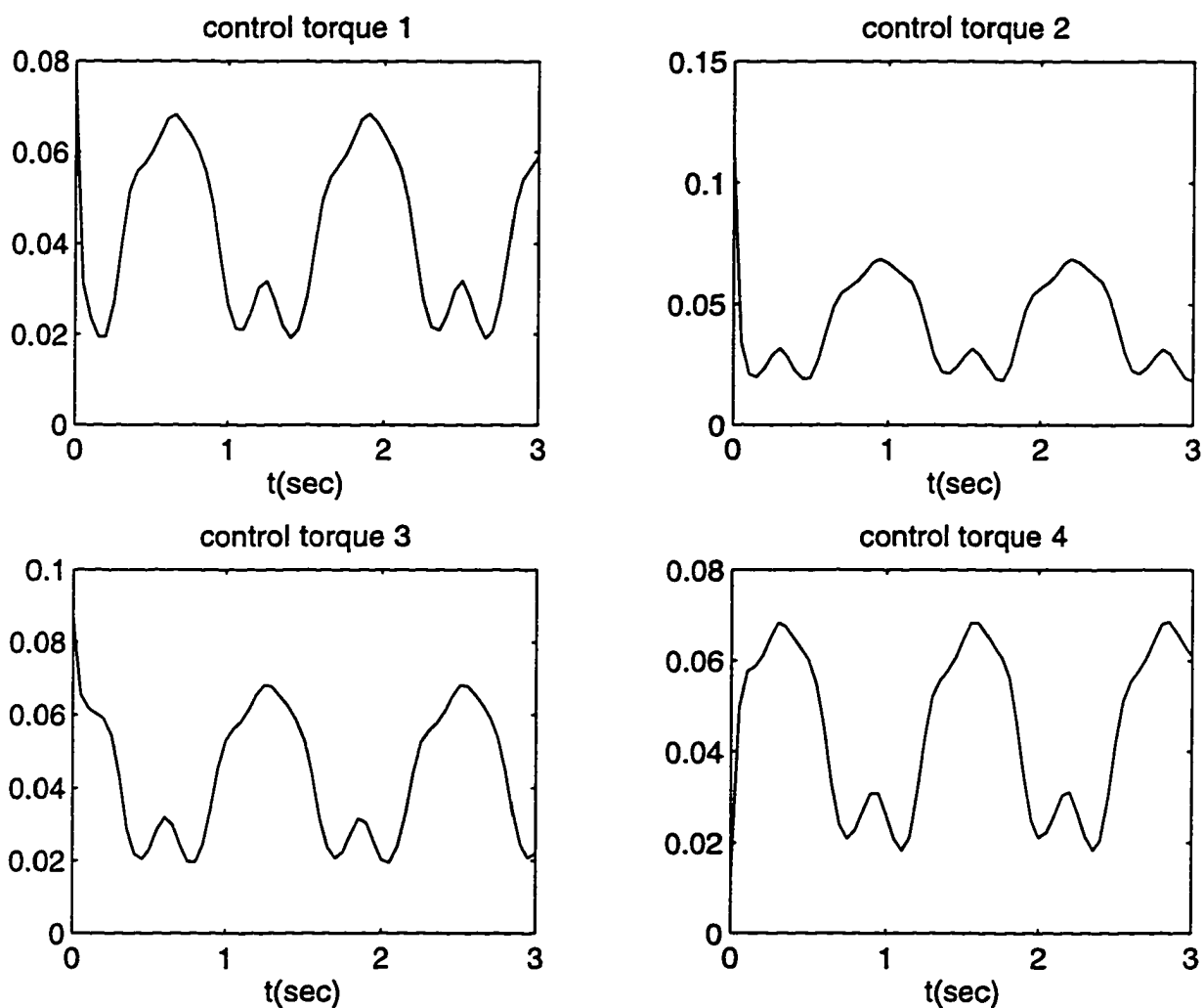


Figure 5.15 Control torques exerted on each motors. Friction is present. Observer is used

5.1.2 Elastic Case

The elastic modulus k was taken as $1000N/m^2$. This value is much lower than would be expected in practice but was taken to accentuate the effect of elasticity.

The desired trajectory is a circle with radius $4cm$. We choose

$$\lambda = 8, \sigma = 10, \delta = 0.05, N = 0.05$$

The slow control gains were chosen to be $k_v = 177.6, k_p = 15775.36$ and the fast control gains were chosen as $k_v = 15, k_p = 50$.

The parameter N controls the magnitude of the torque and hence the magnitude of the input voltage. N should be chosen to ensure the input voltage is less than its allowable maximum value.

Two control laws are used, one without sliding mode control, the other with sliding mode control, In the first case, the true trajectory tends to a circle with radius $3.86cm$. There is a discrepancy between the actual trajectory and the desired trajectory. This is due to the disturbance of the residue value of η .

In the second case, the sliding mode control is used to overcome the disturbance, the radius of the true trajectory is $3.99cm$. We see that significant improvement is achieved.

From Figure 5.18, we see that the fast variable η tends to zero rapidly under the action of the fast control u_f .

Simulation results show that the sliding mode control works in the linear region most of time and acts as a high gain control. So the performance improvement is achieved through high gain control. This is consistent with the fact that in the feedback system, large loop gain can decrease the effect of the disturbance and reduce the sensitivity of the system performance to the parameter variation.

The stiff case of the agonistic control problem is the limiting form of its elastic case when the elastic modulus of the tendon approaches infinity. The new phenomenon appeared in the elastic case is the oscillations in the fast variables.

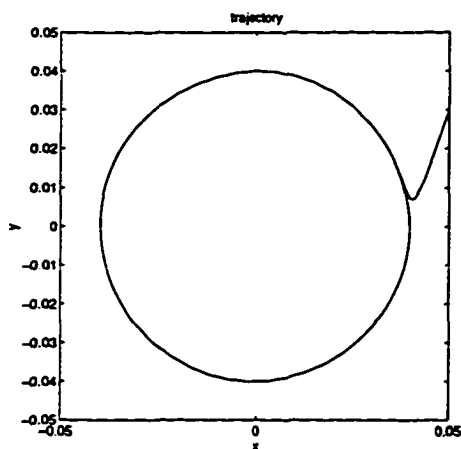


Figure 5.16 Composite control law performance for the agonistic system with elastic tendons

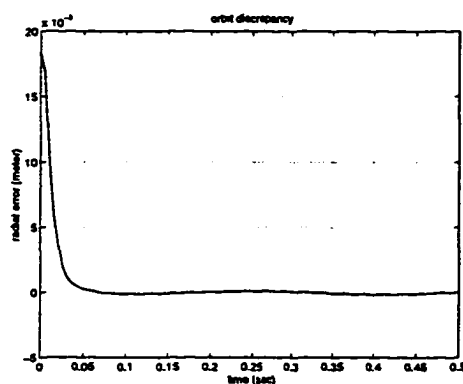


Figure 5.17 Orbit discrepancy

This investigation shows that the effect of elastic tendons in agonistic control can be compensated for by appropriately modifying the control law designed for inelastic tendons. The elastic control entails more information than stiff control. In the elastic case, there is no one to one correspondence between the angular position of the actuator and the position of the workpiece, both are required to be measured. This study assumes all the state variables are available. If, as would be expected, not all these variables can be measured, they must be estimated via observer.

Figure 5.23 through Figure 5.26 shows the simulation results when observer is incorporated into the system. We see that the observer gives good estimates and the system works well although the radial error increases a little bit.

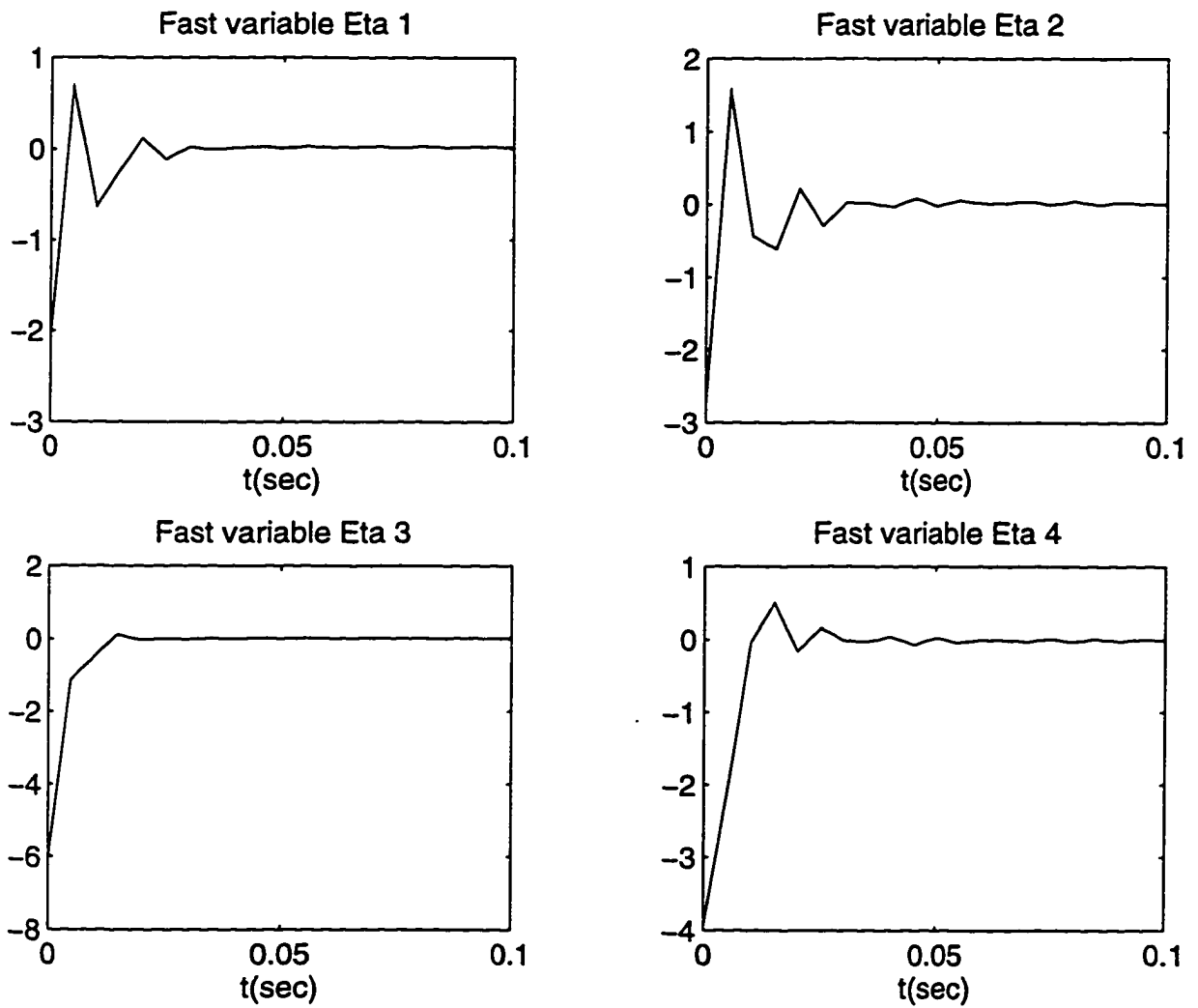


Figure 5.18 Behavior of fast boundary-layer state η

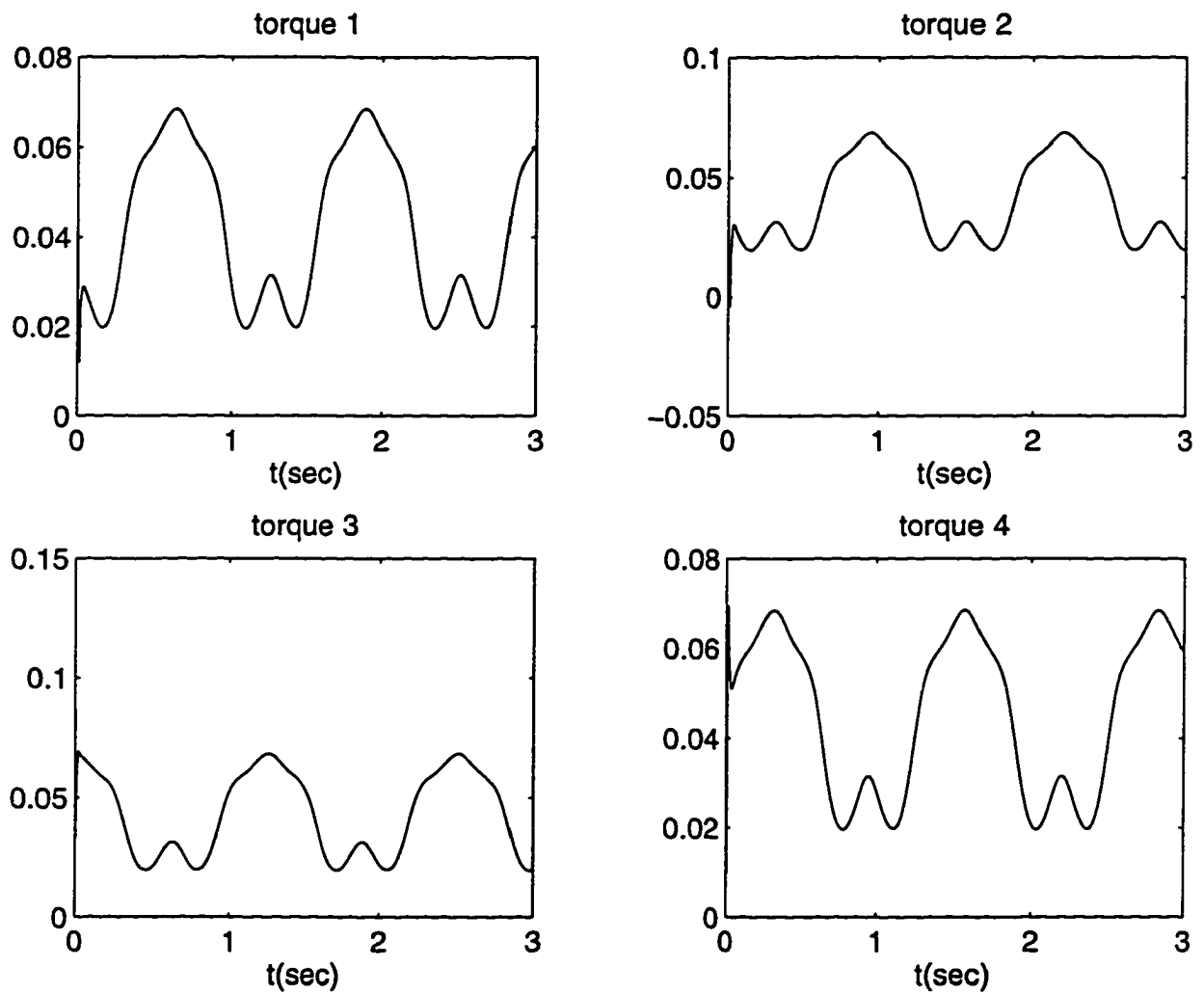


Figure 5.19 Composite control developed in tracking circular trajectory

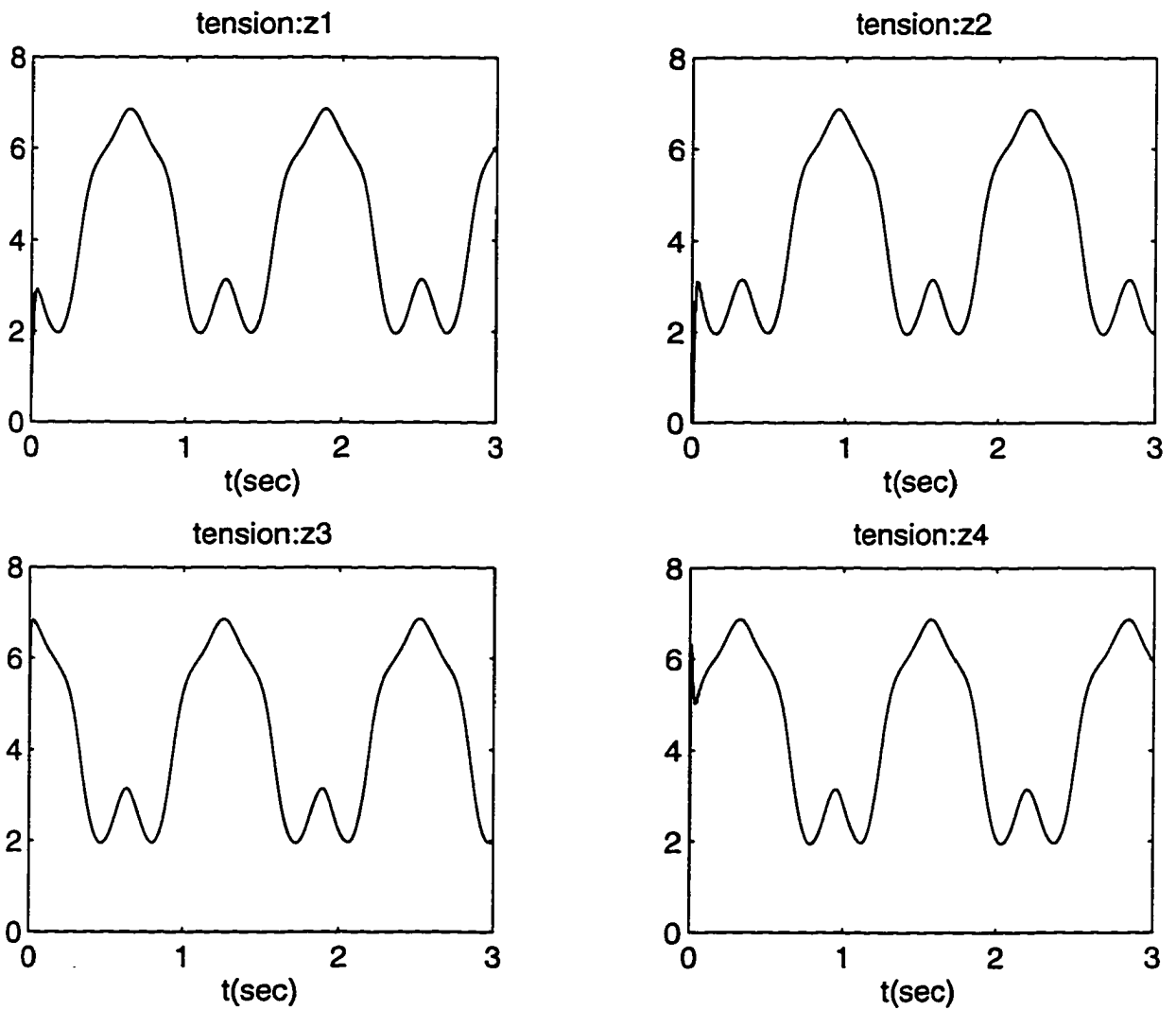


Figure 5.20 Control law maintains positive tensions in the tendons

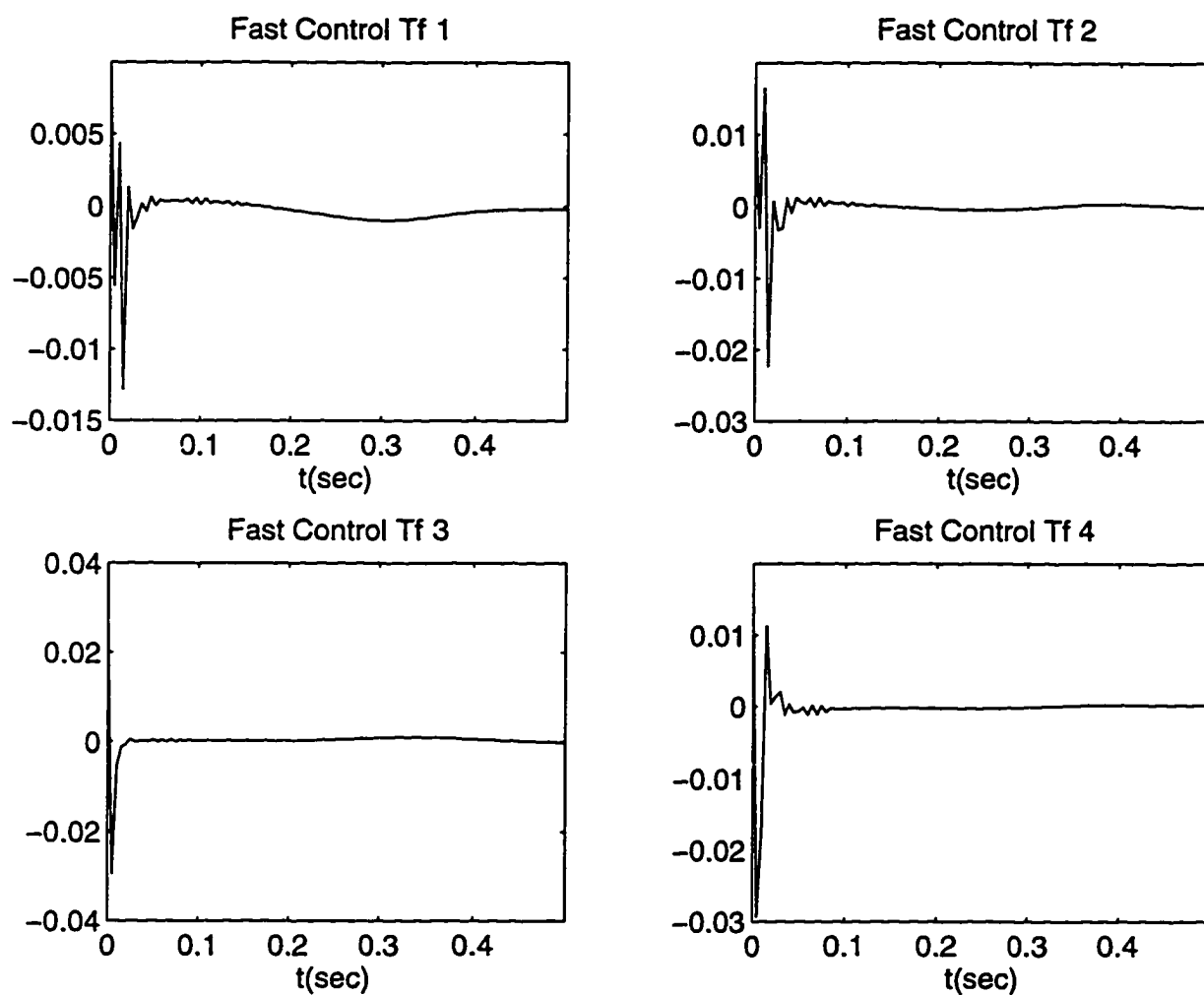


Figure 5.21 Fast control is used to suppress the oscillations appeared in the fast variables

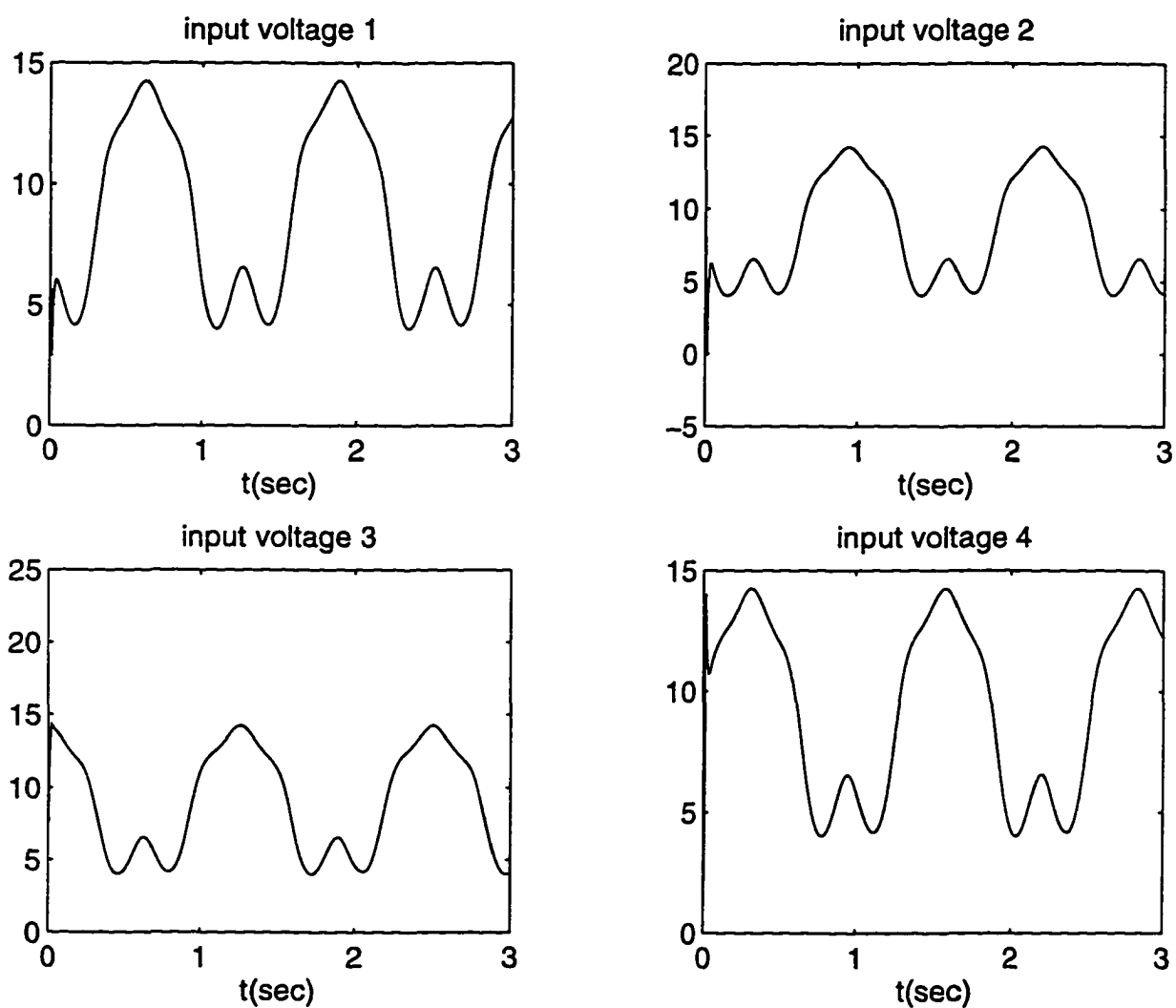


Figure 5.22 Input voltages are less than allowable level, 24 volts

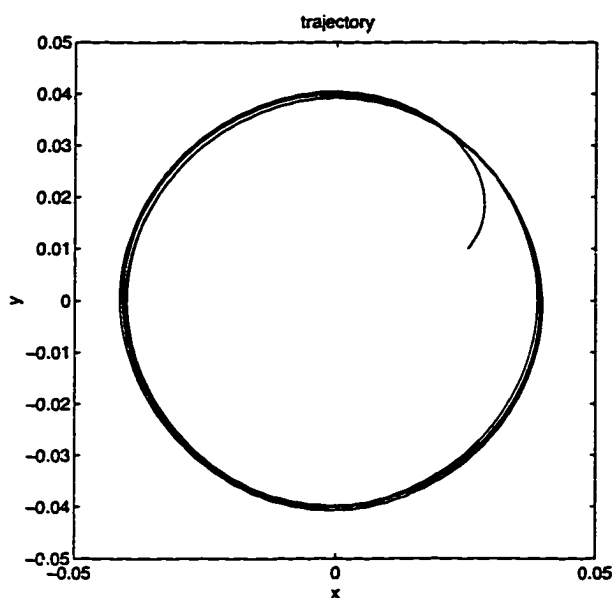


Figure 5.23 Composite control law performance for the agonistic system in the elastic case. Estimated values from observer are used in the control law

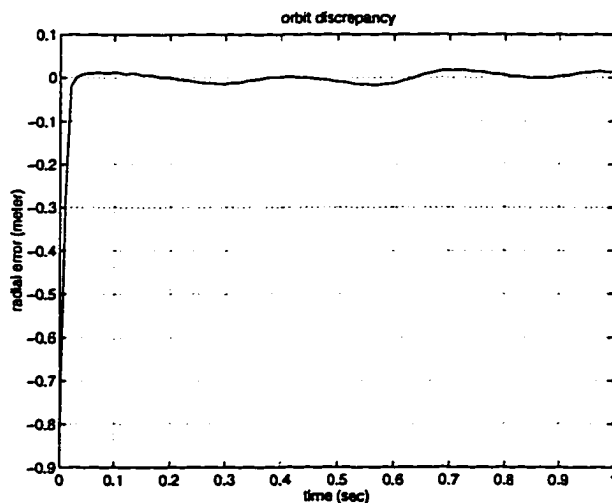


Figure 5.24 Radial error for tracking a circle in elastic case. Observer is incorporated in the control law

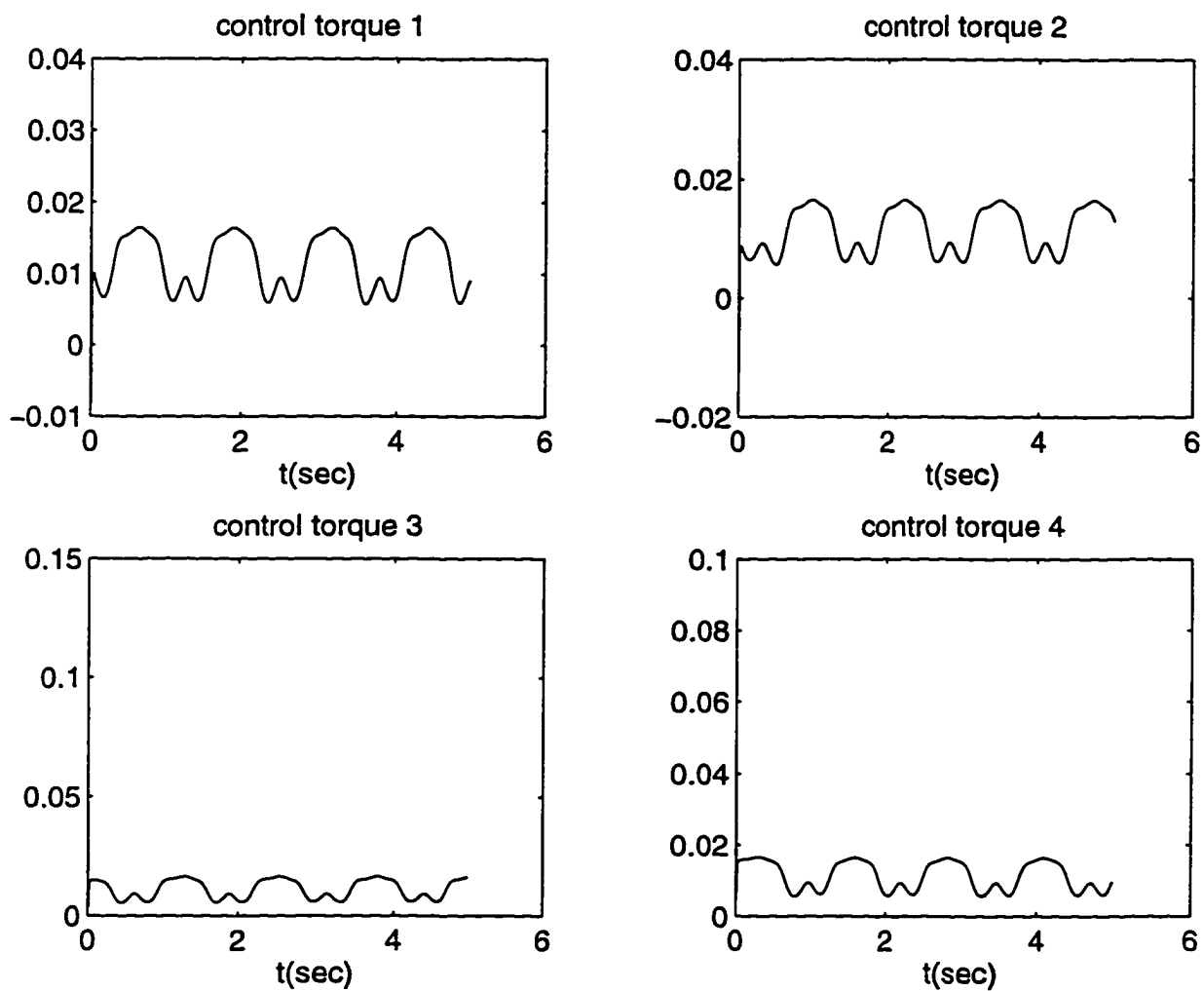


Figure 5.25 Control torques are positive, as physically required

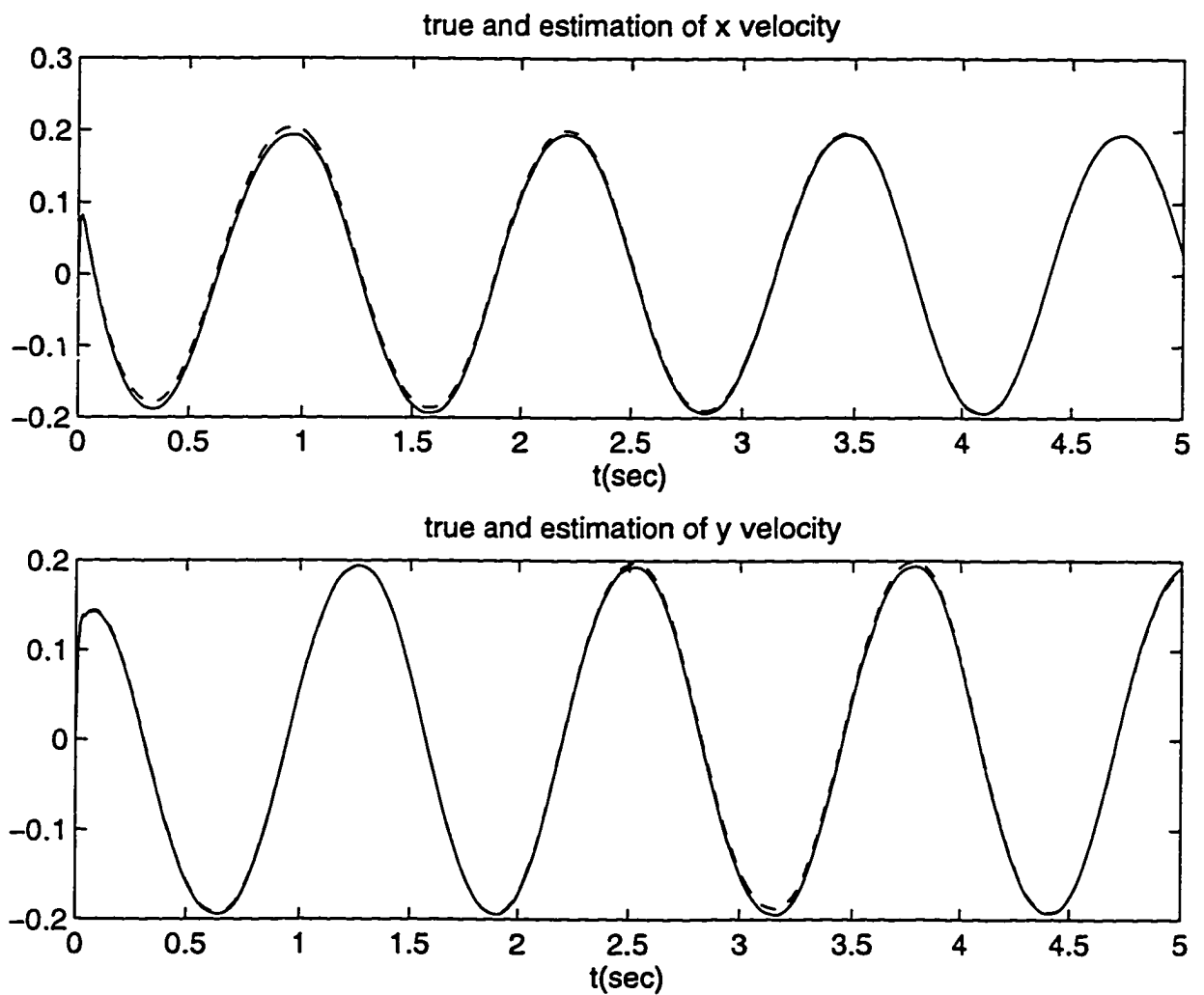


Figure 5.26 True and estimated velocities. The estimated values closely follow the true values

5.2 Decentralized Control Strategy

To evaluate the performance of the decentralized control law described in Chapter 3, we apply the decentralized control law to the actual dynamics model (2.50). The tension is estimated from the observer and the true tension is calculated from (2.14).

The base level for the bias torque was set at $N = 0.05$

A number of simulations were performed. Typical performance is exemplified by the ability of the system to acquire and track a circular trajectory 8cm in diameter. The reference trajectory is defined by

$$x_d = 0.03 \cos(5t), \quad y_d = 0.03 \sin(5t)$$

The desired trajectory is expressed in terms of the coordinates x and y . It should be transformed to the requirements on the angular position of each motor.

The gains in the control law are taken as: $k_v = 177.6$, $k_p = 15775.36$. The initial position of the workpiece is $x_0 = 1\text{cm}$, $y_0 = 1\text{cm}$. N is set to be 0.05. It determines the nominal magnitude of the torque. The result of the simulation are shown in Figure 5.27 through Figure 5.34.

They reveal that the decentralized control scheme has the good ability to track the desired trajectory and keep the tendon in tension at the same time.

However, through simulation, we also find one of the disadvantage of the decentralized control strategy: it can not operate over entire working space. The working domain is smaller than the available area. If the trajectory extends too far from the center, the system may become unstable. Generally, the radius of the desired circle should be less than $\frac{a}{2}$ although theoretically its maximum value can be $\frac{a}{\sqrt{2}}$.

To illustrate this point, we choose the radius of the desired circle as 0.04cm. The simulations are shown in Figure 5.35. we see that the system works well at the initial period of time then goes into disorder.

The above results assume direct measurements of angular velocities of the motors. When such measurements are not available, estimation of the angular

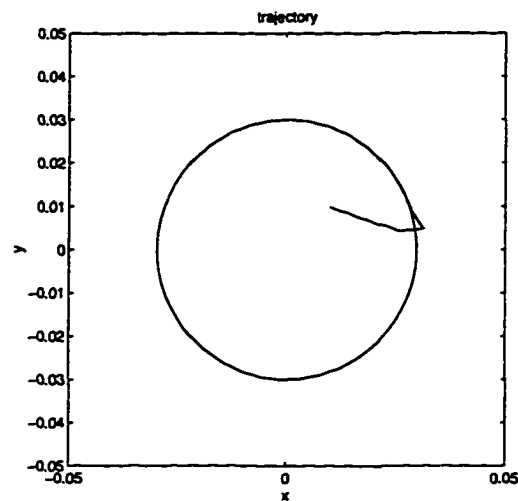


Figure 5.27 Decentralized control law achieves good performance for the agonistic system

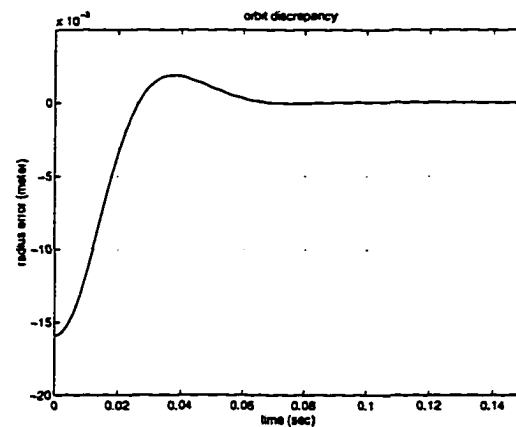


Figure 5.28 Orbit discrepancy. decentralized control strategy. full state feedback velocities can be included in the observer. When the estimated angular velocities are used in the control law, the gains in the PD portion should not be taken too large. This implies the decreased response speed. System bandwidth is sharply reduced. In addition, Use of observer will also result in increased orbit error. This can be seen from Figure 5.38. In that simulation, we choose the gains as $k_v = 15$, $k_p = 50$.

Incorporating observer into decentralized control law will lead to reduced system bandwidth and increased orbit discrepancy.

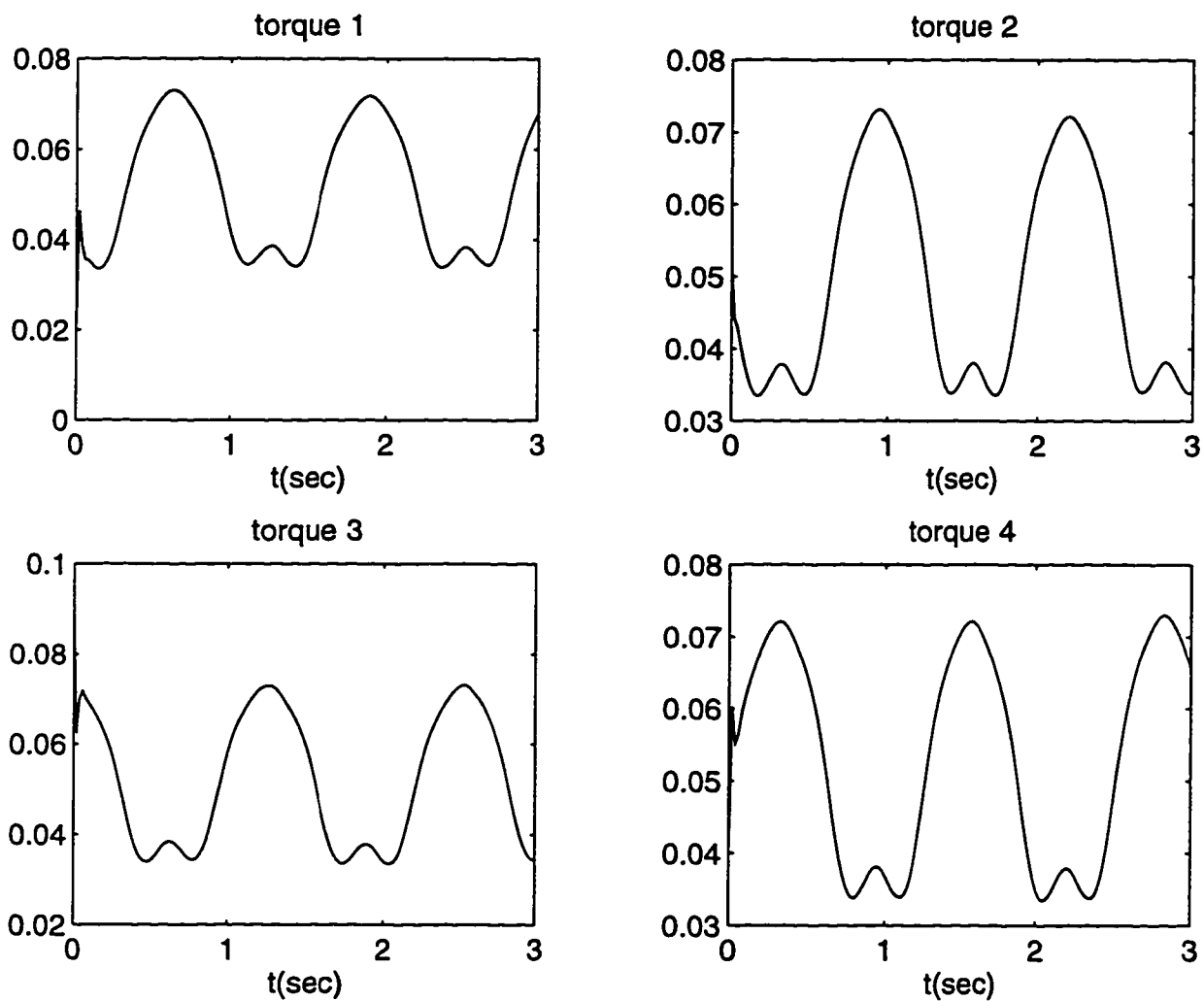


Figure 5.29 Decentralized control law can also maintain the positive tensions in all tendons

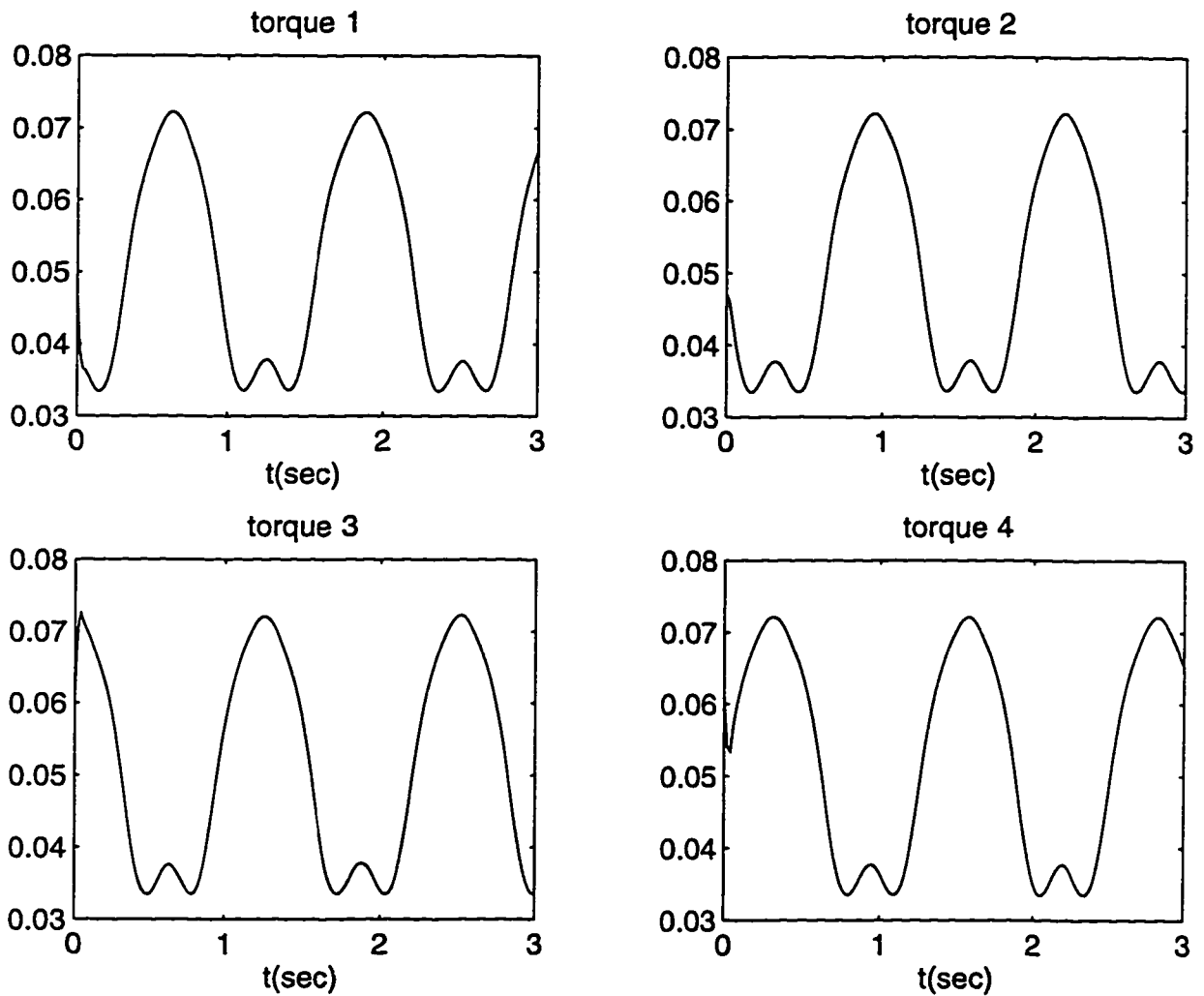


Figure 5.30 The base value in each torque. The base torques are calculated from equilibrium condition

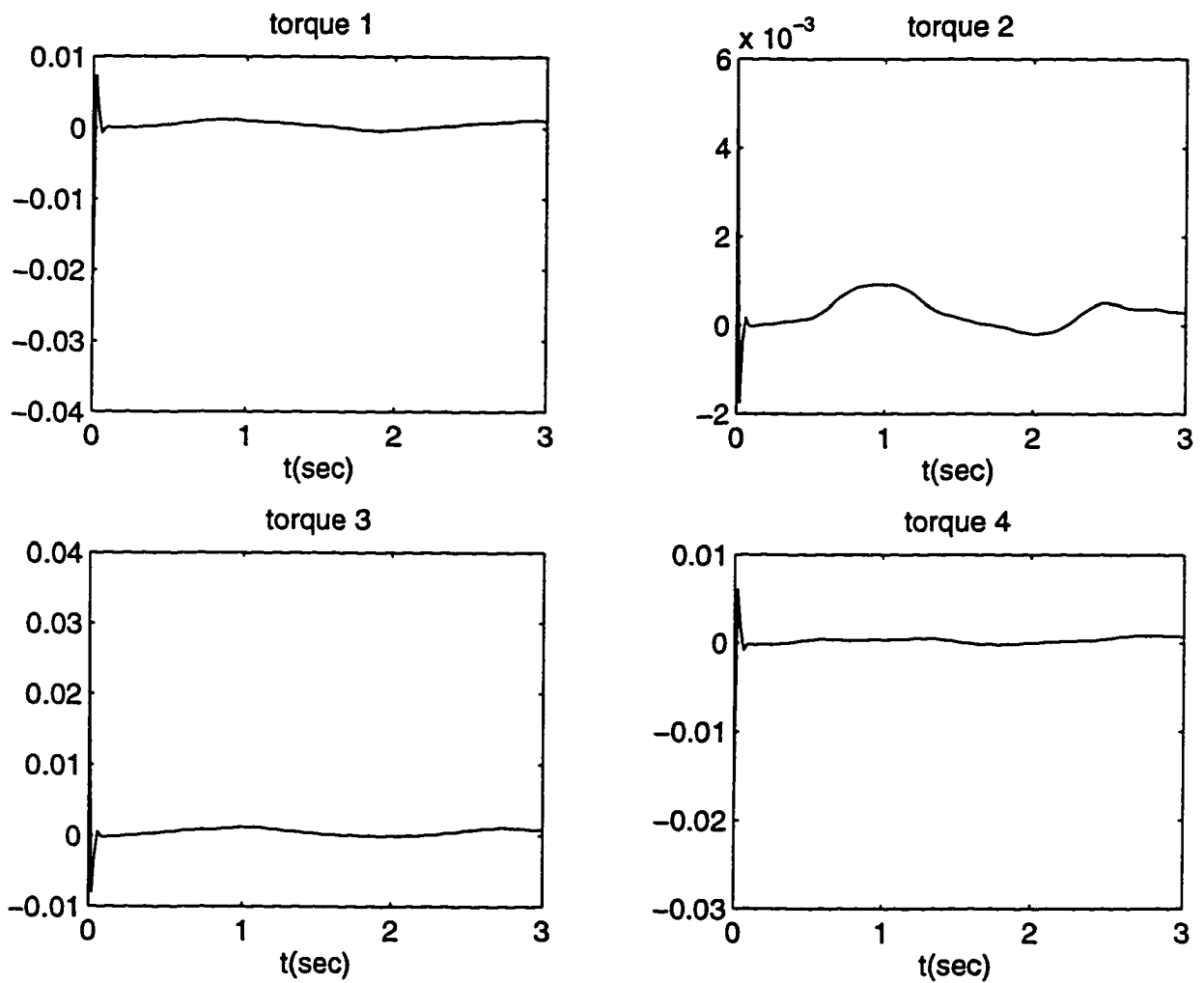


Figure 5.31 The correction part in each torque which is responsible for the movement of the workpiece

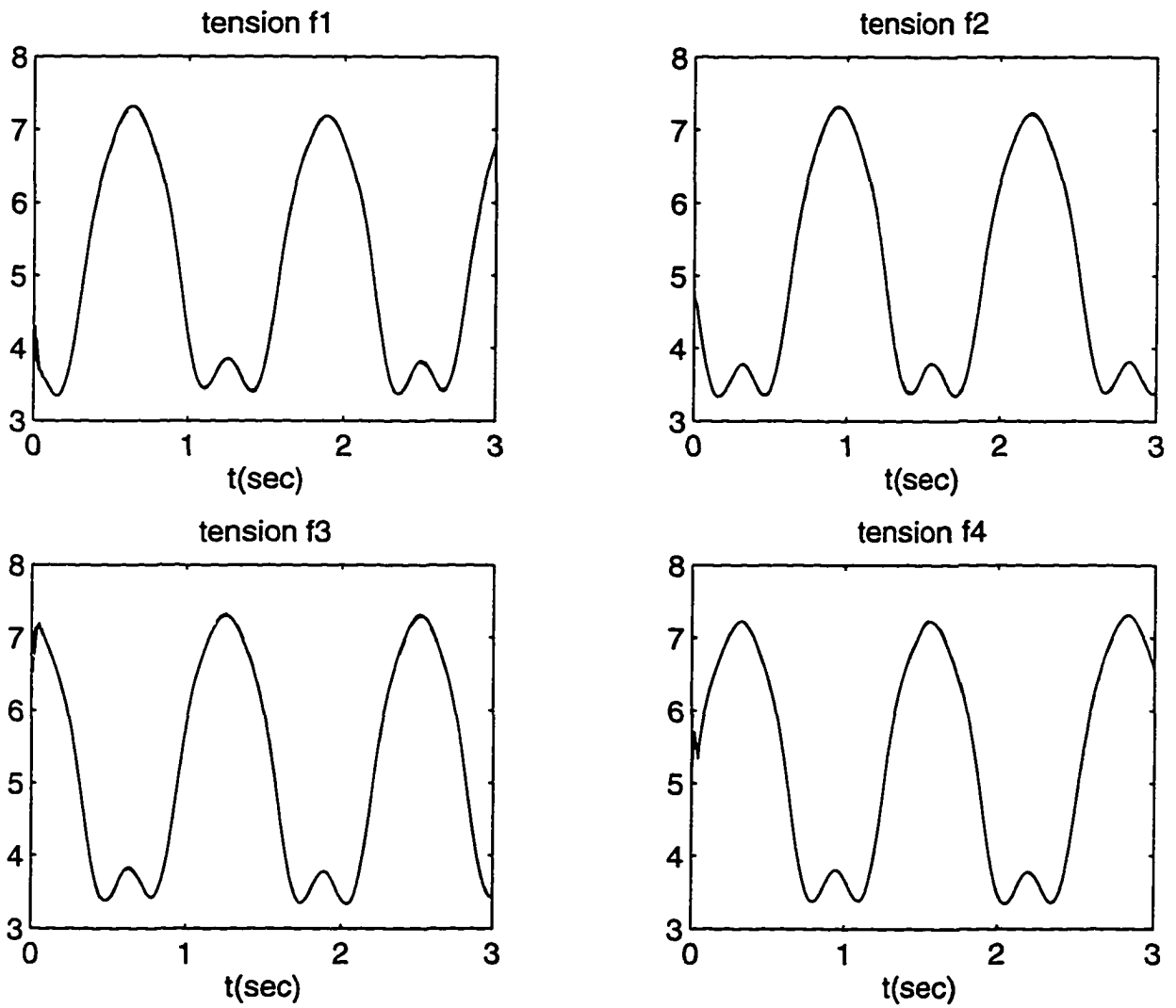


Figure 5.32 Tensions in each tendon. solid line: actual value. dashed line: estimated value

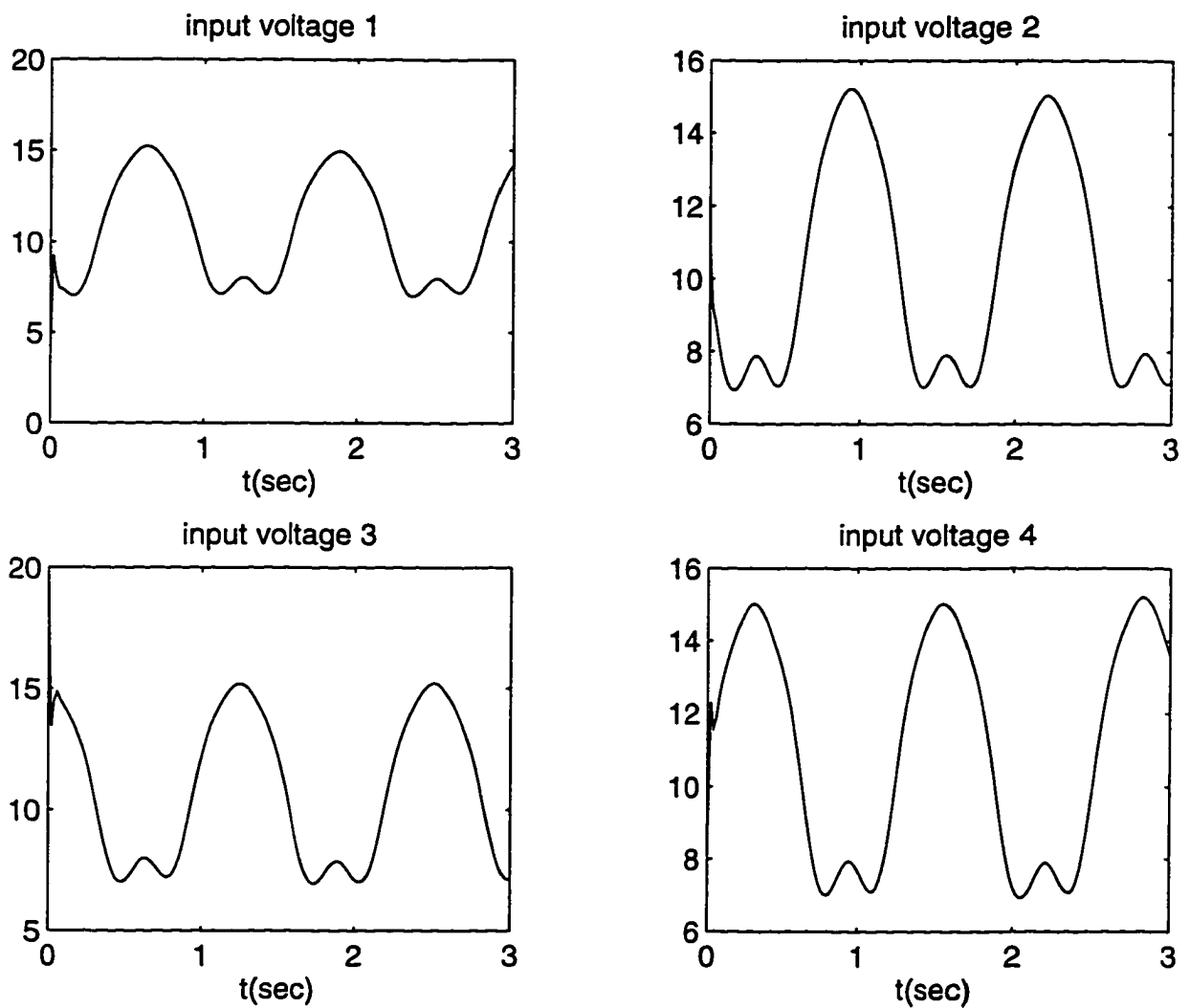


Figure 5.33 Input voltages don't exceed the maximum value 24 volts

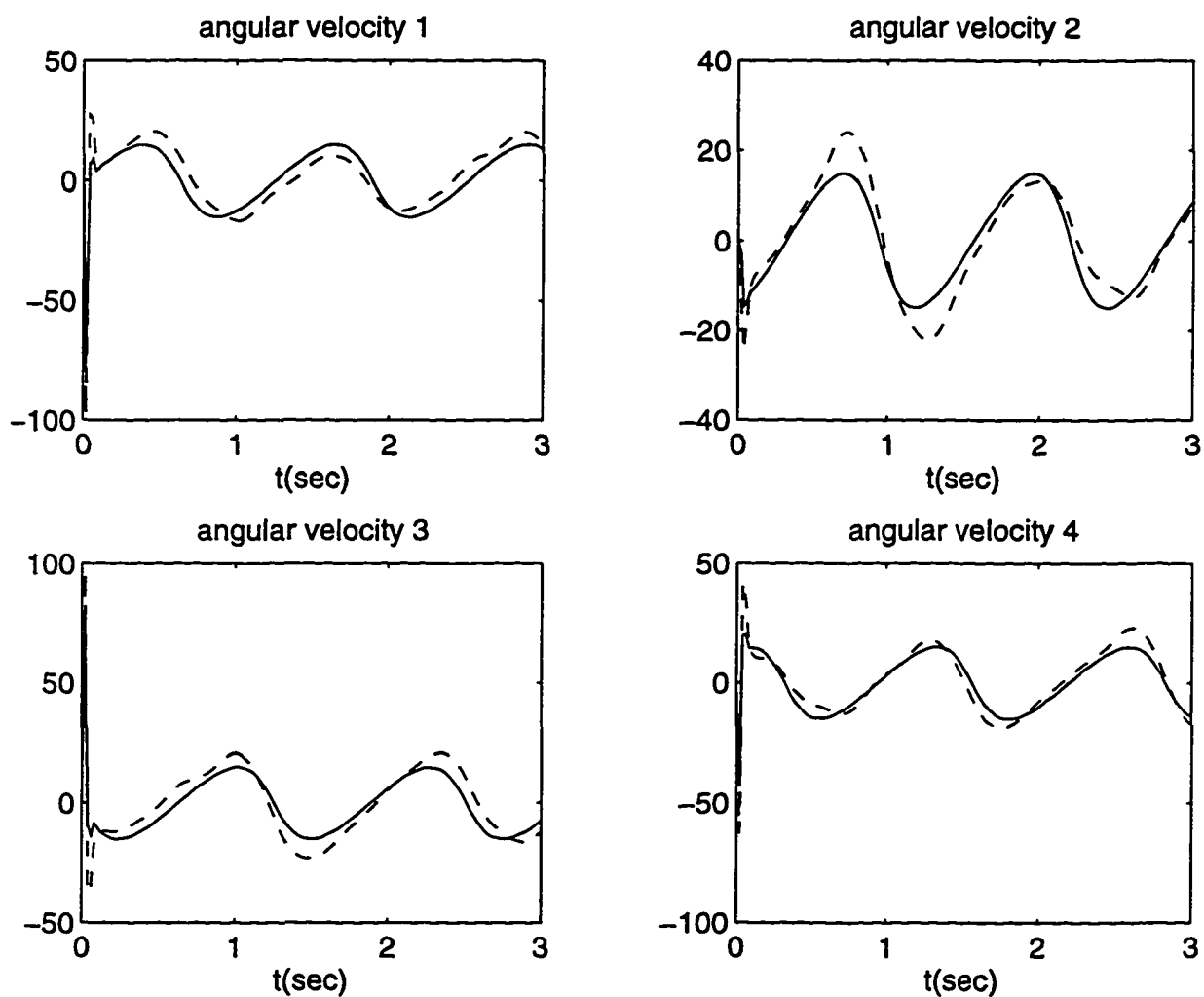


Figure 5.34 True (solid line) and estimated (dashed line) angular velocities of the motors

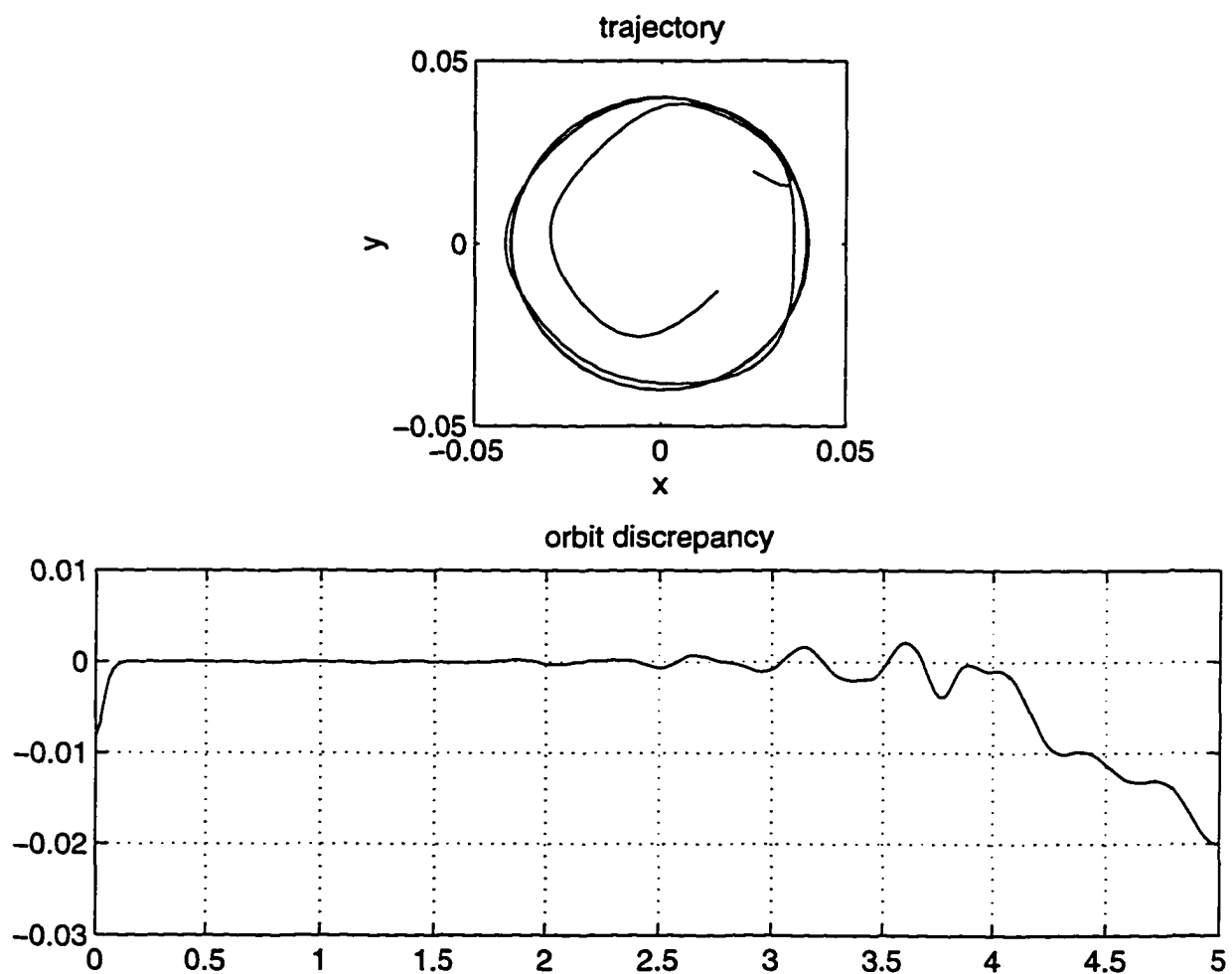


Figure 5.35 The radius of the desired circle is set to be 4 cm to illustrate the effect of decentralized control strategy on the working domain of the workpiece

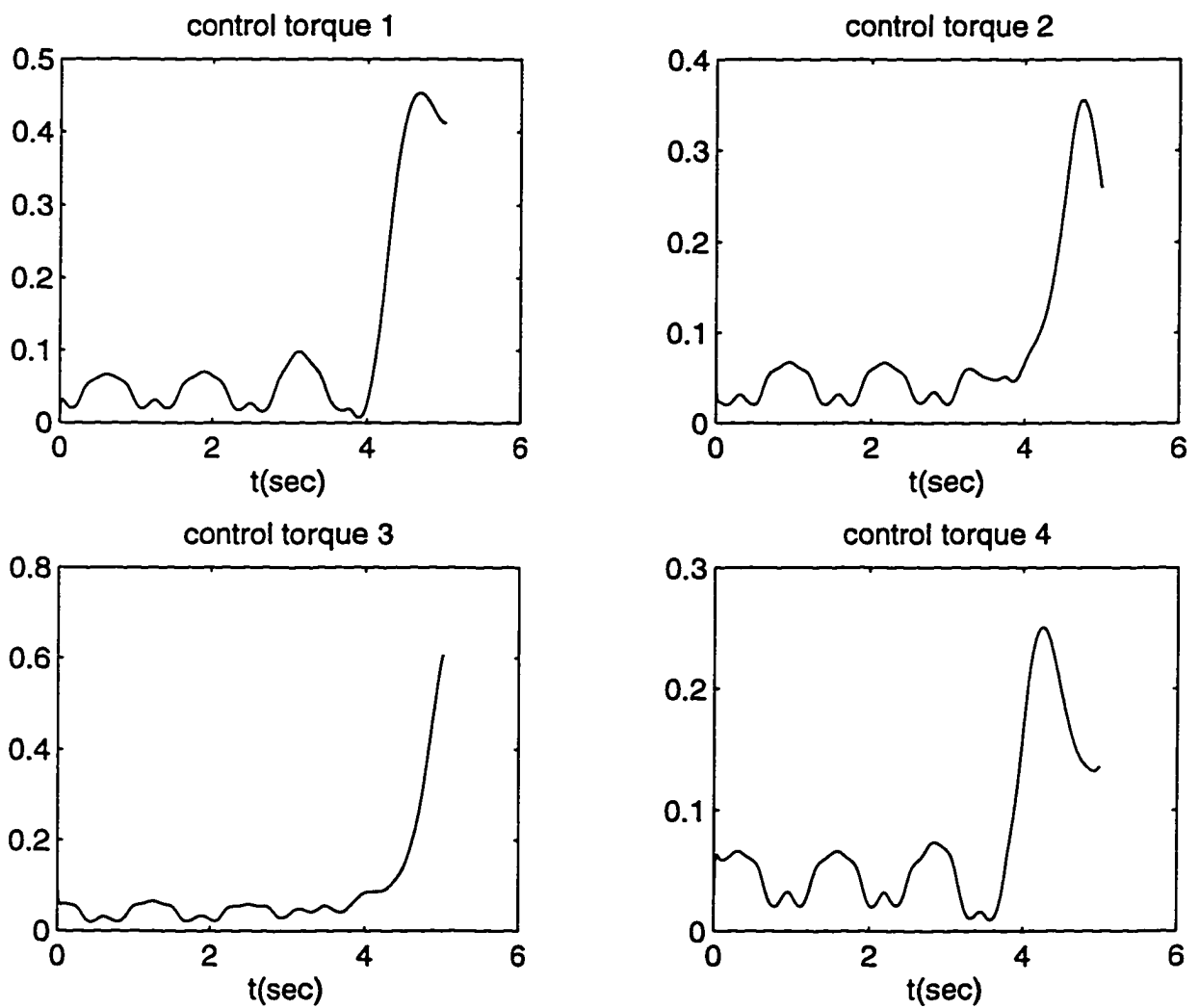


Figure 5.36 Control torques become unstable after some successful period of time

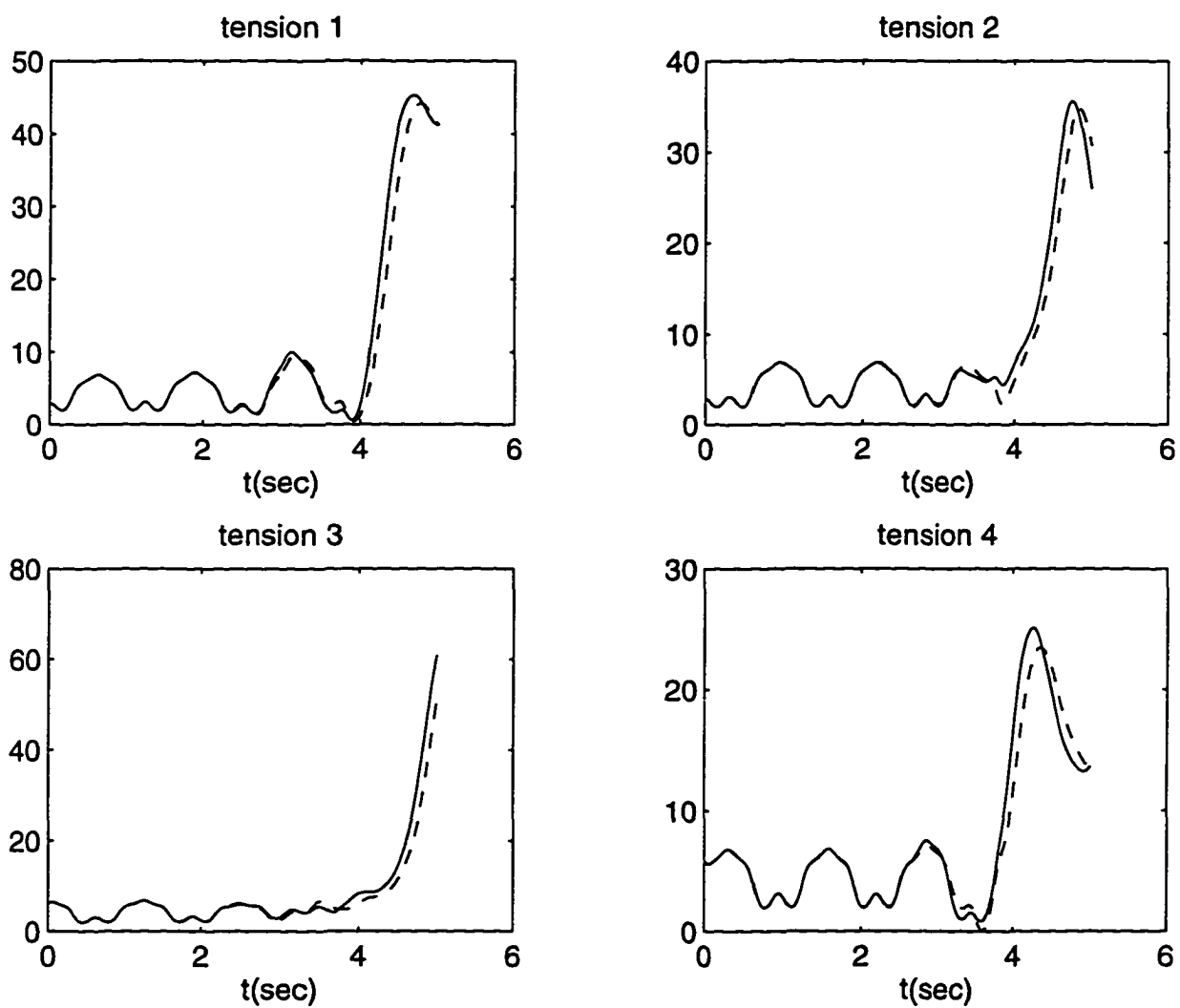


Figure 5.37 True (solid line) and the estimated (dashed line) tensions become larger and larger as the system enters into disorder

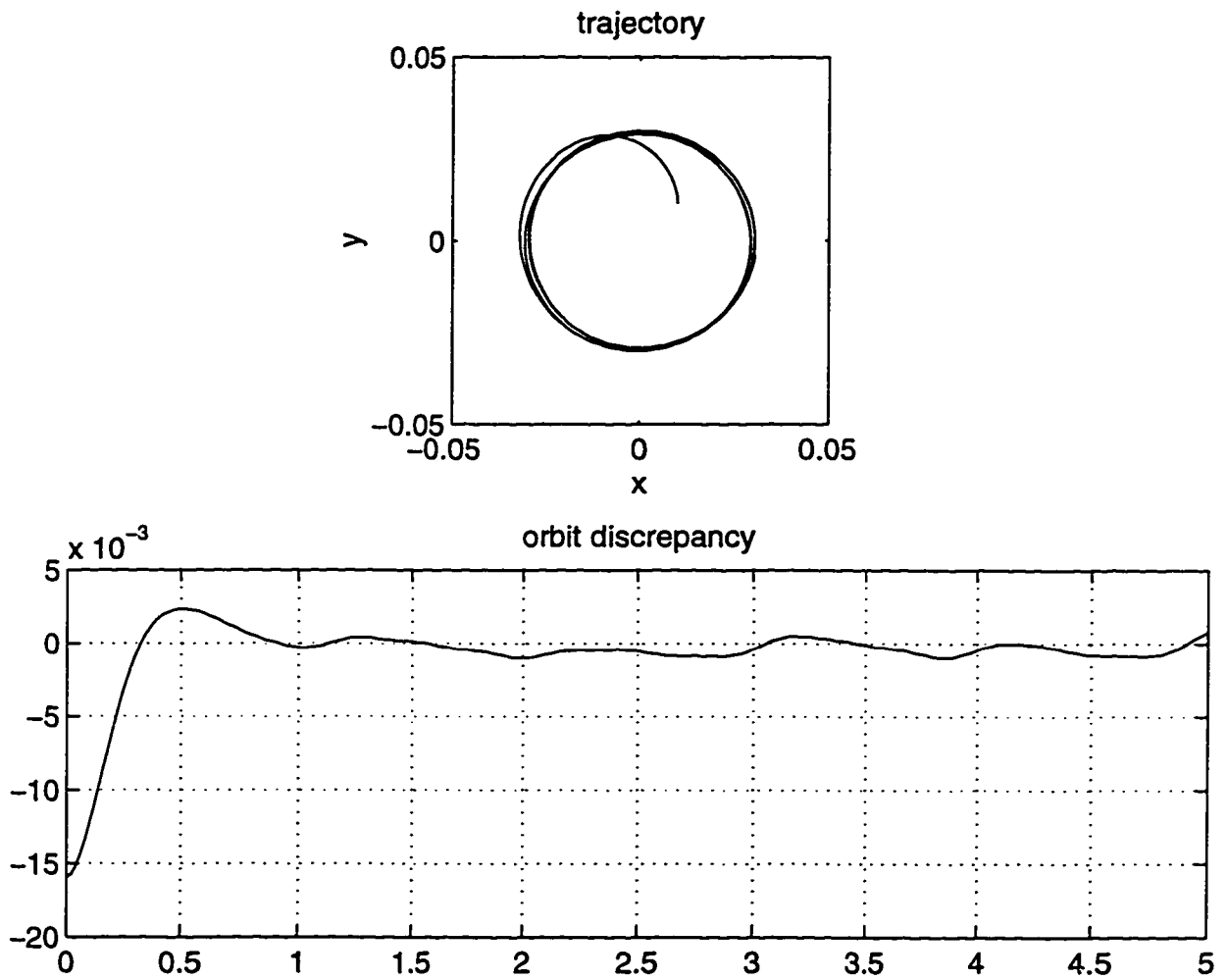


Figure 5.38 Trajectory of the workpiece. The estimated angular velocity is used in the control law

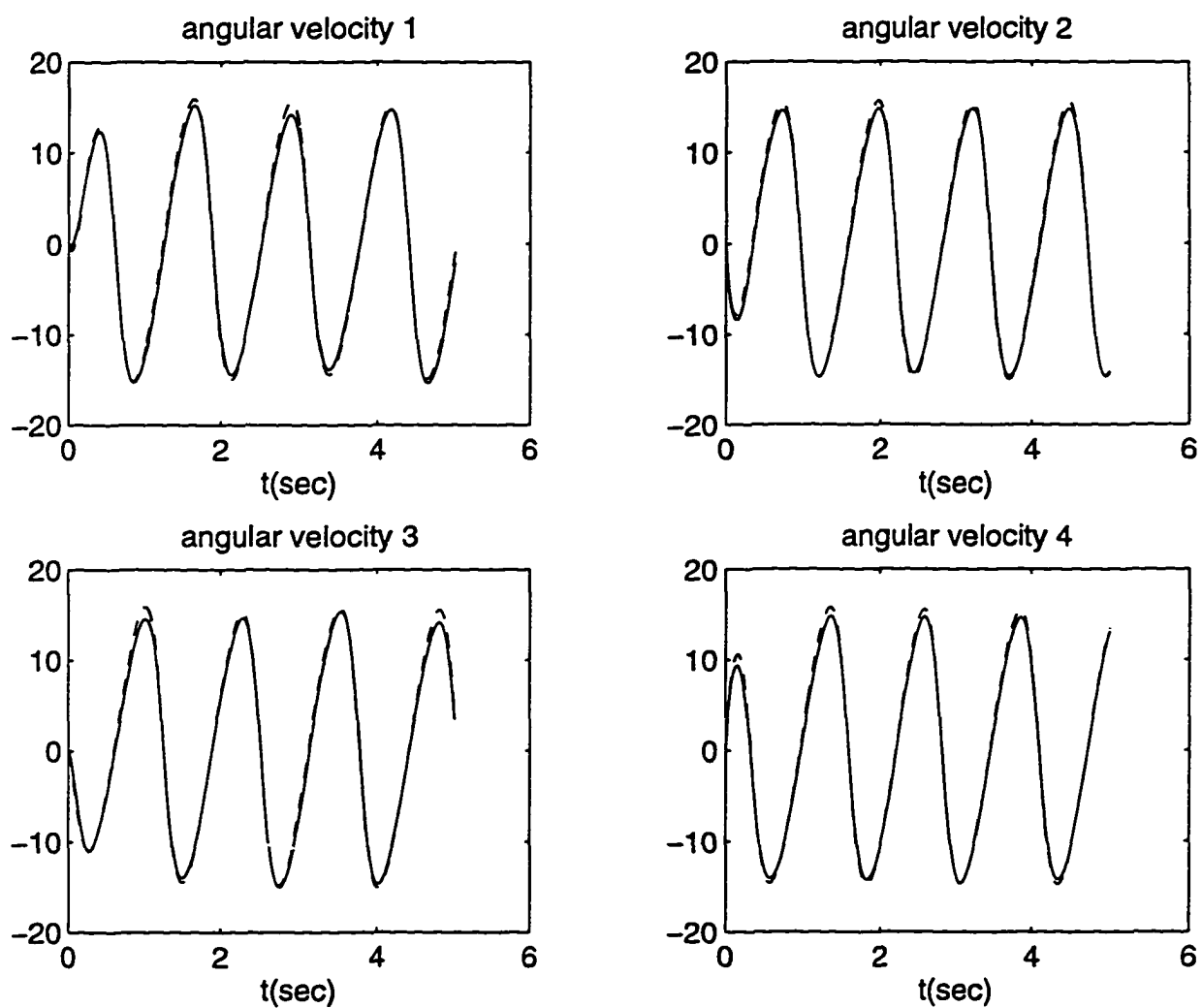


Figure 5.39 True (solid line) and estimated (dashed line) angular velocity of the motor

5.3 Bandwidth of the Agonistic System

Under the computed-torque control law, the nonlinear dynamics of the agonistic system can be linearized as the second-order linear dynamics.

From (Friedland, 1986), the bandwidth W of the second-order linear system is related to the natural frequency ω_n as:

$$\left(\frac{W}{\omega_n}\right)^2 = 1 - 2\zeta^2 + \sqrt{(1 - 2\zeta^2)^2 + 1}$$

If we choose the damping factor ζ as $\frac{1}{\sqrt{2}}$, then, $W = \omega_n$.

The bandwidth is limited by the following factors:

- unmodelled dynamics such as friction
- use of observer
- actuator saturation
- constraint on the controller such as positiveness

Under the physical parameters of the agonistic system, we choose the natural frequency as $\omega_n = 125.6$ rad/sec (20 Hz) and the gains in the controller as

$$k_v = 2\zeta\omega_n = 177.6$$

$$k_p = \omega_n^2 = 15775.36$$

The parameter N is selected as $N = 0.055$ to prevent the torque from becoming negative.

Under these values in the controller, the input voltage will not exceed its allowable maximum value 24 volts.

The closed loop bandwidth is expected to reach 20 Hz.

In addition to the basic requirement on the controller to accomplish the control task such as point-to-point move, or tracking a given trajectory, there are other requirements imposed on the controller.

- The control torques exerted on each motors are nonnegative. This is required to keep the tendons in tension.

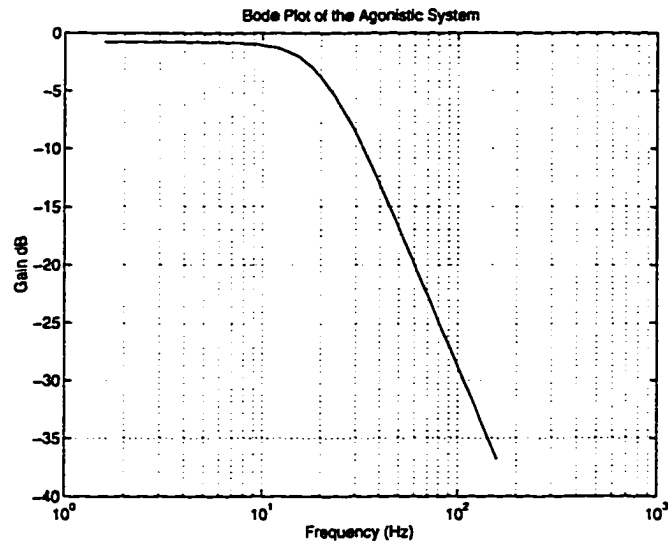


Figure 5.40 The agonistic system has 20 Hz bandwidth

- The input voltage can not exceed its maximum value. In real actuators, there is physical limitation on the input energy.

Under these requirements, the agonistic control becomes a nonlinear multi-variable control problem with constraints on control input. Let u be the control input, then u must satisfies: $0 \leq u \leq \bar{u}$ where \bar{u} is the maximum allowable value. A lot of work has been done on the energy constraints on the input. However, only a few work are seen on the nonnegative control. The general case is not easy.

5.4 Choice of the Control Laws

In the above, we evaluated several control laws through extensive simulations. It is shown that both centralized control and decentralized control can achieve control task with high accuracy, have high bandwidth, and at the same time, satisfy the other requirements imposed on the control input (preserving positiveness and not exceeding maximum values). When observer is incorporated, centralized control still works well. However, the performance of decentralized control is severely degraded. Specifically, the bandwidth is sharply reduced and the tracking error is increased. In addition, decentralized control has a main disadvantage: the working domain of the

workpiece is smaller than the available area. If the trajectory extends too far from the center, the system will become unstable. This is the price paid for using simple linear controller instead of complex nonlinear controller.

As for the comparison between computed-torque method and passivity-based method, their performances are essentially the same. But the passivity-based method has an advantage: its stability is guaranteed. Hence, larger uncertainties may be accommodated. The drawback of passivity-based method is that the error dynamics is very complicated and depends on the inertia matrix $M(q)$, hence, the real-time position of the workpiece. Computed-torque method is not passive and may therefore suffer from instabilities in the presence of uncertainties. But its error dynamics is very simple and independent of the inertia matrix.

5.5 Comparison with Hummingbird System

Both agonistic system and Hummingbird system are minipositioners. It is interesting to make a comparison between these two systems.

- **Cost:** The Hummingbird is very high while the agonistic system is potentially very inexpensive.
- **Speed:** Hummingbird system is capable of making a 5 millimeter move in 11 ms (Zai et al, 1992). Agonistic system is capable of making a 10 mm move in 100 ms.
- **Precision:** The positioning accuracy of the Hummingbird system is in the order of a micrometer. The positioning accuracy of the agonistic system is in the order of micrometer for the set-point task and in the order of 10^{-4} meter for a tracking task. The actual accuracy depends on the unmodelled dynamics (such as friction), optical encoder and DC motor.
- **Bandwidth:** The agonistic system has the 20 Hz bandwidth. As of Hummingbird system, we don't know the exact value of its closed loop bandwidth.

We only know that its servo motor has a bandwidth 273 Hz (Zai, et al, 1992). But from the Hummingbird's rapid dynamic response, we infer that the Hummingbird system should have higher bandwidth than the agonistic system. Actually, this comparison is not fair, since larger motors are used in the Hummingbird system than one proposed for the agonistic control (In Hummingbird system, torque constant for actuators is 5.75×10^{-2} kg-m/A).

Conclusion:

Hummingbird system is an expensive, high speed and high precision minipositioner.

Agonistic system is a cost-effective, high speed with moderate precision positioning device.

CHAPTER 6

SUMMARY AND CONCLUSIONS

In this dissertation, a new positioning method, agonistic control, is investigated. A thorough analysis of the system in both stiff and elastic cases are performed. The dynamic model is established. It is a highly nonlinear multivariable system. Based on this nonlinear model, a control law is synthesized. The specific requirement in agonistic system is that the control torque must be positive to keep the tendons in tension. Also, the control input can't exceed its allowable level. Fine tuning the parameters in the control law can meet these different requirements.

In the stiff case, the control law is composed of two parts. The first part is a feedforward control to cancel the nonlinear dynamics. The second part is a PD control which is used to position the poles of the error dynamics at the desired locations.

The stiff case of the agonistic control problem is the limiting form of its elastic case when the elastic modulus of the tendon approaches infinity. The new phenomenon appeared in the elastic case is the oscillations in the fast variables. This resonant behavior imposes bandwidth limitations on the control algorithm that is designed assuming perfect rigidity and will cause stability problems. This can be dealt with effectively by use of singular perturbation method. This investigation shows that the effect of elastic tendons in agonistic control can be compensated for by appropriately modifying the control law designed for inelastic tendons. Specifically, the control law consists of the control law (slow control) designed based on rigid model, together with a correction term (fast control) to damp out the oscillations incurred by the finite elasticity of the tendon. The slow control drives the system to track the desired trajectory. Robustness of the controller is enhanced by using sliding mode control.

The simulation results demonstrate the feasibility of designing a control law to coordinate the input voltages to four actuators for agonistic control.

The elastic control entails more information than stiff control. In the stiff case, due to the holonomic constraints, the position of the workpiece can be inferred from the angular positions of the motors which are measured with optical encoders mounted on each motor. In the elastic case, however, the position of the workpiece is independent of the angular positions of the motors. There is no one to one correspondence between two quantities. Therefore, additional position sensor is needed to detect the position of the workpiece.

For the need of the velocity information which is usually unavailable, an observer is used. Assuming that the geometric coordinates x, y of the workpiece are accessible for measurement, a nonlinear observer is constructed to estimate the corresponding velocities which are used instead of the actual velocities in the control law, based on "extended separation principle". In the design of observer for elastic case, linear uncertain system theory is used. It is shown that the observer is globally stable.

For the real time implementation, a decentralized control law is designed. A simple linear second order model is used instead of complex nonlinear model used in centralized version. The control scheme presented embodies a key concept: the total torque is the superposition of the base value and the correction value. It has the desirable feature that the total torque and the tension in the tendon are always positive. The decentralized control strategy makes the implementation of the controller very easy and parallel processing architecture become possible.

REFERENCES

1. Bram de Jager, "Acceleration assisted tracking control" IEEE Control Systems Magazine, pp20-27, Oct. 1994.
2. L.C. Zai, L.F. Durfee, D.G. Manzer et al, "Control of a Hummingbird minipositioner with a multi-transputer MARC controller" Proc. IEEE Int. Conf. on Robotics and Automation, Nice, France, pp534-541, 1992.
3. J.P. Karidis, G. McVicker et al, "The Hummingbird mini-positioner: providing three-axis motion at 50G's with low reactions" Proc. IEEE Int. Conf. on Robotics and Automation, Nice, France, pp685-692, 1992.
4. C.C. Neumann, "Closed-loop laser beam alignment along active robot arm" Proc. of SPIE, Vol. 1821, Boston, MA, Nov. 1992.
5. L.W. Chang, "A robust motion control of actuators in disk files" Proceedings of American Control Conference, Boston, MA, pp49-55, 1991.
6. S.C. Jacobsen, H. Ko, E.K. Iversen and C.C. Davis, "Antagonistic control of a tendon driven manipulator" Proceedings of IEEE Int. Conf. on Robotics and Automation, AZ, pp1334-1339, 1989.
7. J.M. Wendlandt and S.S. Sastry, "Design and control of a simplified stewart platform for endoscopy" Proc. IEEE Decision and Control, Lake Buena Vista, FL, pp357-362, 1994.
8. S. Kawamura, W. Choe, S. Tanaka and S.R. Pandian "Development of an ultrahigh speed robot FALCON using wire drive system" Proceedings of IEEE Int. Conf. on Robotics and Automation, Nagoya, Japan, pp215-220, 1995.
9. T. Morizono, K. Kurahashi and S. Kawamura "Analysis and control of a force display system driven by parallel wire mechanism" Proceedings of Japan-USA Symposium on Flexible Automation, Boston, MA, Vol.1, pp63-70, 1996.
10. M. Ishii and M. Sato, "A 3D interface device with force feedback: a virtual work space for pick-and-place tasks" Proceedings of IEEE Int. Symposium of Annual Virtual Reality, Seattle, WA, pp331-335, 1993.
11. J.L. Synge and B.A. Griffith, *Principles of Mechanics*, McGraw Hill, New York, NY, 1942.
12. P. LaSalle and S. Lefschetz, *Stability by Lyapunov's Direct Method*, Academic Press, New York, NY, 1961.

13. M. Takegaki and S. Arimoto, "A new feedback method for dynamic control of manipulators" ASME J. Dyn. Syst. Measure. Control, Vol.102, pp119-125, 1981.
14. B. Paden and R. Panja, "Gloably asymptotically stable PD+ controller for robot manipulators" Int. J. Control, Vol.47, No.6, pp1697-1712, 1988.
15. R. Kelly, "A simple set point robot controller by using only position measurements" 12th World Congress IFAC, Sydney, Australia, Vol.6, pp173-176, 1993.
16. R.H. Middleton and G.C. Goodwin, "Adaptive computed torque control for rigid link manipulations" Systems and Control Letters, Vol.10, pp9-16, 1988.
17. M.W. Spong, M. Vidyasagar, *Robot Dynamics and Control*, John Wiley & Sons, New York, NY, 1989.
18. A.Ben-Israel, T.N.E. Greville, *Generalized Inverses*, John Wiley & Sons, New York, NY, 1974.
19. B. Friedland, *Advanced Control System Design*, Prentice Hall, Englewood Cliffs, NJ, 1996.
20. J.J.E. Slotine and W. Li, "On the adaptive control of robot manipulators" Int. J. Robotics Research, Vol.6, pp49-59, 1987.
21. M.W. Spong, "Modeling and control of elastic joint robots" Trans. of ASME, J. of Dynamic Systems, Measurement and Control, vol.109, pp310-319, Dec. 1987.
22. R. Marino and S. Nicosia, "Singular perturbation techniques in the adaptive control of elastic robots" IFAC Symposium on Robot Control, Barcelona, Spain, 1985.
23. F. C. Hoppensteadt, "Properties of solutions of ordinary differential equations with small parameters" Comm. Pure Appl. Math., vol.24, pp807-840, 1971.
24. J.H. Chow and P. Kokotovic, "Two time scale feedback design of a class of nonlinear systems" IEEE Trans. Automatic Control, vol.23, pp438-443, 1978.
25. A. Saberi and H. Khalil, "Stabilization and regulation of nonlinear singularly perturbed systems-composite control" IEEE Trans. Automatic Control, Vol.30, p739-747, 1985.
26. J.J.E. Slotine and W. Li, *Applied Nonlinear Control*, Prentice-Hall, Englewood Cliffs, NJ, 1991.

27. J.J.E. Slotine and S. Sastry, "Tracking control of nonlinear systems using sliding surfaces with application to robot manipulators" *Int. J. of Control*, Vol.38, No.2, 1983.
28. B. Friedland, *Control System Design*, McGraw Hill, New York, NY, 1986.
29. T.J. Tarn, A.K. Bejczy, X. Yun and Z. Li, "Effect of motor dynamics on nonlinear feedback robot arm control" *IEEE Trans. on Robotics and Automation*, Vol.7, No.1, 1991.
30. 1995-1996 Catalog, Servo Systems Co.
31. B.R. Barmish, "Necessary and sufficient conditions for quadratic stability of an uncertain linear systems" *J. Opt. The. Appli.* Vol.46, pp399-408, 1985.
32. I.R. Petersen and C.V. Hollot, "A Riccati equation approach to the stabilization of uncertain linear systems" *Automatica*, Vol.22, pp397-411, July 1986.
33. I.R. Petersen, "A stabilization algorithm for a class of uncertain linear systems" *Systems and Control Letters*, Vol.8, pp 351-357, 1987.
34. K. Zhou and P.P. Khargonekar, "On the stabilization of uncertain linear systems via bounded invariant Lyapunov functions" *SIAM J. Contr. and Opt.* Vol.26, No.6, pp1265-1273, 1988.
35. P.V. Kokotovic, H.K. Khalil and J. O'Reilly, *Singular Perturbation Methods in Control: Analysis and Design*, Academic Press, London, 1986.
36. A. Vinkler and L.J. Wood, "A comparison of several techniques for designing controllers of uncertain dynamic systems" *Proc. IEEE Int. Conf. on Decision and Control*, San Diego, CA, pp31-38, 1978.
37. S.S.L. Chang and T.K.C. Peng, "Adaptive guaranteed cost control of system with uncertain parameters" *IEEE Trans. Automatic Control*, Vol.17, pp474-483, August 1972.
38. P.P. Khargonekar, I.R. Petersen and K. Zhou, "Robust stabilization of uncertain linear systems: Quadratic stabilizability and H^∞ control theory" *IEEE Trans. Automatic Control*, Vol.35, No.3, pp356-361, 1990.
39. S.D.G. Cumming, "Design of observers of reduced dynamics" *Electronic Letters*, Vol.5, No.10, pp213-214, 1969.
40. D. Yang and B. Friedland "Two dimensional agonistic control: elastic case" *Proceedings of Japan-U.S.A. Symposium on Flexible Automation*, Boston, MA, Vol.1, pp95-101, July, 1996.
41. H. Hemami and F.C. Weimer, "Modeling of nonholonomic dynamic systems with applications" *Trans. of ASME, J. of Applied Mechanics*, Vol.48, pp177-182, March 1981.

42. S. Arimoto, F. Miyazaki and S. Kawamura, "Cooperative motion control of multiple robot arms or fingers" IEEE Int. Conf. on Robotics and Automation, Raleigh, NC, pp1407-1412, 1987.